

# DEVELOPMENT OF AN ENERGY DISSIPATION SYSTEM BASED ON METAL EXTRUSION

By Herbert Kartluke and Philip G. Luckhardt

November 1966

GPO PRICE \$ \_\_\_\_\_

CFSTI PRICE(S) \$ \_\_\_\_\_

Hard copy (HC) 3.00

Microfiche (MF) 1.50

9 653 July 65

Prepared under Contract No. NASW-1185 by  
TECHNIDYNE INCORPORATED  
West Chester, Pennsylvania

Langley Research Center  
NATIONAL AERONAUTICS AND SPACE ADMINISTRATION

N67 16773  
107  
Q10-51317  
(NACA OR OR YMX OR AD NUMBER)

(THIRD)  
1  
(CODE)  
32  
(CATEGORY)

# **DEVELOPMENT OF AN ENERGY DISSIPATION SYSTEM BASED ON METAL EXTRUSION**

**By Herbert Kartluke and Philip G. Luckhardt**

**November 1966**

**Prepared under Contract No. NASW-1185 by  
TECHNIDYNE INCORPORATED  
West Chester, Pennsylvania**

**Langley Research Center  
NATIONAL AERONAUTICS AND SPACE ADMINISTRATION**

## ABSTRACT

An energy dissipation system based upon the inverse extrusion process was developed, with aluminum billets serving as the working medium. The resulting "shock strut," a tubular telescoping mechanism, was evolved by comparative evaluation of deceleration profile characteristics experienced in absorbing the kinetic energy of a falling body.

Suitable shock strut designs utilizing aluminum billets of about 1.5 cubic inches were tested at impact velocities up to 40 feet per second with dropped weights exceeding 400 pounds. It was found that deceleration levels not exceeding 20 g's were within the system capability. Further development could result in even further decreases in deceleration levels. In a given system, the deceleration level varies inversely with the dropped weight and is essentially independent of impact velocity. The best system consistently exceeded 60,000 foot-pounds of energy absorbed per pound of aluminum actually expended. Shock strut design involves a trade-off between the acceptable peak "g" level, the overall length, and the energy absorption efficiency.

## TABLE OF CONTENTS

	<u>Page</u>
INTRODUCTION . . . . .	1
Scope of Investigation . . . . .	2
Theoretical Considerations . . . . .	2
Evaluation of Absorber Characteristics . . . . .	4
EQUIPMENT . . . . .	6
Dropping Apparatus . . . . .	6
Shock Struts . . . . .	6
Instrumentation . . . . .	10
SHOCK STRUT DEVELOPMENT . . . . .	17
Preliminary Strut No. 1 . . . . .	17
Preliminary Strut No. 2 . . . . .	33
Concurrent Developments . . . . .	40
Summary . . . . .	41
EXPERIMENTAL INVESTIGATIONS . . . . .	43
Evaluation Methods . . . . .	43
Investigation of Design Effects . . . . .	50
System Design Considerations . . . . .	81
SUMMARY AND DISCUSSION . . . . .	85
Constant Force . . . . .	85
Major Design Effects . . . . .	85
Design for Use . . . . .	86
Limitations of Shock Strut Concept . . . . .	89
CONCLUSIONS . . . . .	90
APPENDIX A - ADDITIONAL SHOCK STRUT PERFORMANCE DATA . . . . .	91



## LIST OF FIGURES

<u>Figure</u>		<u>Page</u>
1	Deceleration Profile . . . . .	5
2	Schematic Arrangement of Energy Absorber Test Installation .	7
3	Apparatus in Position for Test Drop . . . . .	8
4	Schematic Drawing of Shock Strut Assembly . . . . .	9
5	Instrumentation for Photographic Record of Strut Descent . .	13
6	Diagrams of "Piezotron" Accelerometer . . . . .	14
7	"Piezotron" Filter, Coupler and Accelerometer . . . . .	15
8	Oscilloscope and Polaroid Camera . . . . .	15
9	Velocity and Deceleration as a Function of Distance Traveled: Small-scale Strut . . . . .	18
10	Orifice Rings and Entry Angles, Strut Design No. 1 . . . . .	20
11	Effect of Orifice Angle on Average Deceleration: Strut Design No. 1 . . . . .	22
12	Effect of Billet Nose Configuration on Deceleration: Strut Design No. 1 . . . . .	24
13	Specially Drilled Lead Billet for Impact-Reduction Tests: Strut Design No. 1 . . . . .	25
14	Effect of Billet Nose Configuration on Deceleration: Strut Design No. 1 . . . . .	26
15	Effect of Billet Nose Configuration on Deceleration: Strut Design No. 1 . . . . .	27
16	Effect of Billet Nose Configuration on Deceleration: Strut Design No. 1 . . . . .	28
17	Effect of Billet Nose Configuration on Deceleration: Strut Design No. 1 . . . . .	29
18	Effect of Billet Nose Configuration on Deceleration: Strut Design No. 1 . . . . .	30

# LIST OF FIGURES (Continued)

<u>Figure</u>		<u>Page</u>
19	Effect of Billet Nose Configuration on Deceleration: Strut Design No. 1 . . . . .	31
20	Effect of Billet Nose Configuration on Deceleration: Strut Design No. 1 . . . . .	32
21	Effect of Billet Nose Configuration on Deceleration: Strut Design No. 2 . . . . .	34
22	Effect of Billet Nose Configuration on Deceleration: Strut Design No. 2 . . . . .	35
23	Effect of Billet Nose Configuration on Deceleration: Strut Design No. 2 . . . . .	36
24	Effect of Billet Nose Configuration on Deceleration: Strut Design No. 2 . . . . .	38
25	Work Hardening of Aluminum Billets, Strut Design No. 2 . . .	39
26	Deceleration Profiles: Comparison of Acquisition Methods, Strut Design No. 3 . . . . .	48
27	Graphically Determined Curve Superimposed on Accelerometric Curve: Strut Design No. 3 . . . . .	49
28	Shock Strut Performance (Drop No. 103) . . . . .	51
29	Shock Strut Performance (Drop No. 111) . . . . .	52
30	Shock Strut Performance (Drop No. 137) . . . . .	53
31	Shock Strut Performance (Drop No. 151) . . . . .	55
32	Shock Strut Performance (Drop No. 153) . . . . .	56
33	Shock Strut Performance (Drop No. 158) . . . . .	57
34	Shock Strut Performance (Drop No. 130) . . . . .	59
35	Design of 6061-T5 Billet, Axially Graded for Hardness . . .	60
36	Shock Strut Performance (Drop No. 154) . . . . .	61
37	Shock Strut Performance (Drop No. 143) . . . . .	63

# LIST OF FIGURES (Concluded)

<u>Figure</u>		<u>Page</u>
38	Shock Strut Performance (Drop No. 111) . . . . .	64
39	Shock Strut Performance (Drop No. 150) . . . . .	65
40	Shock Strut Performance (Drop No. 151) . . . . .	66
41	Shock Strut Performance (Drop No. 152) . . . . .	67
42	Shock Strut Performance (Drop No. 153) . . . . .	68
43	Shock Strut Performance (Drop No. 110) . . . . .	69
44	Shock Strut Performance (Drop No. 111) . . . . .	70
45	Shock Strut Performance (Drop No. 113) . . . . .	71
46	Shock Strut Performance (Drop No. 114) . . . . .	72
47	Shock Strut Performance (Drop No. 116) . . . . .	73
48	Shock Strut Performance (Drop No. 117) . . . . .	74
49	Shock Strut Performance (Drop No. 119) . . . . .	75
50	Shock Strut Performance (Drop No. 163) . . . . .	76
51	Shock Strut Performance (Drop No. 151) . . . . .	77
52	Bending of Shock Strut as Result of Oblique Impact Test . .	79
53	Shock Strut Performance (Drop No. 138) . . . . .	80
54	Deceleration Mode as a Function of Billet Hardness and Load Weight . . . . .	87
55	Energy Absorption Efficiency as a Function of Impact Energy.	88

LIST OF TABLES

<u>Table</u>		<u>Page</u>
I	Shock Strut Dimensions . . . . .	11
II	Weights of the Three Strut Systems . . . . .	11
III	Effect of Orifice Entry Angle on Extrusion Factor, Small Scale Strut . . . . .	19
IV	Effect of Orifice Entry Angle on Average Deceleration: Strut Design No. 1 . . . . .	21
V	Drops Using Area Ratio of 1.50:1 . . . . .	44
VI	Drops Using Area Ratio of 1.23:1 . . . . .	45
VII	Drops with 6061-T6 Aluminum Alloy Hollow Billets . . . . .	46
VIII	Accelerometer Data Verification . . . . .	47
IX	Extrusion Factor Variation with Billet Geometry . . . . .	81

## INTRODUCTION

Consideration given in recent years to methods for absorbing the kinetic energy of decelerating vehicles has indicated that high energy-absorption accompanies the plastic deformation of metals. Another energy absorption principle, that of friction, is considered to have the greatest potential of any method of energy absorption <sup>1</sup>. Among various collapsible structures investigated for the landing of space vehicles, the frangible tube, utilizing such principles in undefined relation, is reported to have demonstrated a higher energy absorption capability than any deceleration system yet investigated. <sup>1</sup>

Under Contract NASW-1185, the National Aeronautics and Space Administration authorized Technidyne Incorporated to investigate an energy-absorption vehicular landing system based on the inverted extrusion of metals.

Direct extrusion involves a process wherein a metal billet is forced through a container by a ram and is extruded through a die at the end remote from the ram. Inverted extrusion is a process wherein the billet is fixed within the container, and the head of the ram becomes the die.

In direct extrusion processes, the total extrusion force varies appreciably due to the changing friction between the moving billet and the container wall. In inverted extrusion, the total extrusion force is constant with travel, due to the elimination of friction between billet and container wall. Whereas in direct extrusion processes it is usually desirable to minimize frictional forces between the extruding billet and the die orifice and cylinder walls, in this indirect application such interfacial friction contributes to energy absorption and should be maximized since the concern is with controlled, rather than rapid extrusion rate.

The deceleration system devised to apply such an extrusion principle is a tubular telescoping mechanism, the operation of which can be briefly described as follows: At impact, the movable (inside) tubular ram thrusts the die in contact with the fixed billet, deceleration being then coincident with the extrusion of billet metal through the die into the ram cavity.

In addition to the advantages of low cost, simplicity of actuation, and a potential saving in weight, this system is not limited by the tensile strength of the shock-absorbing member as is the frangible tube, and, importantly, it promises control of the deceleration rate through variation in the geometry of the billet and of the die, and/or through variation of the physical properties of the billet.

---

<sup>1</sup> Esgar, J. B., "Survey of Energy-Absorption Devices for Soft Landing of Space Vehicles", NASA Technical Note D-1308, National Aeronautics and Space Administration, Washington, June 1962.

## Scope of Investigation

The aims of this work have been to acquire engineering information on the potential of the extrusion energy absorber and to ascertain the approximate requirements of a system offering the most efficient energy absorption and deceleration control.

Specifically, the object of such an energy dissipation system is to provide a landing within the deceleration and deceleration-onset rate limitations dictated by the landing structure and its contents. The maximum permissible deceleration depends on such factors as the structural strength of the vehicle, whether it is manned or unmanned, instrumentation limitations, etc. It has been stated [1] that for a manned vehicle, the maximum g-load should preferably be of the order of 4 to 8 g's, although in some applications decelerations up to 35 g's are permissible. A wider range of decelerations may be allowed for unmanned vehicles. Less information is available concerning the deceleration-onset rate, although it is postulated [1] that man may be able to withstand up to 1500 g's per second.

Within the above limitations, the specific requirements of a landing system depend upon the total vehicle weight, the travel distance during deceleration, and the velocity at deceleration onset. For this work involving metal extrusion energy absorbers, weights up to a maximum of 500 pounds and free falls from a maximum of 25 feet, providing a terminal velocity of approximately 40 feet per second, embraced the operational ranges of interest.

The development included the design and assembly of a drop-test rig, three shock struts, and instrumentation to record the performance of the system. Extrusion arrays were tested to determine (a) deceleration profile (including peak g-loading), and (b) energy absorption efficiency (total energy absorbed per unit weight of the absorbing system). Data were compiled to permit the design of absorbers which will meet potential combinations of peak g-load and absorption per unit weight criteria.

## Theoretical Considerations

The relationships of the significant variables of the energy-absorbing system are expressed by classical falling body, force and work-energy equations and by an empirically-determined equation for extrusion force:

$$\text{Falling Body} \quad s = \frac{v^2}{2g} = \frac{a \theta^2}{2} \quad (1)$$

$$a = \frac{v^2}{2s} = \frac{2s}{\theta^2} \quad (2)$$

$$\theta = \sqrt{\frac{2 s}{a}} \quad (3)$$

$$v = \sqrt{2 g s} \quad (4)$$

Force

$$F = \phi Y A_1 \ln A_1/A_2 \quad (5)$$

$$F = m a \quad (6)$$

Derived Extrusion Factor

$$\phi = \frac{m a}{Y A_1 \ln A_1/A_2} \quad (7)$$

Work Energy

$$Fl = mgs = \frac{m v^2}{2} \quad (8)$$

where

- s = drop height
- v = terminal velocity after free fall
- g = acceleration due to gravity
- a = average deceleration
- $\theta$  = deceleration time
- F = force required for deceleration
- $\phi$  = extrusion factor
- Y = yield strength of extrusion material
- $A_1$  = billet cross-sectional area
- $A_2$  = orifice cross-sectional area
- m = mass of the load
- l = distance of ram travel

In evaluating inverted extrusion as an energy absorption process according to the foregoing relationships, the following variables affecting the equation input were considered:

<sup>2</sup> Developed from an equation presented in C. E. Pearson and R. N. Parkins, The Extrusion of Metals, John Wiley & Sons, Inc., New York, 1960.

Billet: Physical properties of material (hardness and yield strength), diameter, cross section, length, and temperature.

Orifice Ring: Entry angle, and ratio of entry area to exit area (die area ratio; with solid billets, this is equivalent to the extrusion ratio).

Overall System: Total weight (affecting length and wall thickness of strut components), height of drop (terminal velocity), system temperature, and frictional losses.

### Evaluation of Absorber Characteristics

The various extrusion systems developed were evaluated in an effort to establish geometries and extrusion materials to provide acceptable deceleration rates and efficient energy absorption for various intended purposes. The two preferred conditions--minimum deceleration level and high-energy absorption efficiency--must be "traded off" in the design of any particular system. Generally high energy absorption efficiencies were found to correspond with high mode g-levels, and the converse. In some situations it may be desirable to minimize absorption system weight and attach secondary importance to the g-levels developed during impact; in this case a system exhibiting higher absorption efficiency may be demanded. In other cases, the primary concern may be to minimize g-levels, with system weight and absorption efficiency being of lesser import.

Deceleration Profile. - In evaluating performance of a given system, the deceleration profile (deceleration vs. time) is of importance. An idealized profile is shown by the solid lines in Figure 1. Actual shock-absorbing systems usually produce results varying to some degree from this idealized pattern. In some instances, there may be a peak at the onset of deceleration, as shown by the dotted line, or the deceleration may rise just prior to the end of the event, or other variations may occur. In this work, effort was directed toward a pattern approximating the idealized curve.

From fundamental principles of integration, the area under the curve is equivalent to the terminal velocity of the impacting load. Average deceleration can be determined by integrating this area and dividing by the length of the base line. The area under the curve is in g-seconds; thus division by the base line (seconds) will yield average deceleration in g's.

As used herein, the term "average" is applied when the above determination is made; the term "mode" is used to indicate the most frequently occurring deceleration level (i.e., the plateau level of the profile).



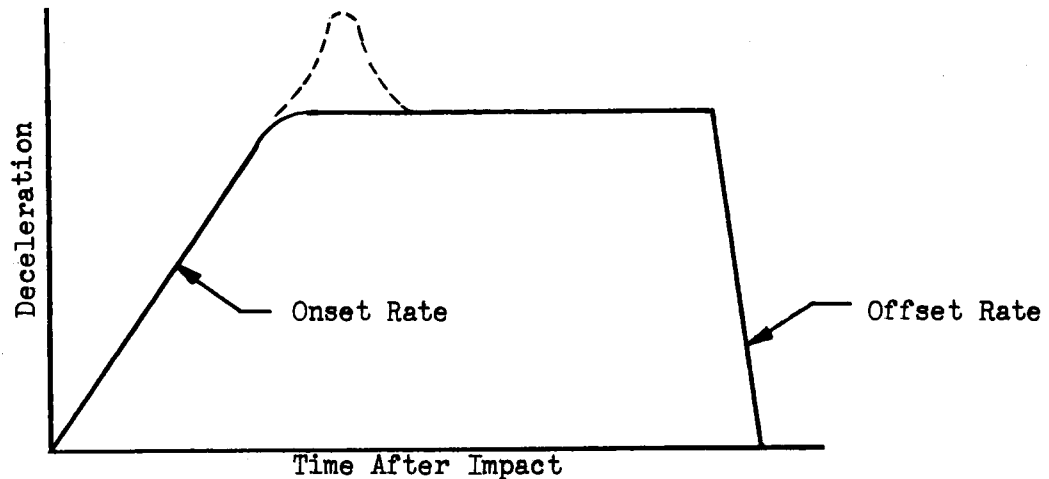


Figure 1

#### DECELERATION PROFILE

Energy Absorption Efficiency. - Another significant parameter is the energy absorption efficiency or the ratio of energy absorbed to the weight of material used in the absorption process. An efficiency value of 30,000 foot-pounds absorbed per pound of absorbing material actually utilized is said to be representative of the performance of the best systems currently available [1, 3].

The energy absorbed by the extrusion shock strut is the weight of the loaded drop box multiplied by the height of the drop; the weight of the material used is computed as the weight of the material extruded. For example, if the weight of the extruded billet material is 0.09 pound after a 10-foot drop with a load weight of 270 pounds, the ratio of energy absorbed to absorbent material weight would be expressed:

$$e = \frac{(270 \text{ lb})(10 \text{ ft})}{(0.09 \text{ lb})} = 30,000 \text{ foot-pounds per pound.}$$

<sup>3</sup> McGehee, J. R., "Experimental Investigation of Parameters and Materials for Fragmenting-Tube Energy Absorption Process," NASA Technical Note D3268, National Aeronautics and Space Administration, February 1966, p. 36.

## EQUIPMENT

The basic array of equipment necessary for accomplishing the experimental objectives included the dropping apparatus, the shock strut, and the instrumentation.

### DROPPING APPARATUS

The dropping apparatus, shown in Figure 2, consisted of a 35-foot length of 10 inch, wide-flange "I" beam anchored in a concrete pad. Brackets were welded to the top of the beam to support a 1/2-ton electric hoist. Figure 3 is a photograph of the apparatus ready for a test drop, with the first preliminary strut in position.

The beam was mounted at an angle of  $5^\circ$  from the perpendicular, with the upper end supported by a steel catwalk connecting the second floors of adjacent buildings. The weight box could thus roll down the length of the beam and maintain contact by means of a second set of rollers on the underside of the flange. A set of rollers riding on the edges of the flange prevented sideward motion.

The shock-strut assembly was bolted to the bottom of the weight box on the ground. The weight box was gripped by the jaws of the release mechanism and hoisted up the beam as far as desired and then released. Raising the box to its highest position provided a maximum free fall of 25 feet.

The impact plate was set in mortar at an angle of 5 degrees to horizontal to provide perpendicular contact. Oblique landings were made by using a second impact plate supported at an angle of 13 degrees to the perpendicular of the line of descent of the weight box.

### SHOCK STRUTS

The basic design of the shock strut, or inverted extruder assembly, is shown schematically in Figure 4. It consists of a mounting block (1) which is bolted to the bottom of the weight box and into which is threaded a length of steel tubing (2) which serves as the container for the extrusion billet (3). When the billet has been placed in the container, an orifice ring (4) is put in place and the tubular ram (5) is inserted into the container. A plug closes the end of the ram.

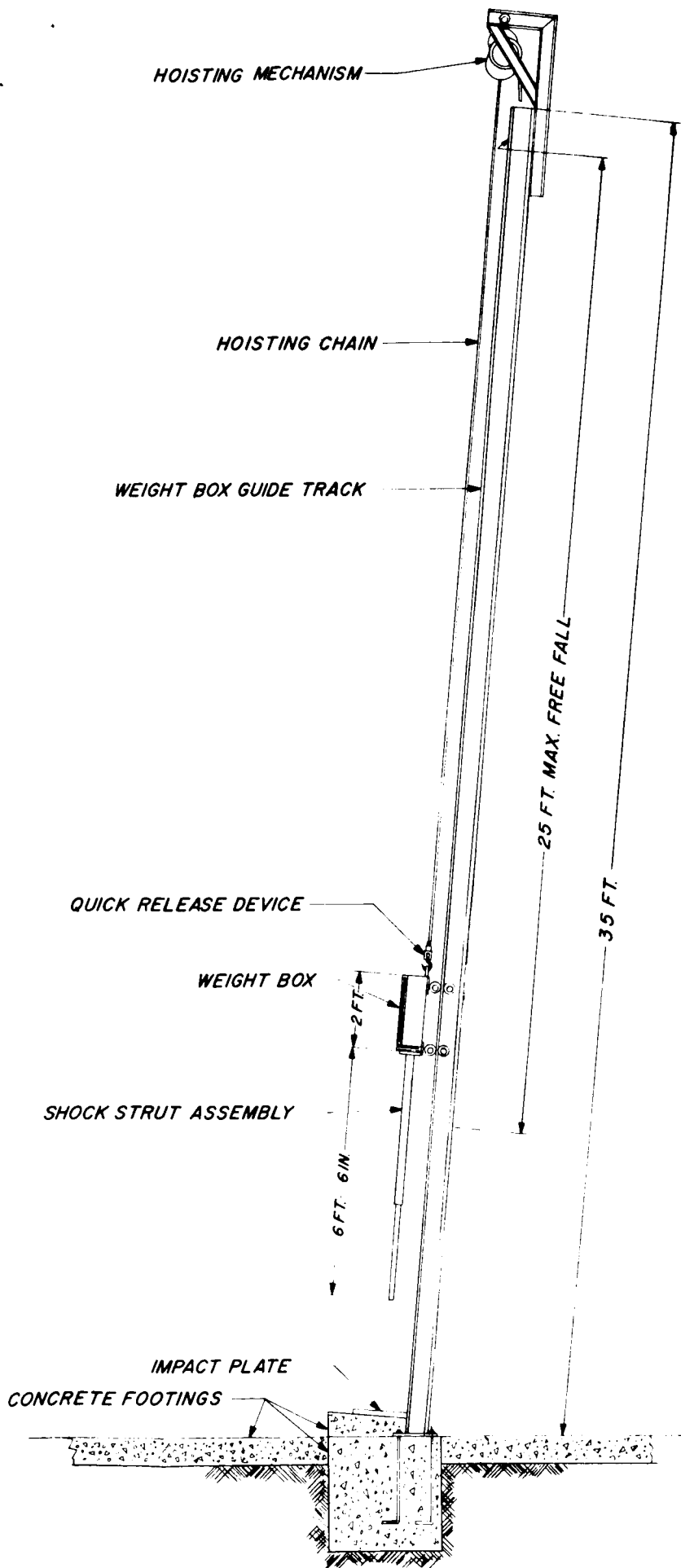


Figure 2  
 SCHEMATIC ARRANGEMENT OF ENERGY  
 ABSORBER TEST INSTALLATION

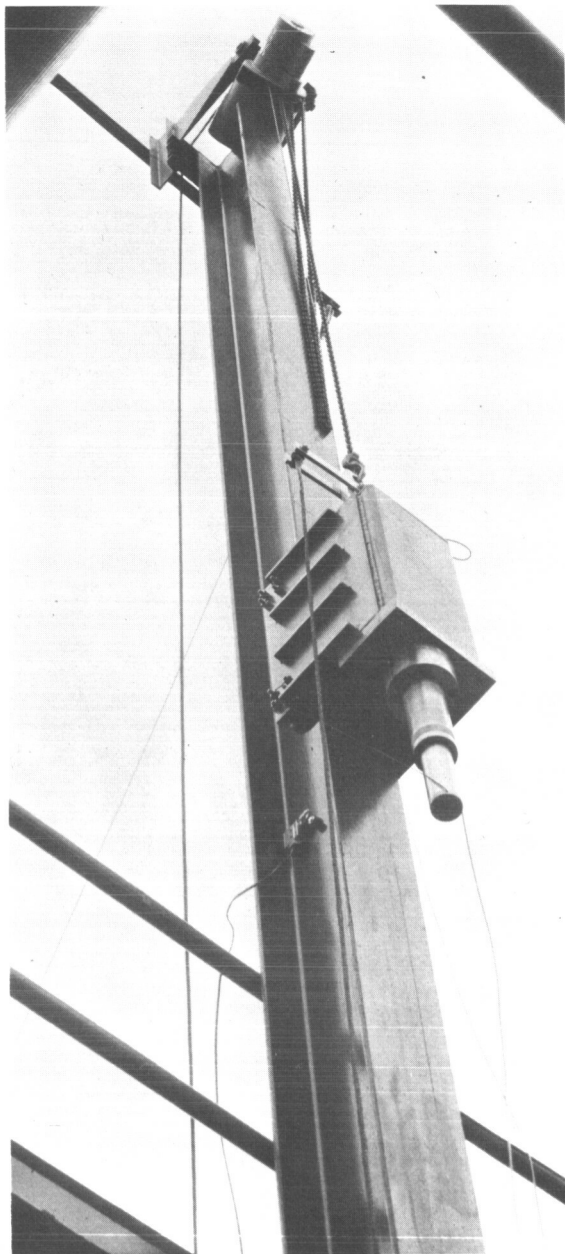


Figure 3

APPARATUS IN POSITION FOR TEST DROP

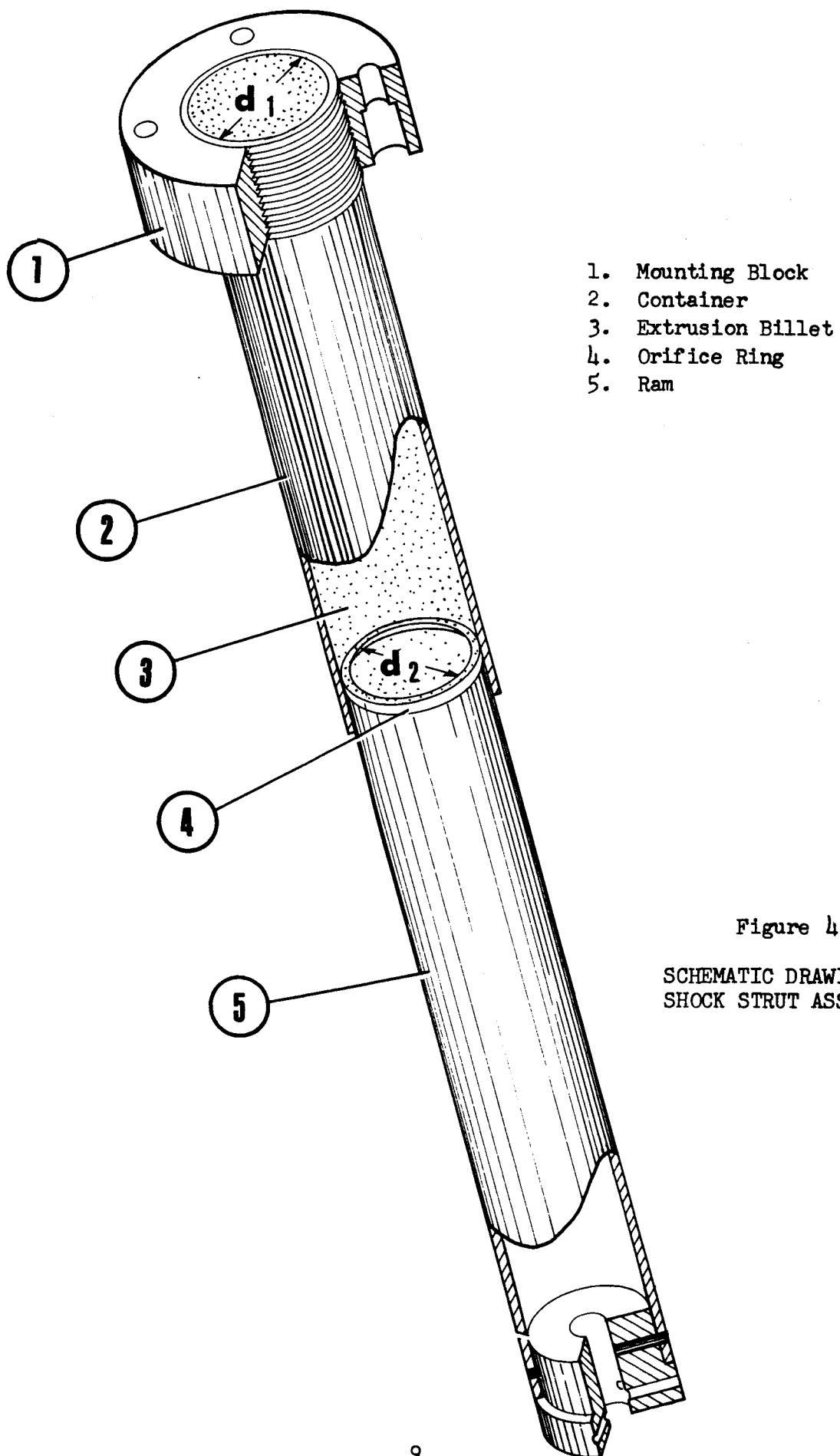


Figure 4

SCHEMATIC DRAWING OF  
SHOCK STRUT ASSEMBLY

Three strut designs were employed, two of these being preliminary struts used in establishing design criteria for the third strut--the ultimate test apparatus of this program. Following conservative design practice, the components for the first preliminary strut were constructed with relatively large cross-sections and thick walls. The second-preliminary strut was characterized by greater length and smaller cross section, but was also thick-walled. During experimentation with these two struts, it was determined that the weight of the assembly could be reduced without sacrificing operating performance by the use of a short, thin-walled strut of small cross-sectional area, and such was the design of the third strut. Comparative dimensions of the three struts, are shown in Table I. In Table II weights of the components and total systems are compiled.

In each design, the billet container and the ram were fabricated from commercially available 4130 seamless steel tubing. Single-material billets were fabricated from lead and aluminum. Compound billets were assembled in two designs: The first provided radial change in material properties by using aluminum annular sections with titanium tubular inserts, and the second provided axial change in properties, using axially-sequenced aluminum washers of varying hardness.

One of the major factors determining the force required for extrusion is the ratio  $d_1^2/d_2^2$  (see Figure 4), since this establishes the diametral reduction. Numerous orifice rings of differing inside diameter were employed throughout these experiments. All were of hardened DBL steel, as were the end caps of the rams.

## INSTRUMENTATION

The major instrumentation system required was for the measurement of deceleration-related factors; additional instruments were used for special temperature and stress determinations.

### Deceleration Measurement

Two instrumentation concepts were used for determination of load deceleration: (1) graphical derivation from high-speed photography of the impact event and (2) direct measurement using accelerometers mounted on the shock strut assembly. Ancillary instrumentation was used for determining load velocity before impact and for triggering oscilloscope and camera.

Table I  
SHOCK-STRUT DIMENSIONS

<u>Container</u>	<u>Strut 1 (inches)</u>	<u>Strut 2 (inches)</u>	<u>Strut 3 (inches)</u>
Length (Approx.)	12	48	10
Outside Diameter	3.528	2.500	1.500
Inside Diameter	2.480	1.595	1.130
Wall Thickness (Approx.)	0.524	0.452	0.185
<u>Ram</u>			
Length (Approx.)	13	48	8
Outside Diameter	2.48	1.595	1.125
Inside Diameter	2.365	1.382	1.027
Wall Thickness	0.055	0.105	0.049

Table II  
WEIGHTS OF THE THREE STRUT SYSTEMS

<u>Components</u>	<u>Strut 1 (13-inch ram length)</u>	<u>Strut 2 (48-inch ram length)</u>	<u>Strut 3 (8-inch ram length)</u>
Weight Box	259 lb	259 lb	259 lb
Container	16 lb	38 lb, 4 oz	2 lb, 8 oz
Ram	5 lb	7 lb, 1 oz	12 oz
Adapter Plate	9 lb, 9 oz	9 lb, 9 oz	9 lb, 9 oz
Hardware	1 lb, 3 oz	1 lb, 3 oz	1 lb, 3 oz
Billet, Lead	9 lb	4 lb, 7 oz	
Billet, Aluminum		2 lb, 1 oz	1 lb, 4 oz
TOTAL, LEAD BILLET	299 lb, 12 oz	319 lb, 8 oz	
TOTAL, ALUMINUM BILLET		317 lb, 2 oz	274 lb, 4 oz

High-Speed Photography. - During much of the program, the descent of the strut was recorded by a high-speed motion picture camera as follows: The shock strut assembly and the steel landing plate were painted with black paint. White reflecting scotch tape was applied to the front edge of the landing plate and to the end of the shock strut ram. A strip of the tape was applied to the bottom end of the container, and a second strip was carefully applied to the container at an accurately measured distance from the bottom strip. The high-speed camera was set up so that its vertical field of view included the white strip on the landing plate and both container strips when the falling strut was at least 6 inches above the landing plate. The camera was mounted on its side so the film would be drawn through horizontally.

With this arrangement, when the film was projected on a screen, the three taped areas appeared as black lines on a white background (or the reverse, depending upon whether negative or reversal film was used). The line on the landing plate established a zero reference, while the two strips on the container established a fixed distance reference for distance scaling purposes; a time reference was obtained by exposing the edge of the film to a 120-cps timing light.

To obtain data from a film, it was necessary to mark only the center of each timing pip so that it would appear on the projection screen, and to run the film through a slow-speed analyzer projector.

Figure 5 shows the "Fastax" camera mounted on the ringstand, sighting on the impact zone. The camera power supply appears at the base of the stand.

Accelerometric. - At the start of the experimental program, an attempt was made to use a standard quartz accelerometer (Kistler Instrument Corporation, Model 828A) to obtain deceleration data. This instrument proved to be unsatisfactory due to saturation of its electrical circuitry and it was necessary to employ the high-speed photographic method for data acquisition.

Later in the program a newly-developed instrument called the "Piezotron"\* became available. Tests with this instrument demonstrated satisfactory performance and it was used in all experiments with the final apparatus.

The basic circuit diagram and hook-up of the "Piezotron" are shown in Figure 6. This instrument was designed to be nonsaturable and to give linear response up to  $\pm 250$  g's at 10 millivolts output per g. Figure 7 is a photograph of filter, coupler, and accelerometer.

---

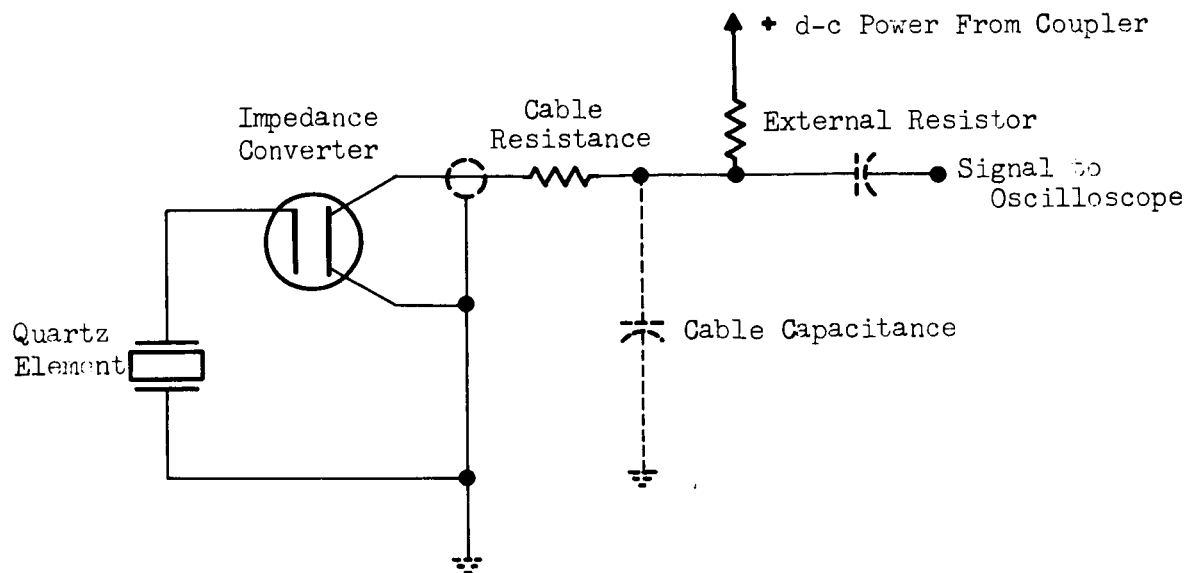
\* "Piezotron", Accelerometer Model 818, Coupler Model 548B, and Filter Model 544A5, Kistler Instrument Corporation, Clarence, N. Y.



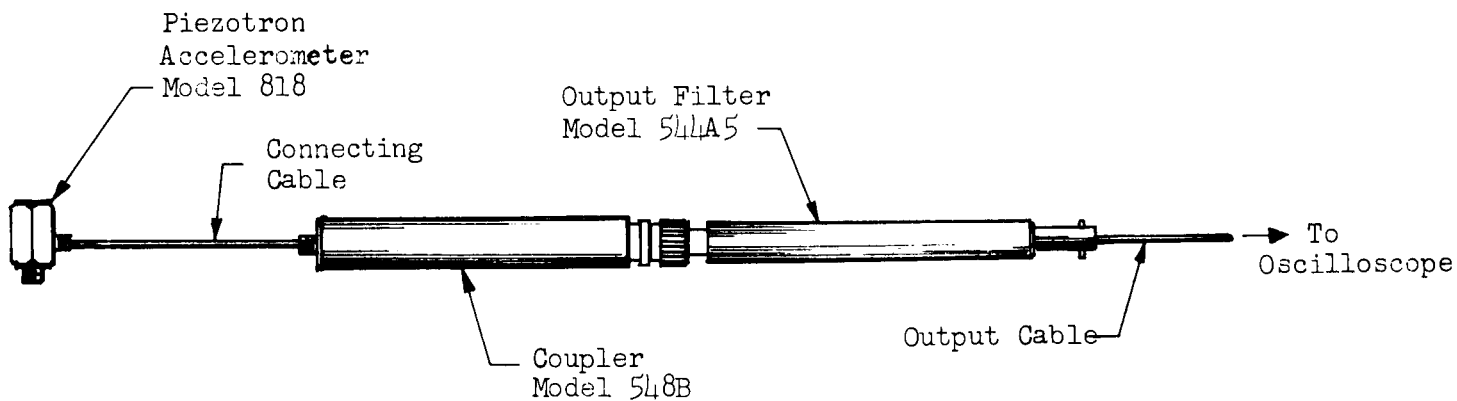


Figure 5

INSTRUMENTATION FOR PHOTOGRAPHIC RECORD OF STRUT DESCENT



a. Basic Circuit Diagram



b. System Diagram

Figure 6

DIAGRAMS OF "PIEZOTRON" ACCELEROMETER

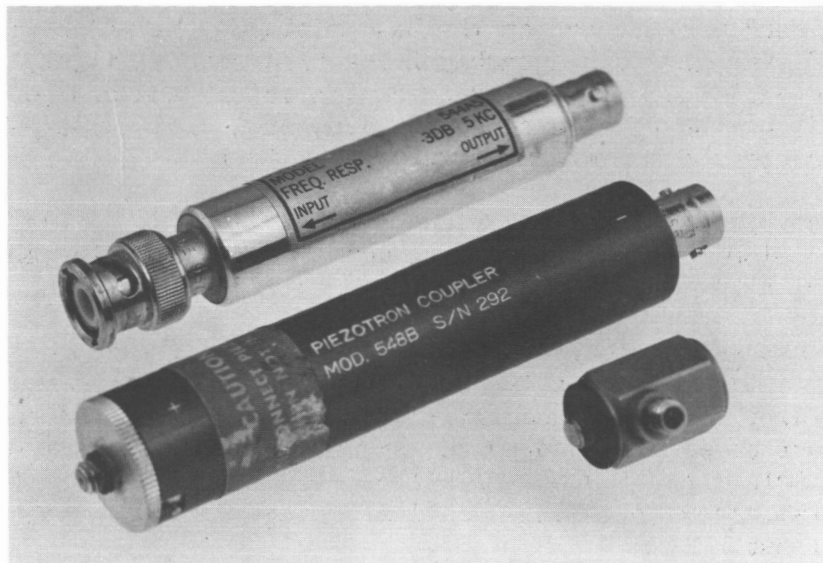


Figure 7

"PIEZOTRON" FILTER, COUPLER AND ACCELEROMETER

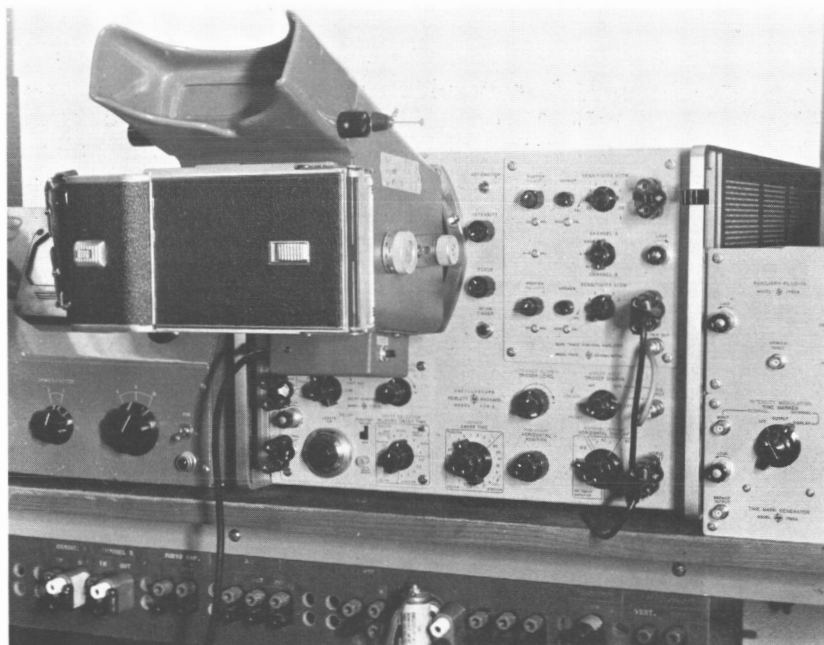


Figure 8

OSCILLOSCOPE AND POLAROID CAMERA

The "Piezotron" was mounted on the base plate of the weight box. Although the use of the filter gave a reasonably noise-free output signal, premature disarming of the oscilloscope trigger by random noise (and consequent loss of the event record) had to be eliminated by using an isolated d-c pulse to trigger the oscilloscope about 2 milliseconds before impact.

The oscilloscope trace was recorded on Polaroid film and later rephotographed by conventional methods for reproduction. The oscilloscope and Polaroid camera are shown in Figure 8.

Ancillary Instrumentation. - Triggering of the oscilloscope for accelerometer measurements was accomplished by use of a microswitch mounted on the "I" beam of the drop tower at a height of from 1/2 inch to 2 inches above the position at impact of an arm mounted on the weight box. Descent of the box brought the arm into contact with the microswitch actuator arm, closing the switch and initiating sweep of the oscilloscope trace approximately 2 milliseconds before impact.

In the photographic method, the start of operation of the high-speed camera was actuated by the same switching operation.

#### Temperature Measurement

Measurement of temperatures developed during impact were made with small-gage Chromel-Alumel thermocouples inserted in a well drilled in the billet and held in place by cement. The hole was of a size such that, upon extrusion, the deformation of the metal would insure intimate contact with the thermocouple. The output voltage was recorded on a strip chart.

#### Stress Measurement

For measurement of hoop stresses in the billet container, bonded wire strain gages were mounted on the outside of the container at the center of the billet area. Outputs of the gages were recorded on a strip chart.

## SHOCK STRUT DEVELOPMENT

The two provisional struts previously described were tested against prior theory to establish criteria for the third test apparatus. Data acquired in these initial studies were not in all cases conclusive, but contributed to the design of the final apparatus.

### PRELIMINARY STRUT NO. 1

The first preliminary strut (Table I) had a billet container ID of approximately 2.5 inches and an orifice ring ID of approximately 2.25 inches, effecting a die area ratio of 1.25:1. Using lead billets, experiments were conducted to evaluate the effects of orifice angle and billet geometry on energy absorption and deceleration.

### Orifice Entry Angle

Orifice entry angle is defined as the apex angle of the cone formed by the working surface of the orifice ring. Orifice design for the first strut was influenced by preliminary deceleration tests conducted with small-scale devices to obtain information on extrusion process variables involved in the absorption of impact energy.

The characteristics of the small-scale device were:

$$A_1 = 0.307 \text{ square inches}$$

$$A_2 = 0.101 \text{ square inches}$$

$$A_1/A_2 = 3.05$$

$$L = 1.75 \text{ inches}$$

$$m = \frac{207 \text{ pounds}}{g}$$

$$Y = 1780 \text{ pounds per square inch}$$

Extrusion material = lead

The drop and the deceleration characteristics were measured with a high-speed Waddell camera sighting directly on the zone of impact. Data from a typical run are plotted in Figure 9.

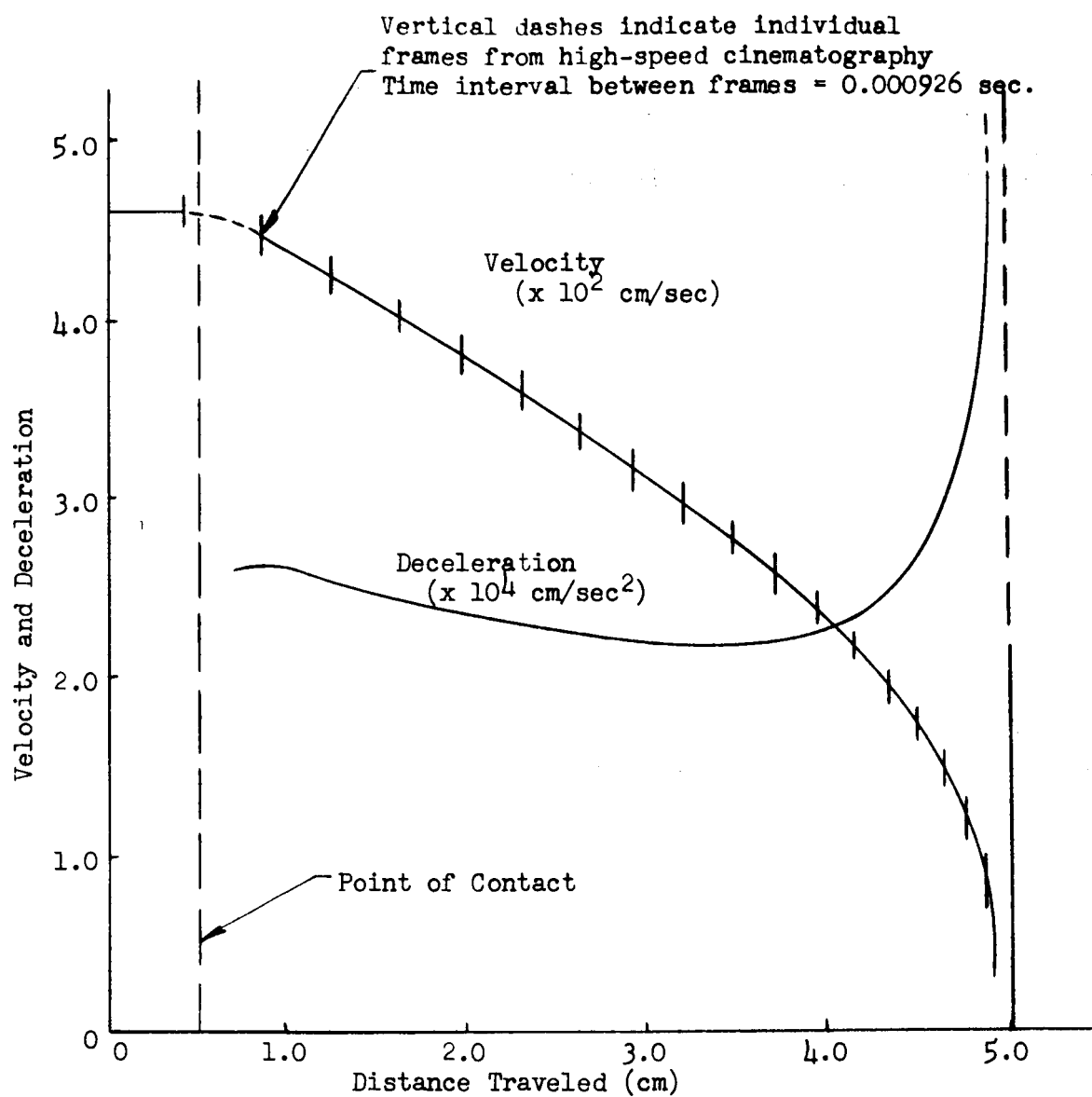


Figure 9

VELOCITY AND DECELERATION AS A FUNCTION OF  
DISTANCE TRAVELED: SMALL-SCALE STRUT

These data permitted evaluation of the extrusion factor  $\phi$  in the design equation (5). In Figure 9, the average deceleration is approximately  $2.25 \times 10^4$  cm/sec<sup>2</sup>, or approximately 23 g's. Since the mass being decelerated was 207 pounds, the extrusion force is

$$F = (207) (23) = 4761 \text{ pounds.}$$

This value of  $F$  can be substituted in equation (7), along with the known values of  $Y$ ,  $A_1$ , and  $A_2$ , and the equation solved for  $\phi$ :

$$\phi = \frac{4761}{(1780) (0.307) \ln (3.05)} = 7.76.$$

This value of  $\phi$  is considerably higher than the value of approximately 1.5 obtained under ideal extrusion conditions, and indicates that the process was inefficient from an extrusion standpoint due to the nozzle design and the speed of extrusion. These factors, however, were advantageous from the standpoint of energy dissipation.

Table III shows extrusion factor values as a function of four die entry angles, computed from equation (5).

Table III  
EFFECT OF ORIFICE ENTRY ANGLE ON  
EXTRUSION FACTOR, SMALL-SCALE STRUT

Orifice Entry Angle (deg)	Mean Deceleration (g)	Extrusion Factor $\phi$
60	32.7	5.15
90	46.6	7.35
120	50.2	7.90
180	54.7	8.65

On the basis of these initial small-scale tests, a set of orifice rings for the first test strut was made with included entry angles of 120, 90, and 60 degrees, in order that the character of the initial extrusion force might be varied. Sketches of the cross sections of the four dies are shown in Figure 10. Test results with these rings were compared with those with the 180-degree ring in evaluating the effect of orifice angle on initial impact peak deceleration and on average deceleration.

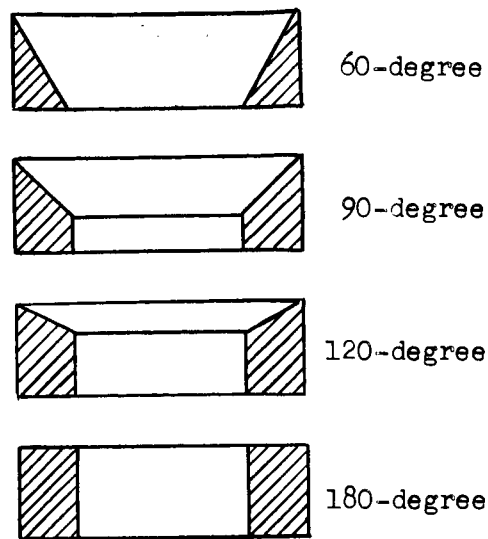


Figure 10

#### ORIFICE RINGS AND ENTRY ANGLES, STRUT DESIGN NO. 1

The deceleration peak produced by initial impact proved to be markedly changed by variation of the entry angle. Due to the rapid rise time, it was difficult to obtain data in the initial impact zone, since the oscilloscope trace moved so rapidly that the film was not heavily exposed. However, the data indicated that the sharp onset peak produced by the 180-degree die was considerably softened as the entry angle was reduced. This finding was of significance in the final design, in which the initial impact was reduced and the deceleration maintained nearly constant until all the energy was dissipated.

To determine the effect of orifice angle on average deceleration, a series of 5-foot test drops was made in which the change in deceleration produced by different entry angles was compared to that produced by the 180-degree shear ring. The data are summarized in Table IV, and a plot of average values is shown in Figure 11. For these data:

- $m = 311.5$  pounds
- $g =$  mean deceleration for an orifice
- $Y = 1.78 \times 10^3$  psi (for lead)
- $A_1 = 4.91$  square inches
- $A_1/A_2 = 1.25$



Table IV

EFFECT OF ORIFICE ENTRY ANGLE ON AVERAGE DECELERATION:  
STRUT DESIGN NO. 1

Material Extruded: Lead  
Free-fall Distance: 5 feet  
Extrusion Ratio: 1.25:1

Test No.	Orifice Angle (deg)	Ram Travel (feet)	Average Deceleration (g)	Average Deceleration (msec)	Mean Value For Orifice (g)
7	60	0.156	32.0	17.5	32.7
8		0.156	32.0	17.5	
9		0.166	30.1	18.6	
10		0.151	33.1	17.0	
11		0.136	36.8	15.2	
12	60	0.156	32.0	17.5	46.6
13	90	0.104	48.0	11.7	
14	90	0.109	45.9	12.2	
15	90	0.109	45.9	12.2	
16	120	0.104	48.0	11.7	50.2
17		0.098	51.0	10.9	
18		0.104	48.0	11.7	
19	120	0.093	53.8	10.4	
20	180	0.104	48.0	11.7	54.7
21		0.078	64.0	8.8	
22		0.088	56.5	9.9	
23	180	0.098	50.5	11.1	

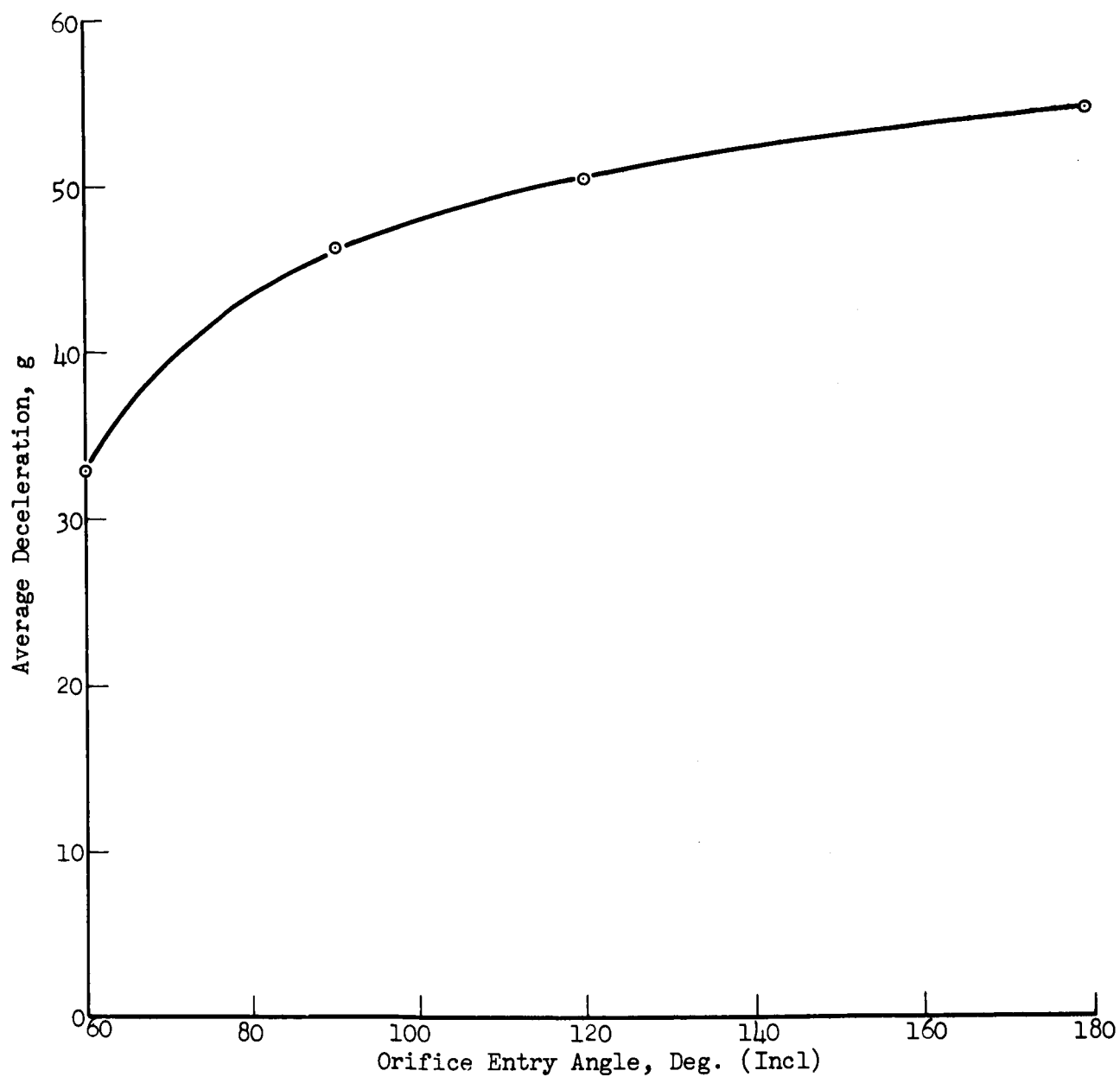


Figure 11

EFFECT OF ORIFICE ENTRY ANGLE ON AVERAGE DECELERATION:  
STRUT DESIGN NO. 1

Material Extruded: Lead  
Free-Fall Distance: 5 feet  
Extrusion Ratio: 1.25:1

Although both peak and average deceleration are seen to decline with a decrease in orifice angle, a 60-degree angle was found to represent the minimum permissible for an extrusion ratio of 1.25:1. It was further established that the 60-degree ring became warped after each impact and possibly added an unknown variable to the tests. As compromise between structural strength and impact softening capability, the 90-degree included angle was adopted for subsequent use.

### Billet Geometry


Having determined the practical limits for the orifice angle, subsequent investigation involved variation of the billet geometry to reduce initial impact deceleration. Various designs calculated to achieve a smoother distribution of energy absorption were tested.

A solid-nosed lead billet dropped from a height of 5 feet produced the deceleration curve shown in Figure 12. The initial sharp rise is due, among other factors, to the energy required to induce flow of the lead through the orifice. The "tail-off" of the curve represents the absorption of the remaining energy.

Additional tests were made with bored-end billets, in an effort to reduce the impact peak by presenting a smaller mass of metal at the billet nose to be induced to flow through the orifice. The nose of a billet was arbitrarily drilled as shown in Figure 13. A 5-foot test drop yielded the deceleration curve presented in Figure 14. The billet produced a gradual rise in deceleration over a period of 8 milliseconds, compared to a sharp rise time of 2 milliseconds for the solid billet. The gradual rise ceased as soon as the orifice ring reached the end of the bored section of the billet. The sharp drop following this point represents the absorption of the remaining energy in inducing extrusion (about 1/16 inch).

Further tests conducted with identical bored-nose billets from heights of 10, 15, 20, and 25 feet showed lower impact decelerations, particularly at the higher drops (Figures 15 through 18). The anomalous rise at the end of the 10 and 15 foot drops is apparently due to mechanical irregularity in the apparatus.

Success in obtaining a distribution of the initial impact energy by the use of partially bored billets suggested the investigation of the effect of completely drilled billets. Two initial drops of 5 and 10 feet were made with a standard lead billet having a 1/4-inch hole drilled axially through its entire length; results are presented in Figures 19 and 20. The sharp initial and terminal rises in deceleration shown in the curves were not fully explainable, and further experimentation with drilled-through billets was carried out later.





Material Extruded: Lead  
 Orifice: 90° (included)  
 Extrusion Ratio: 1.25  
 Billet Nose Configuration: Solid  
 Temperature During Drop: 65°F  
 Drop Height: 5 feet

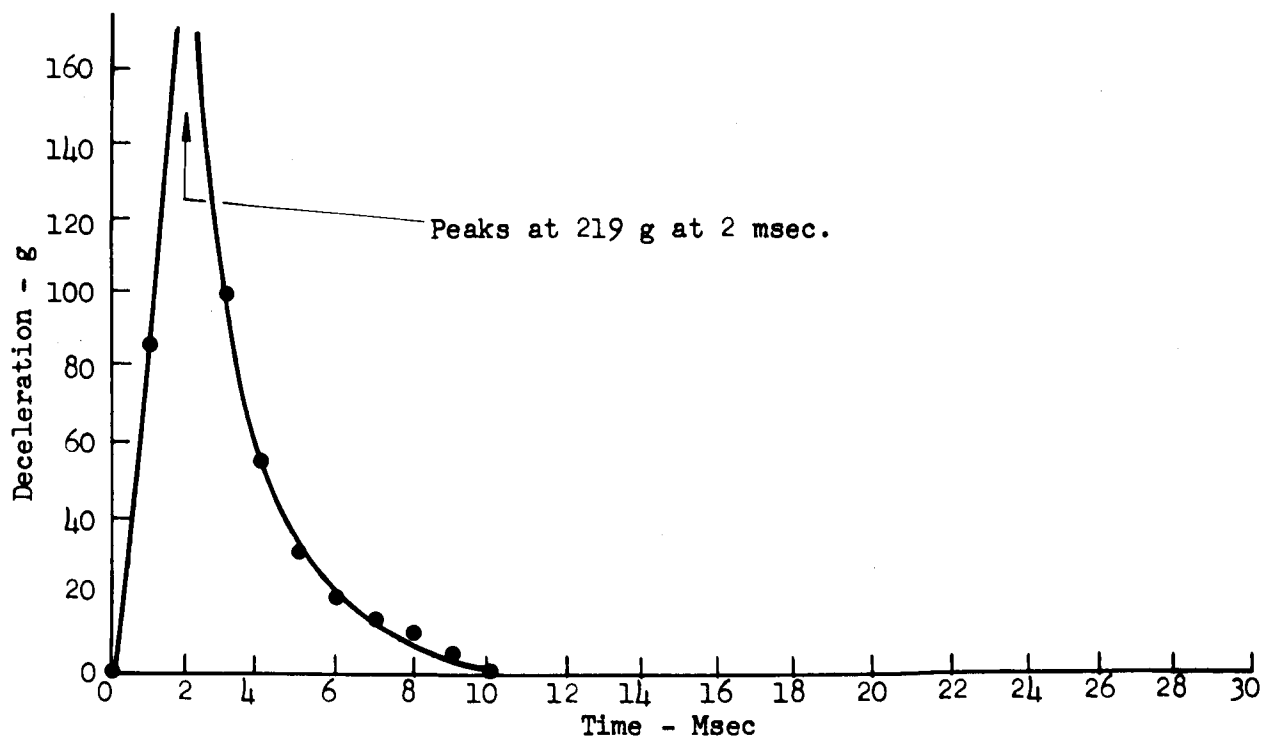
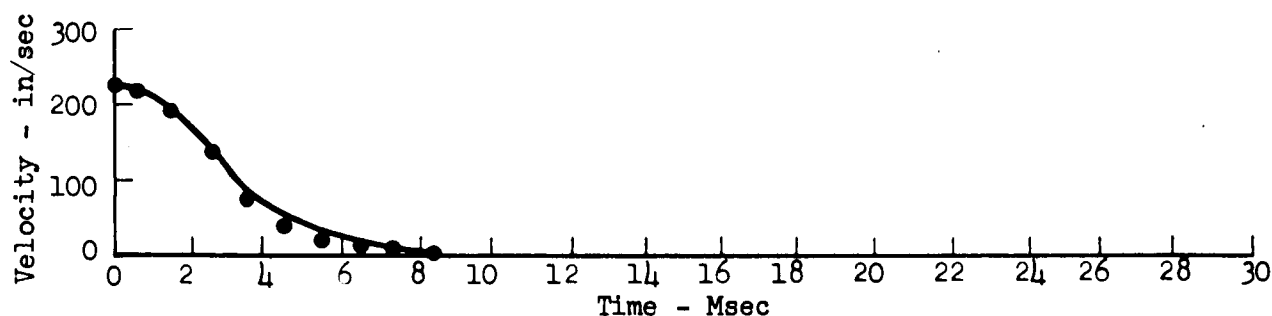
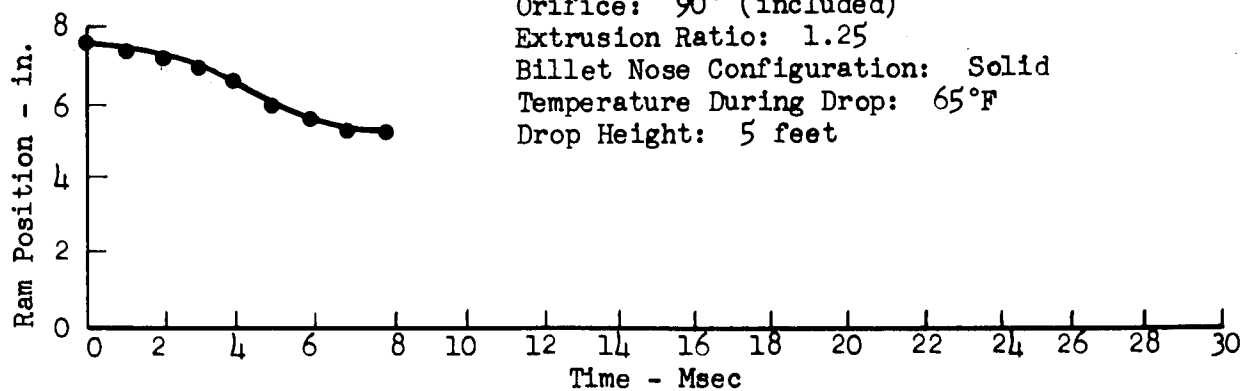
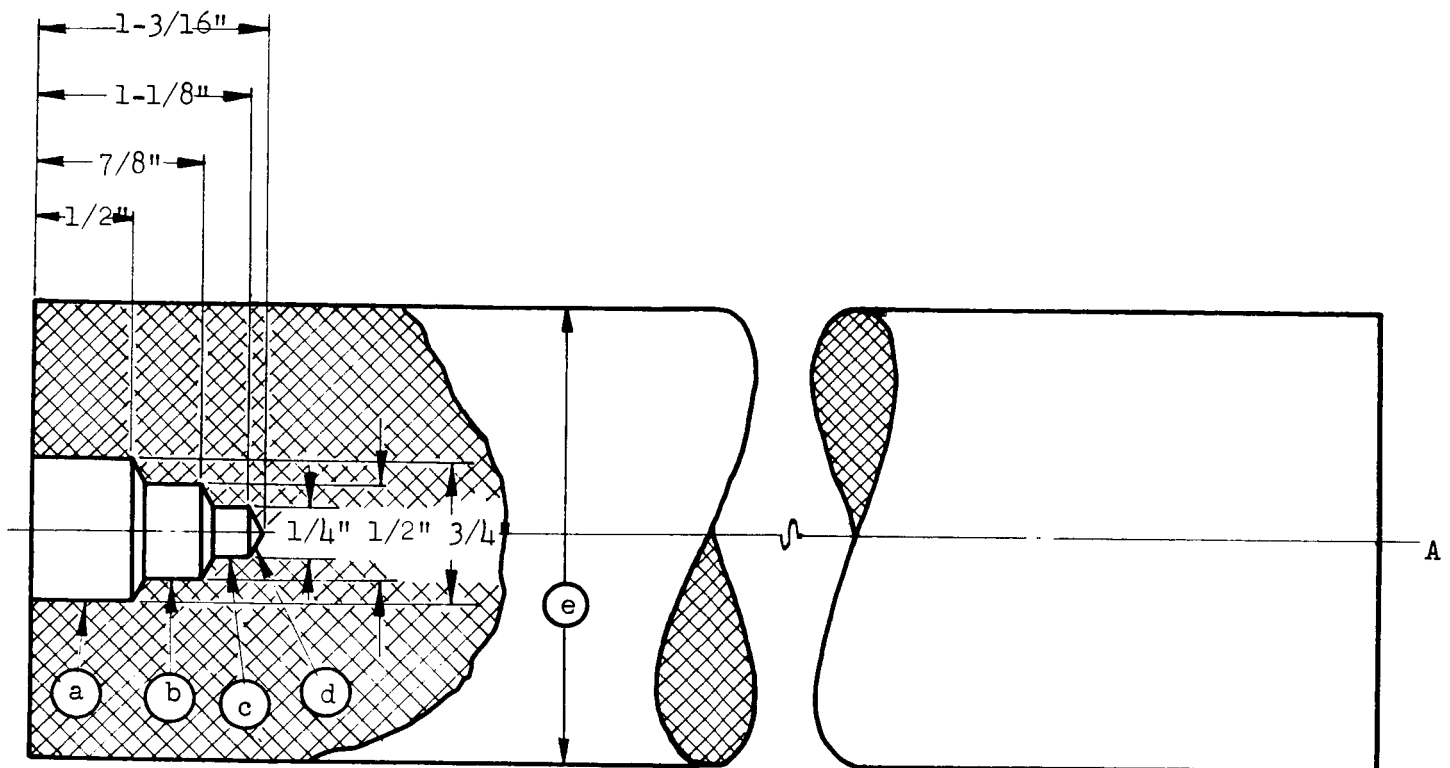


Figure 12

EFFECT OF BILLET NOSE CONFIGURATION ON DECELERATION: STRUT DESIGN No. 1



Extrusion Ratios at    a = 0.89:1  
                               b = 0.95:1  
                               c = 0.99:1  
                               d = 1.25:1  
 Billet Diameter        e = 2.480 in.

Figure 13  
 SPECIALLY DRILLED LEAD BILLET FOR IMPACT-REDUCTION TESTS:  
 STRUT DESIGN NO. 1



Material Extruded: Lead  
 Orifice: 90° (included)  
 Extrusion Ratio: 1.25  
 Billet Nose Configuration: Bored as Shown  
 Temperature During Drop: 65°F  
 Drop Height: 5 feet

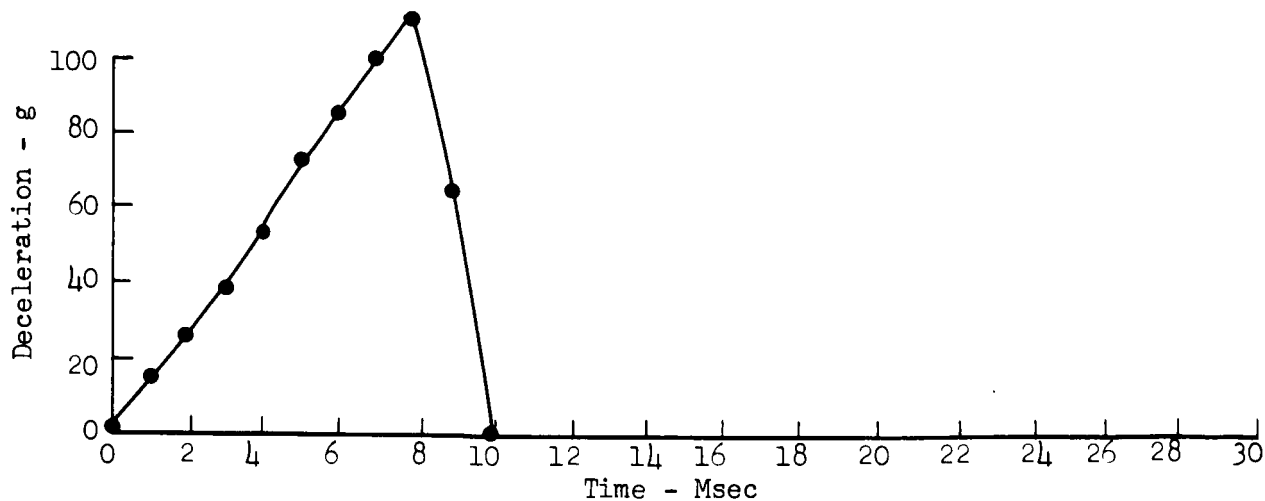
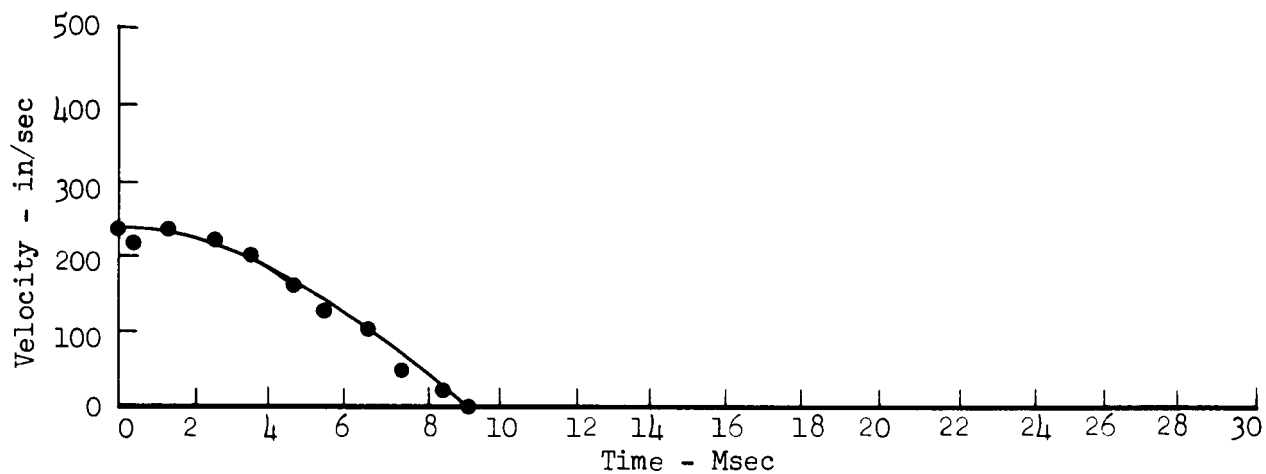
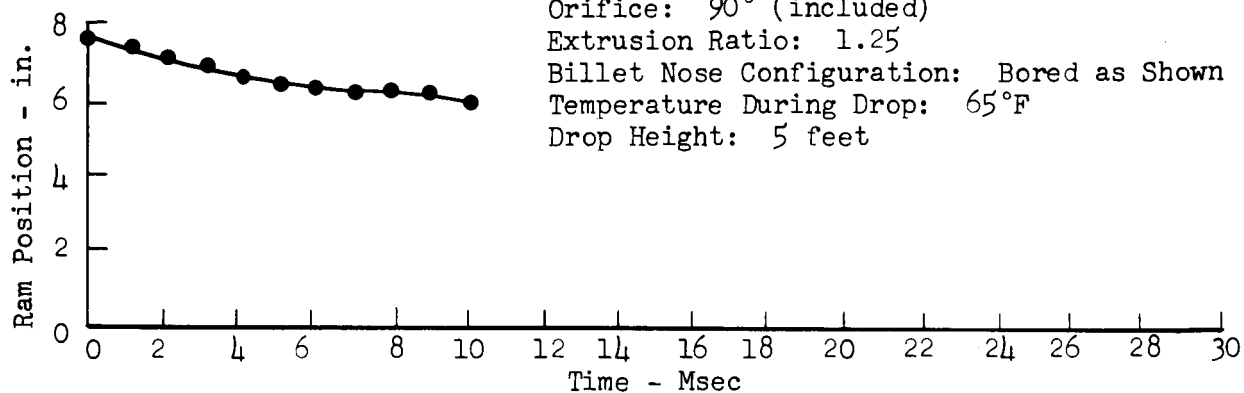


Figure 14  
 EFFECT OF BILLET NOSE CONFIGURATION ON DECELERATION: STRUT DESIGN NO. 1



Material Extruded: Lead  
 Orifice: 90° (included)  
 Extrusion Ratio: 1.25  
 Billet Nose Configuration: Bored as Shown  
 Temperature During Drop: 65°F  
 Drop Height: 10 feet

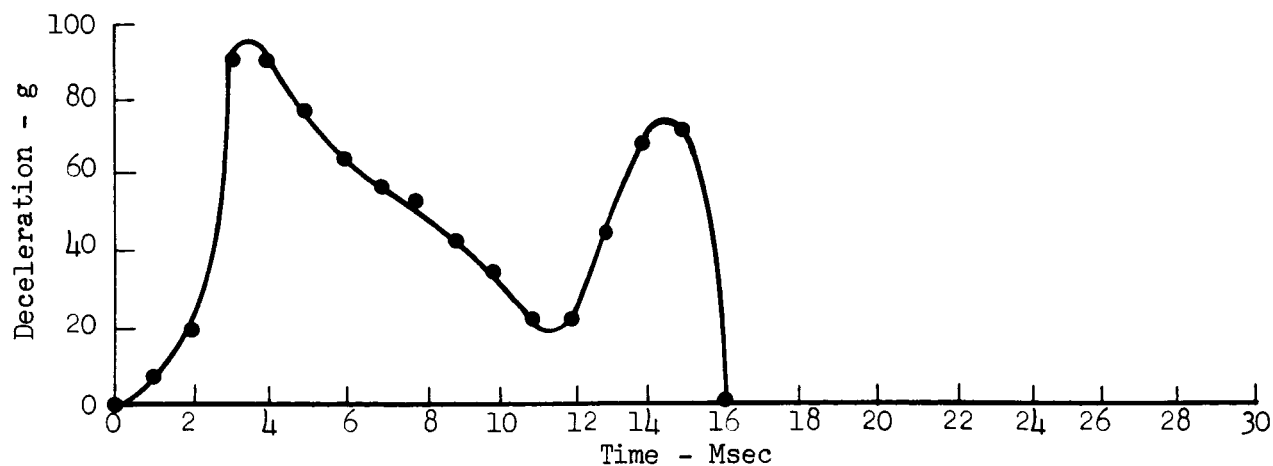
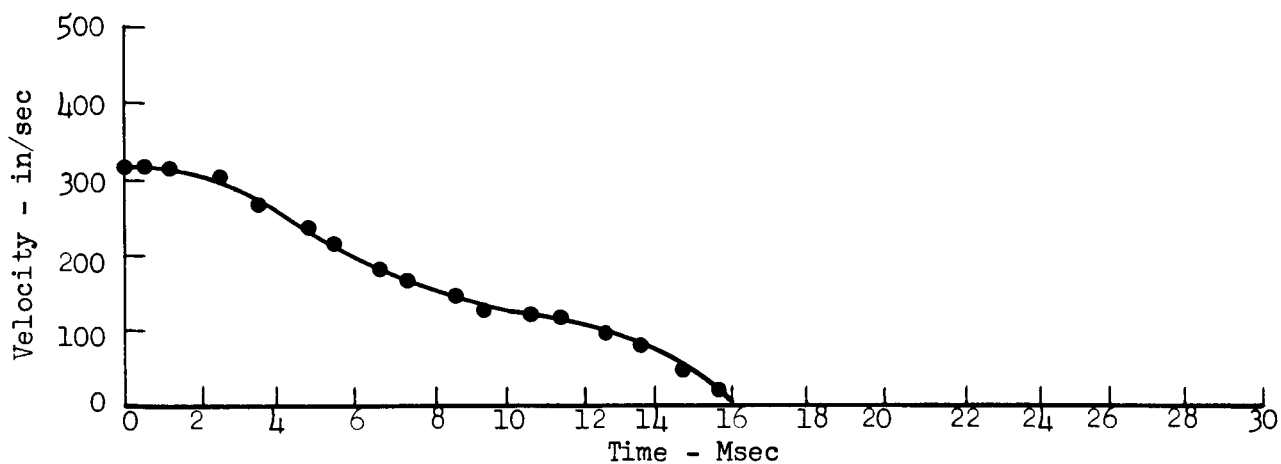
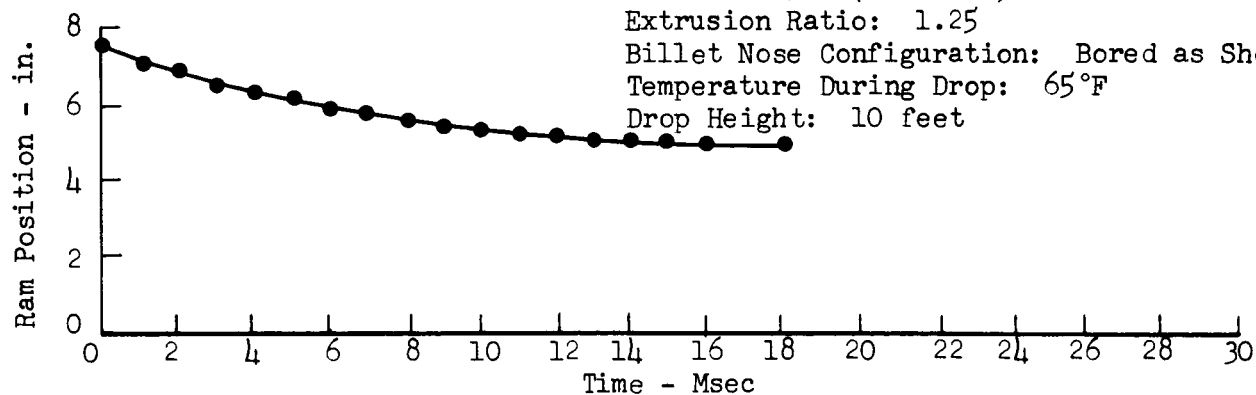
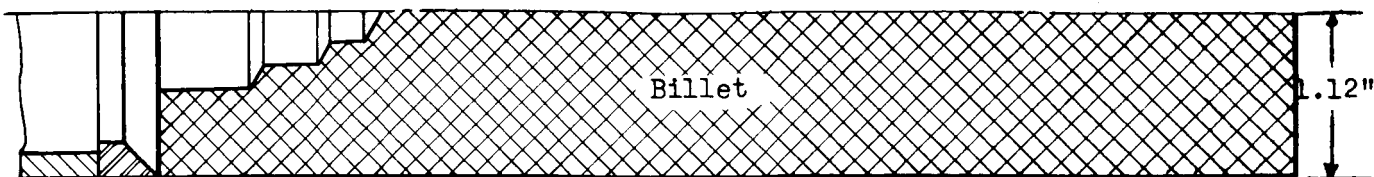


Figure 15

EFFECT OF BILLET NOSE CONFIGURATION ON DECELERATION: STRUT DESIGN NO. 1



Material Extruded: Lead  
 Orifice: 90° (included)  
 Extrusion Ratio: 1.25  
 Billet Nose Configuration: Bored as Shown  
 Temperature During Drop: 65°F  
 Drop Height: 15 feet

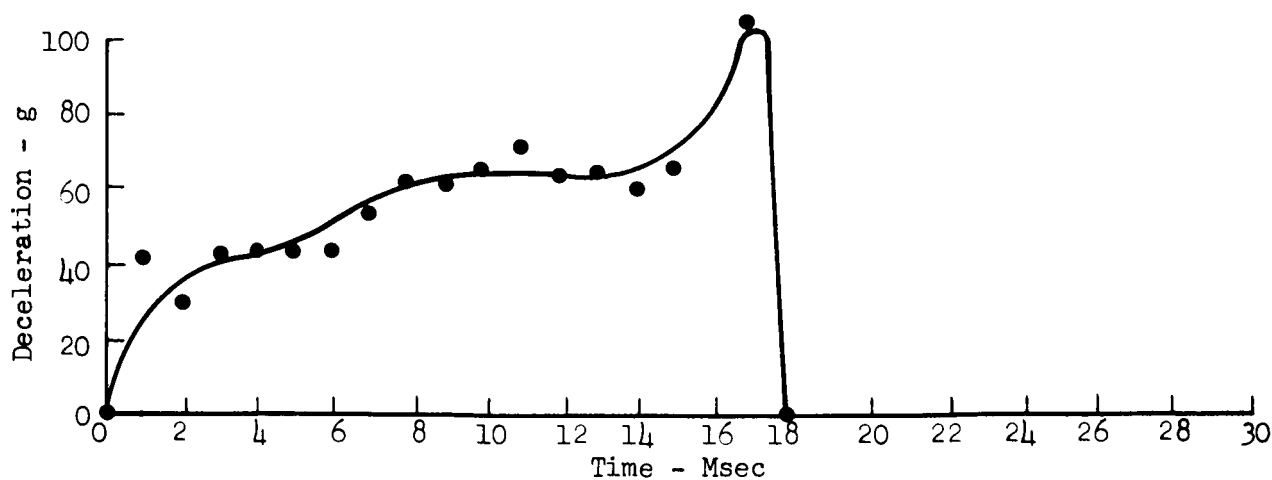
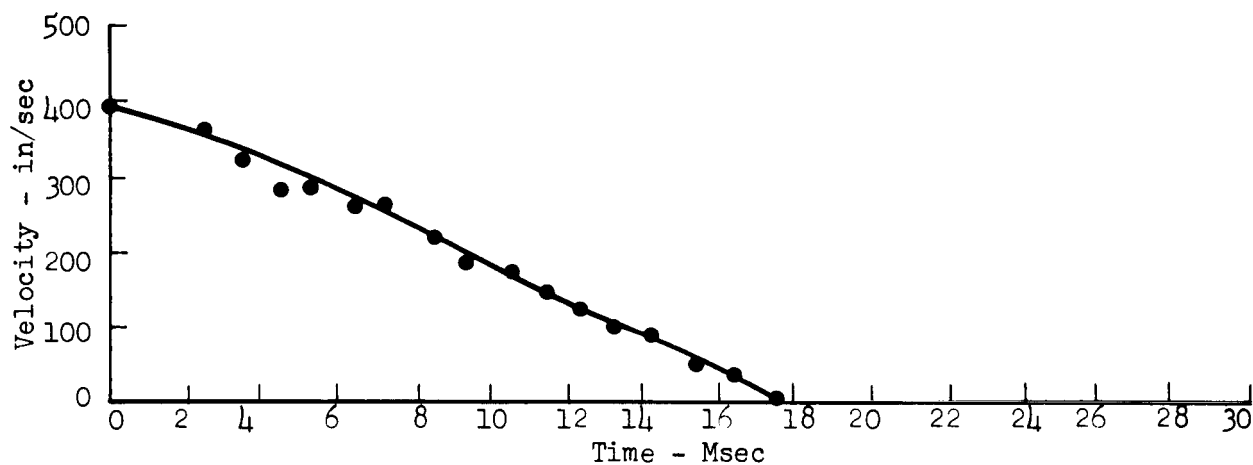
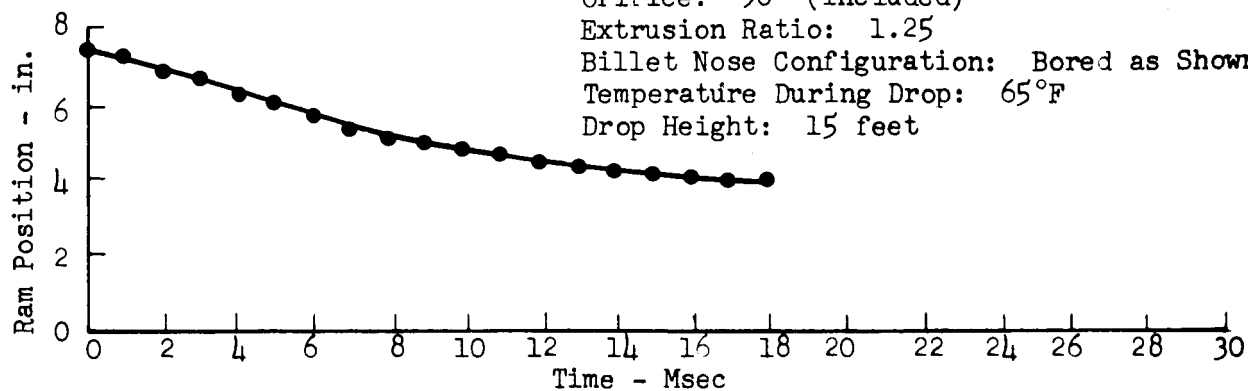


Figure 16

EFFECT OF BILLET NOSE CONFIGURATION ON DECELERATION: STRUT DESIGN NO. 1



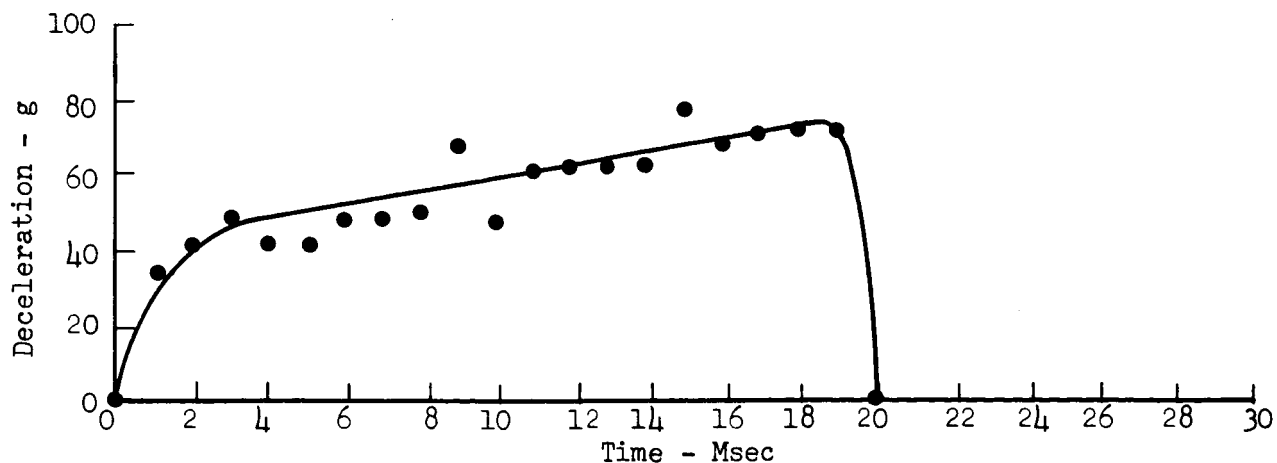
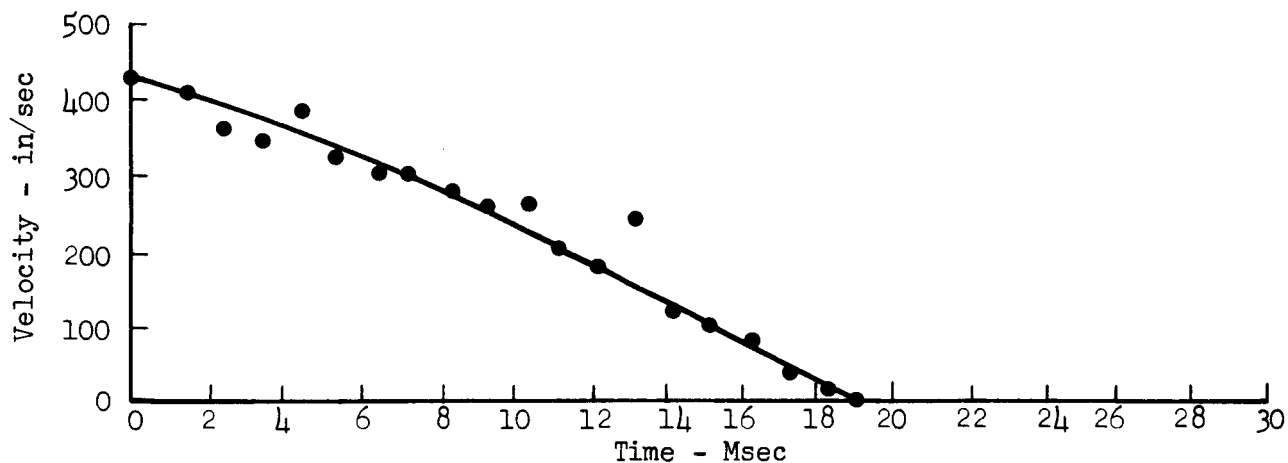
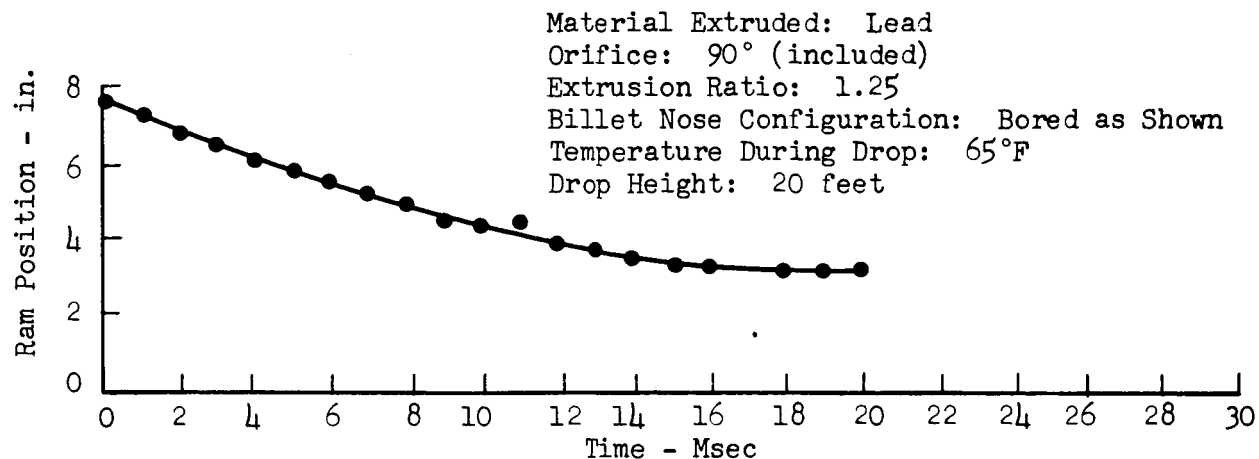


Figure 17

EFFECT OF BILLET NOSE CONFIGURATION ON DECELERATION: STRUT DESIGN NO. 1

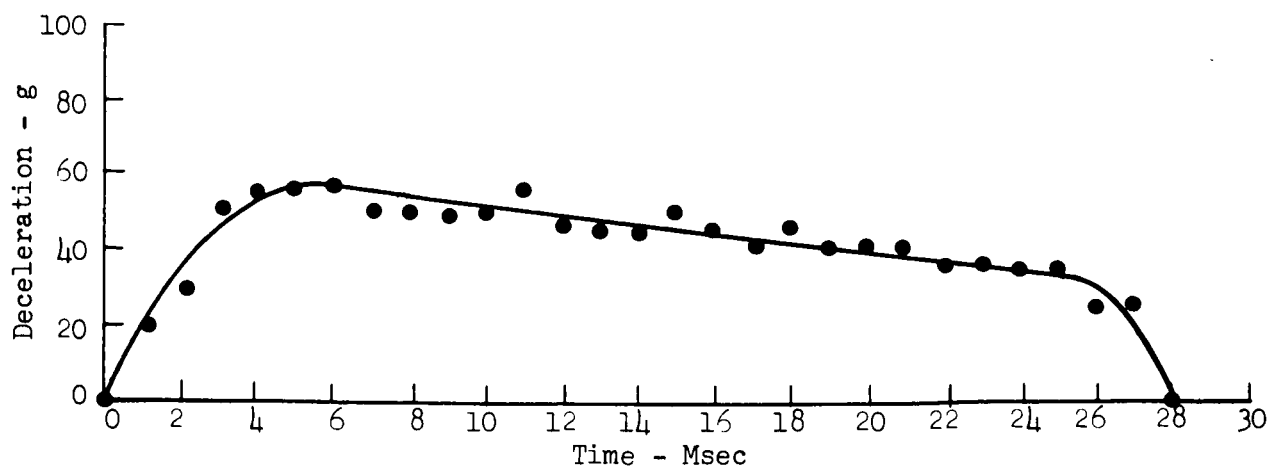
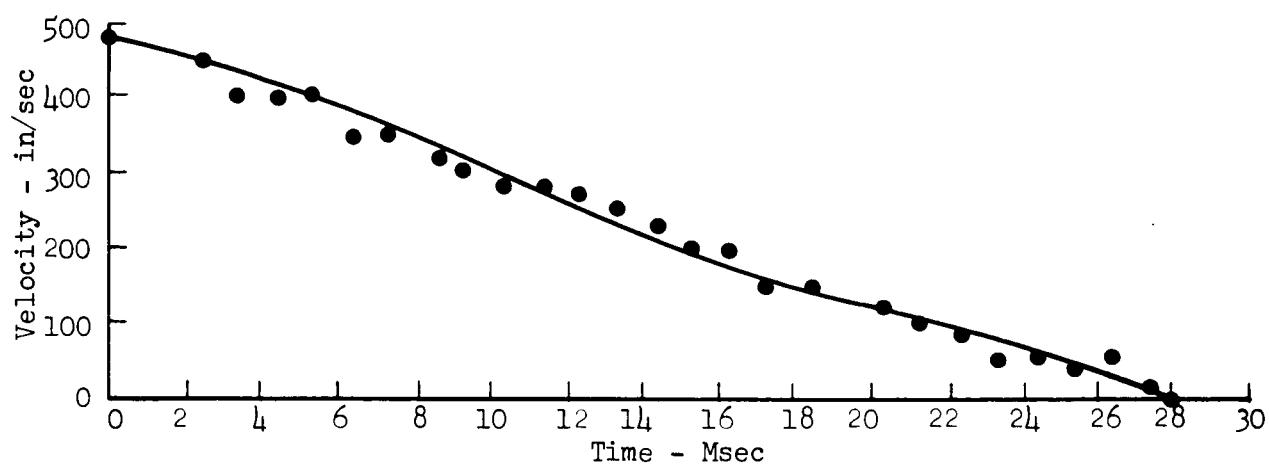
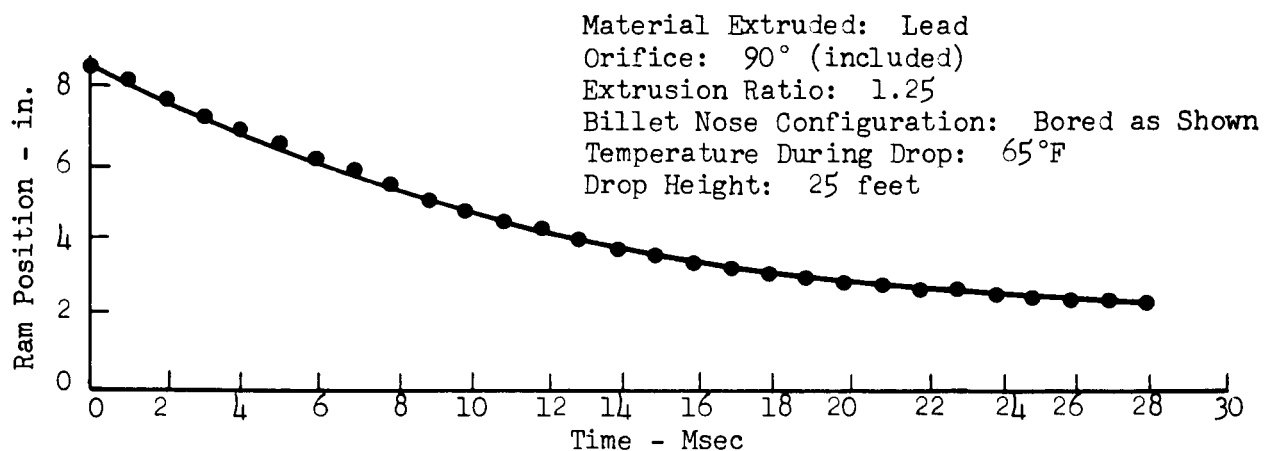
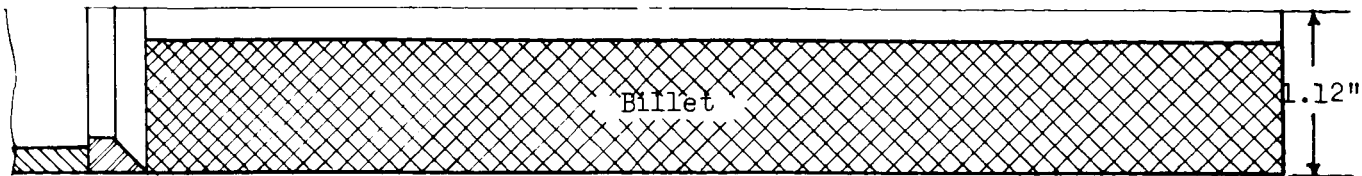


Figure 18

EFFECT OF BILLET NOSE CONFIGURATION ON DECELERATION: STRUT DESIGN NO. 1



Material Extruded: Lead  
 Orifice: 90° (included)  
 Extrusion Ratio: 1.25  
 Billet Nose Configuration: Bored as Shown and  
 Temperature During Drop: 65°F Drilled  
 Drop Height: 5 feet Through

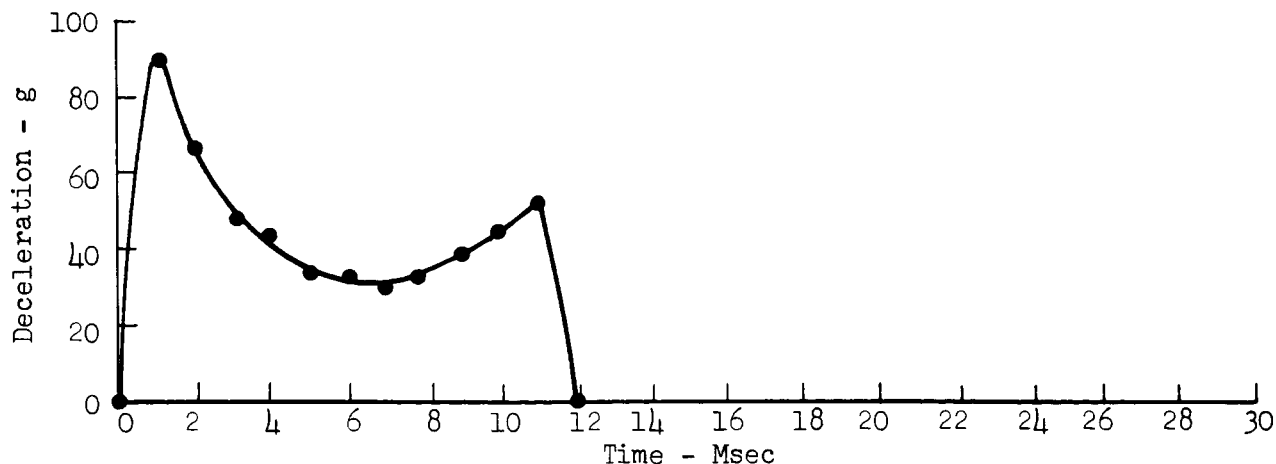
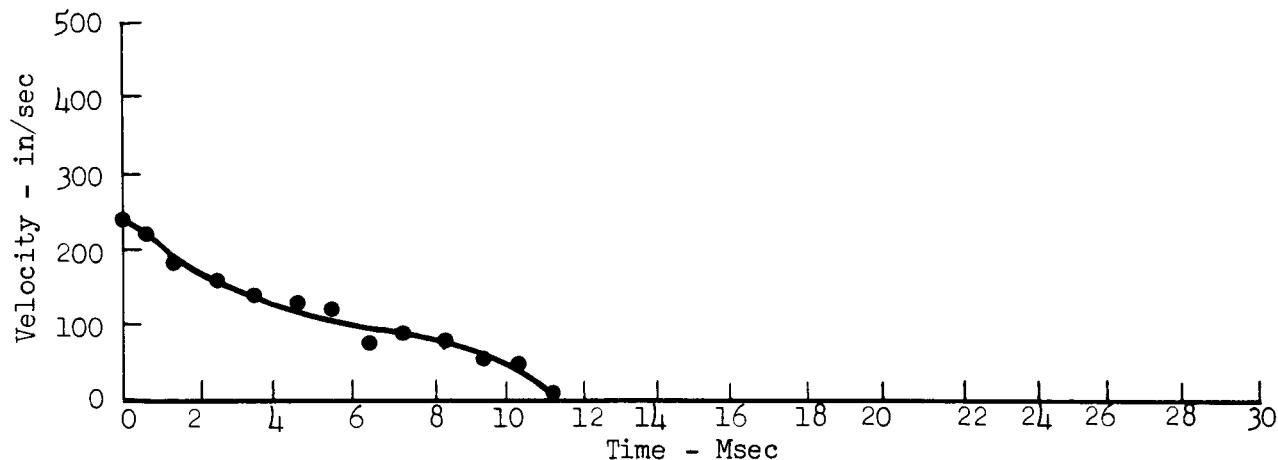
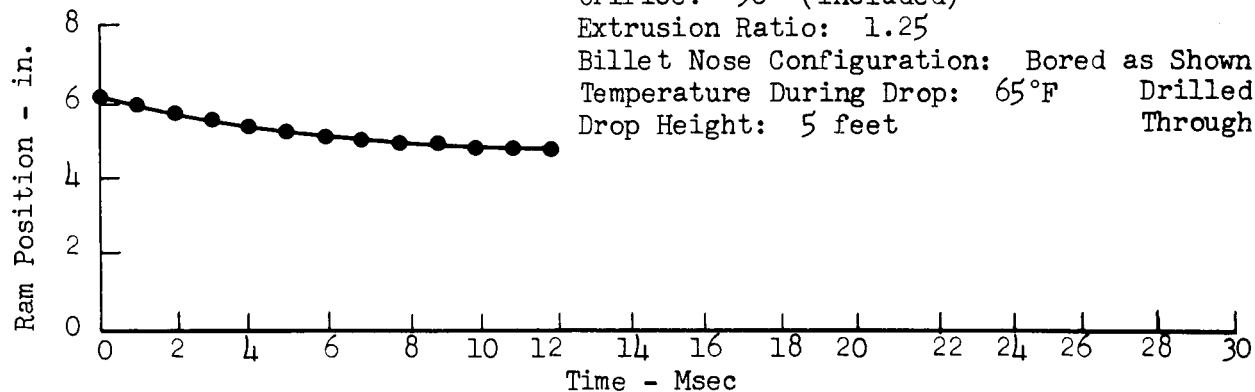


Figure 19

EFFECT OF BILLET NOSE CONFIGURATION ON DECELERATION: STRUT DESIGN NO. 1

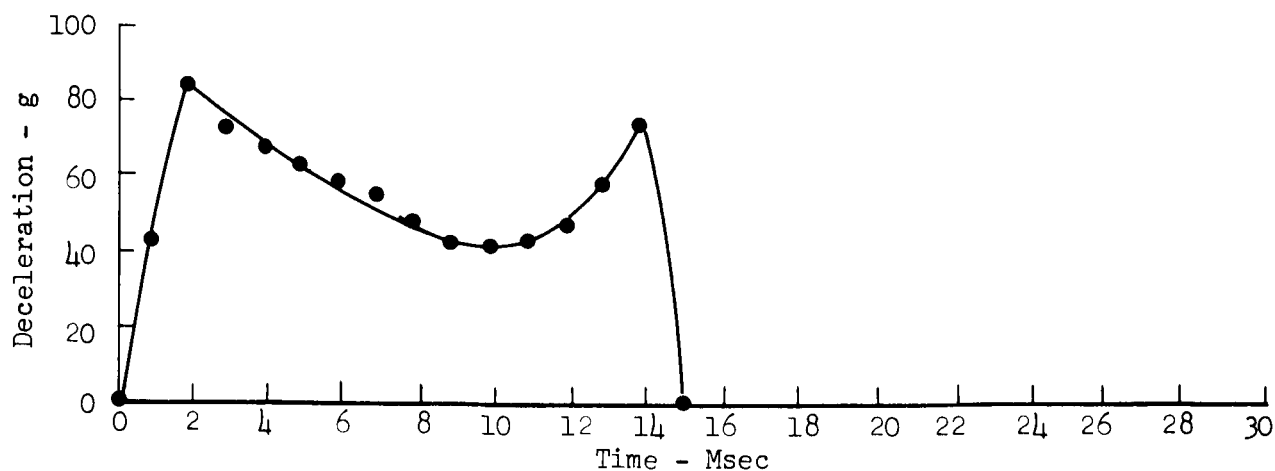
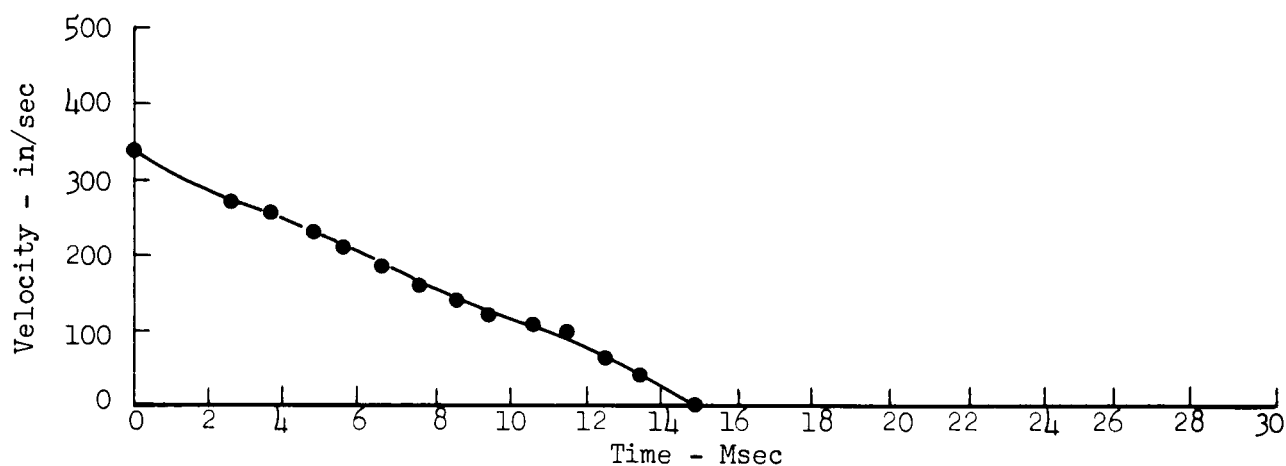
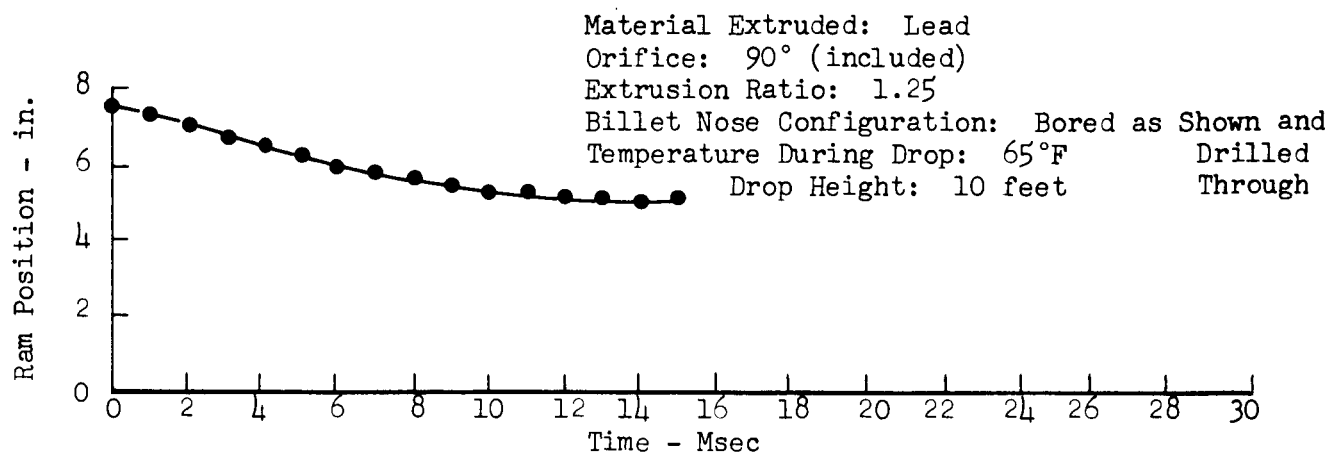
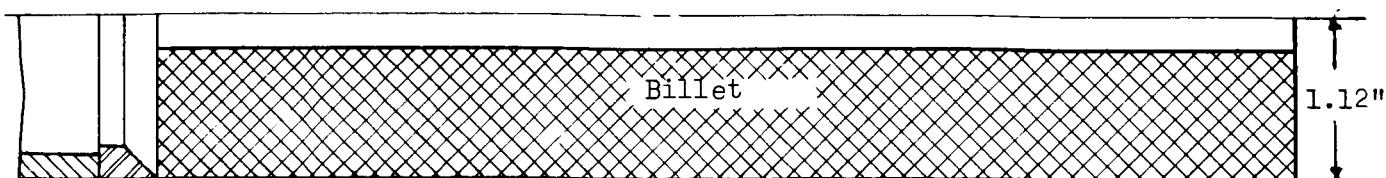


Figure 20

EFFECT OF BILLET NOSE CONFIGURATION ON DECELERATION: STRUT DESIGN NO. 1

## PRELIMINARY STRUT NO. 2

The second preliminary strut, assembled for the purpose of testing effects of billet length and diameter, was used to continue investigations in billet geometry and to initiate work with aluminum billets.

The 48-inch container permitted the billet to have a maximum length of 33 inches. The inside diameter of the billet container measured approximately 1.59 inches. With this smaller diameter, a die area ratio of 1.37:1 was obtained by holding the radial thickness at the orifice ring to a practical minimum.

### Billet Studies

For comparison with the data acquired during work with the first strut, two initial drop tests were conducted with solid lead billets. The results of these tests, made from heights of 5 feet and 10 feet, are shown in Figures 21 and 22. The initial deceleration peak was considerably reduced from that recorded for solid lead billets with the first strut (Figure 12), and a lowered mode is also evident. These results were attributed to the reduced billet diameter, since a smaller mass of lead had to be induced to flow through the orifice, with less absorption of energy. The altered die area ratio, which provided an actual area reduction of 0.70 square inches (compared to 1.17 square inches for the first strut), was also believed to contribute to the reduction of initial impact deceleration. A distribution of the lower deceleration level over longer time intervals was also characteristic of the curves in Figures 21 and 22. As in the case of some of the previous drops with the first strut, the curves exhibited high terminal peaks of deceleration.

In further studies of the onset deceleration spike, 11-inch billets of 1100-0 fully annealed aluminum were drilled in a manner similar to that used in earlier tests with lead billets. An attempt was made to proportion the size of the holes according to the ratio of the yield strengths of lead and aluminum. The first drilled hole in the billet end could not be made as large in diameter as was indicated by this yield strength ratio, since some metal was required for the thermocouple well for temperature measurement. The drilled pattern, as well as data from a typical 5-foot test drop, is shown in Figure 23.

This measurement indicated that decelerations in the range of 20 to 60 g's without an impact spike could be obtained with the open-nosed billets. The curve shows a smooth deceleration over the first 3 milliseconds, followed by a rapid rise; the smooth deceleration occurred during the passage through the

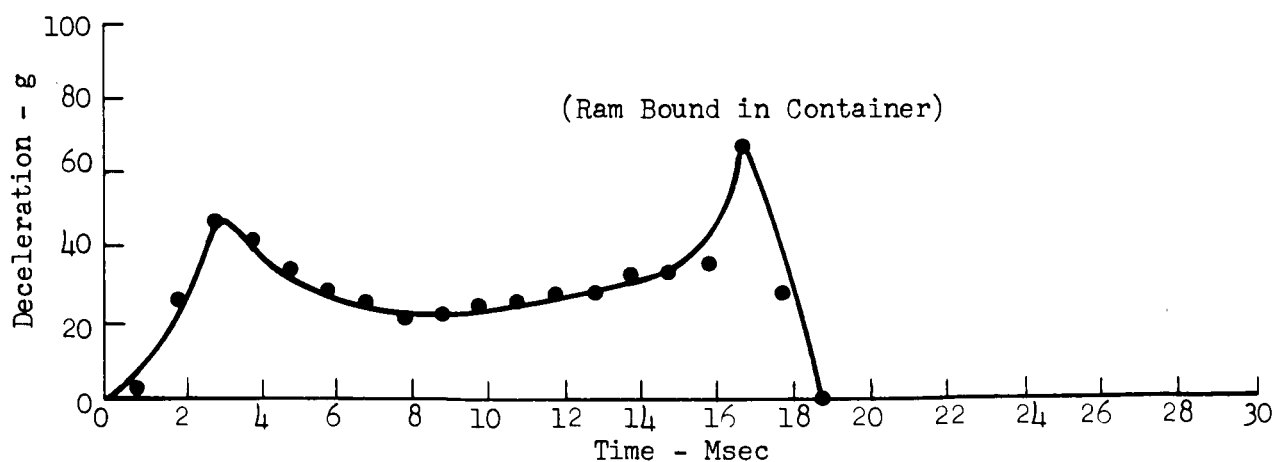
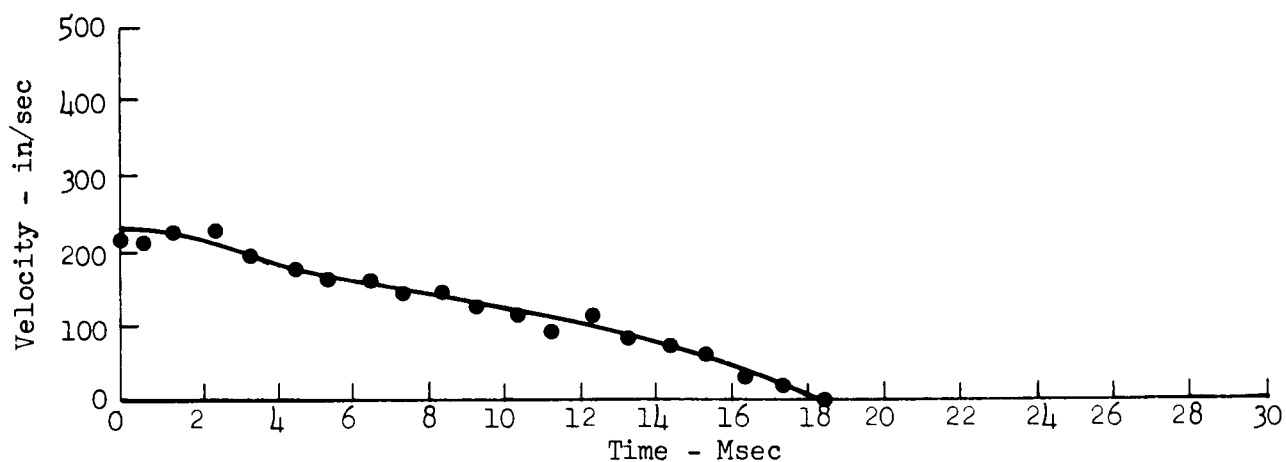
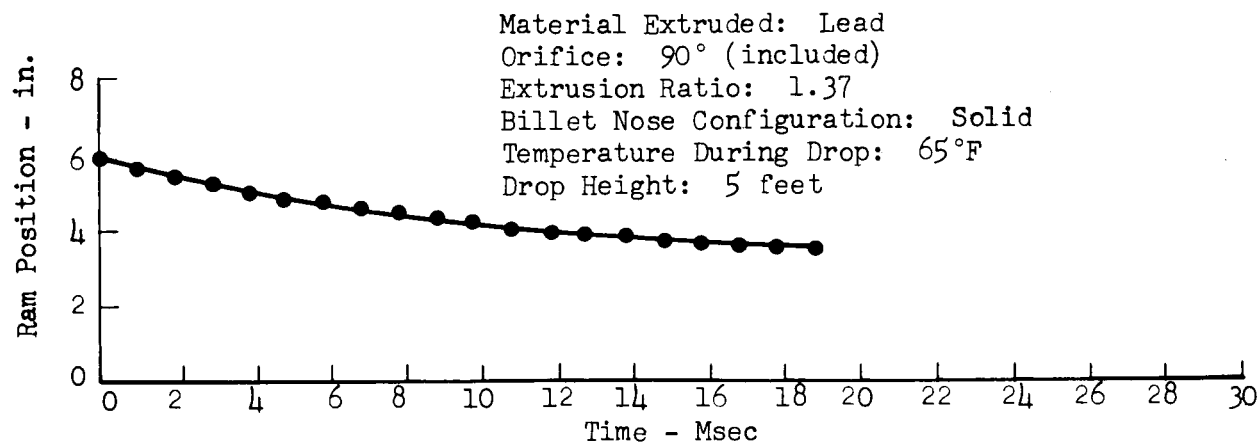
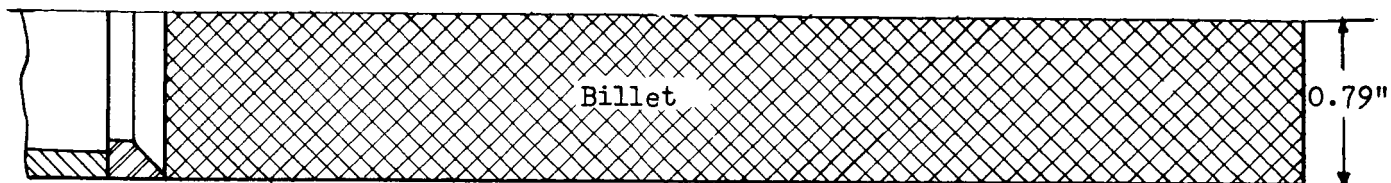


Figure 21

EFFECT OF BILLET NOSE CONFIGURATION ON DECELERATION: STRUT DESIGN NO. 2



Material Extruded: Lead  
 Orifice: 90° (included)  
 Extrusion Ratio: 1.37  
 Billet Nose Configuration: Solid  
 Temperature During Drop: 65°F  
 Drop Height: 10 feet

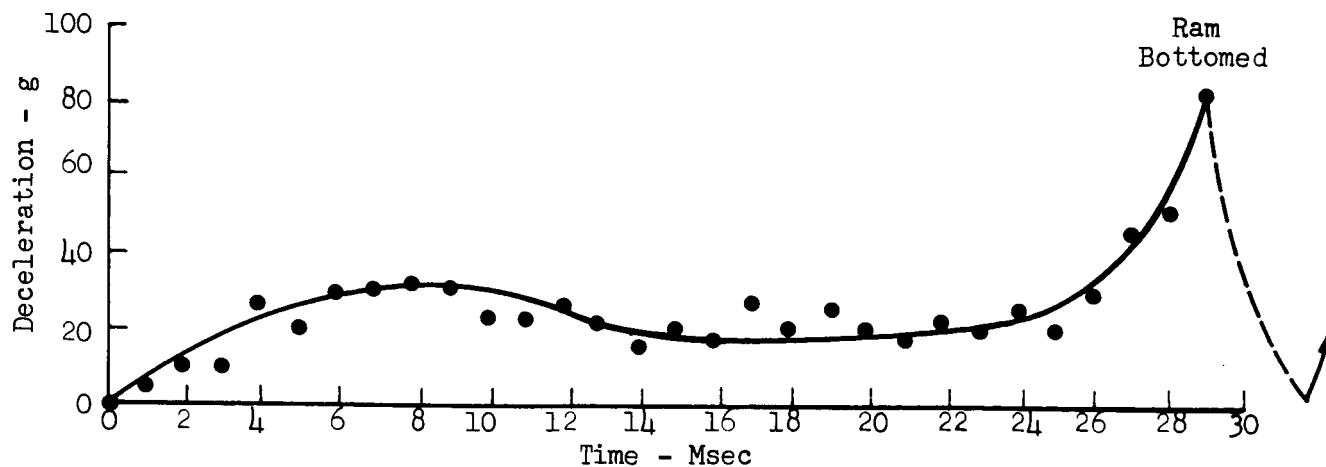
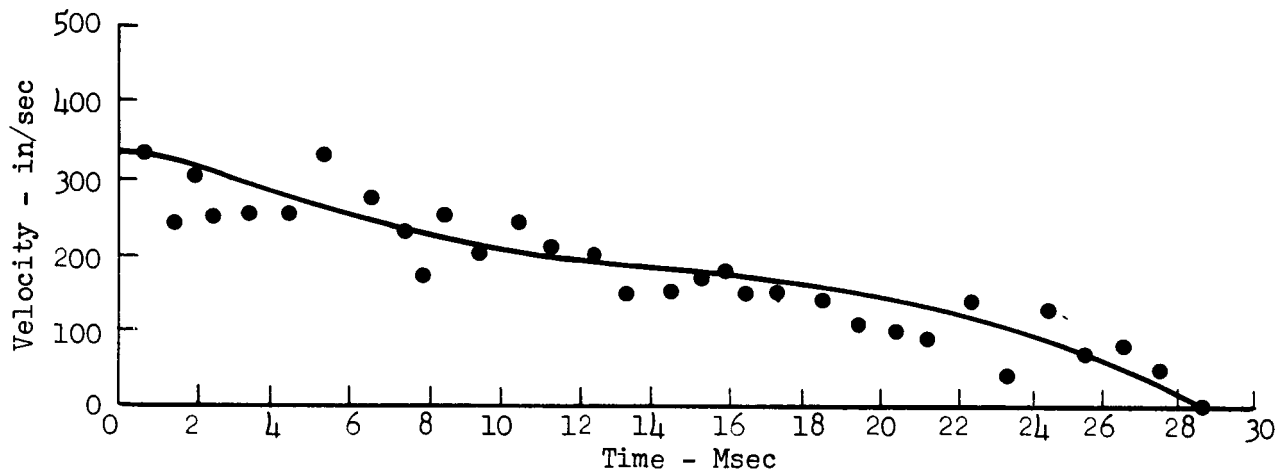
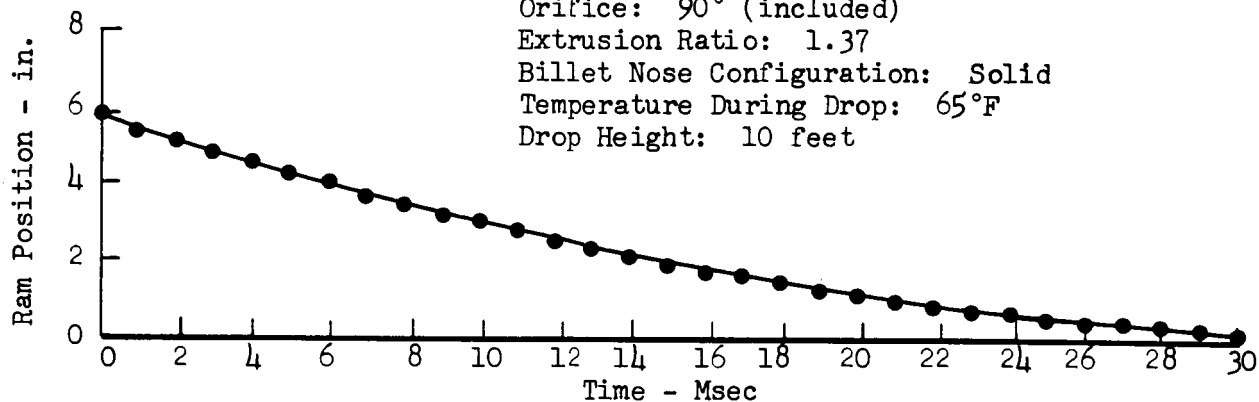
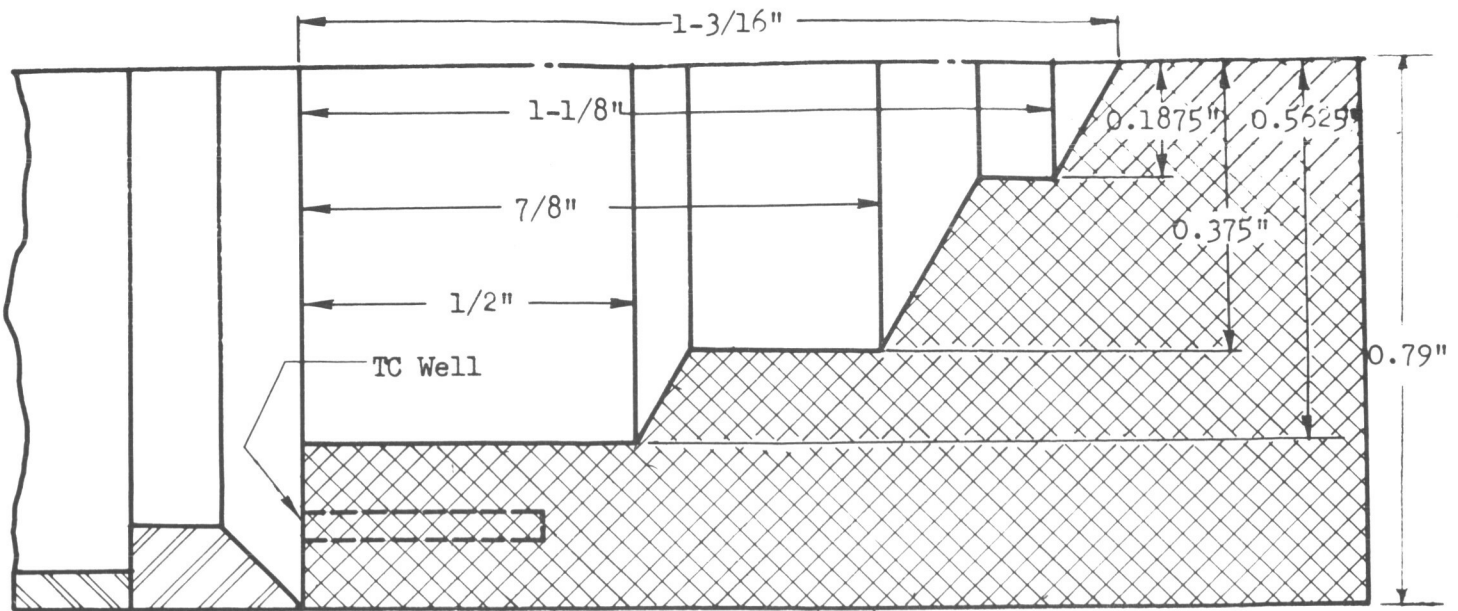
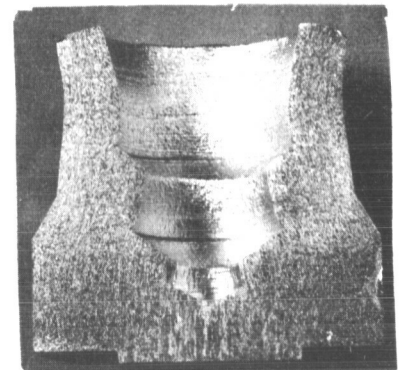
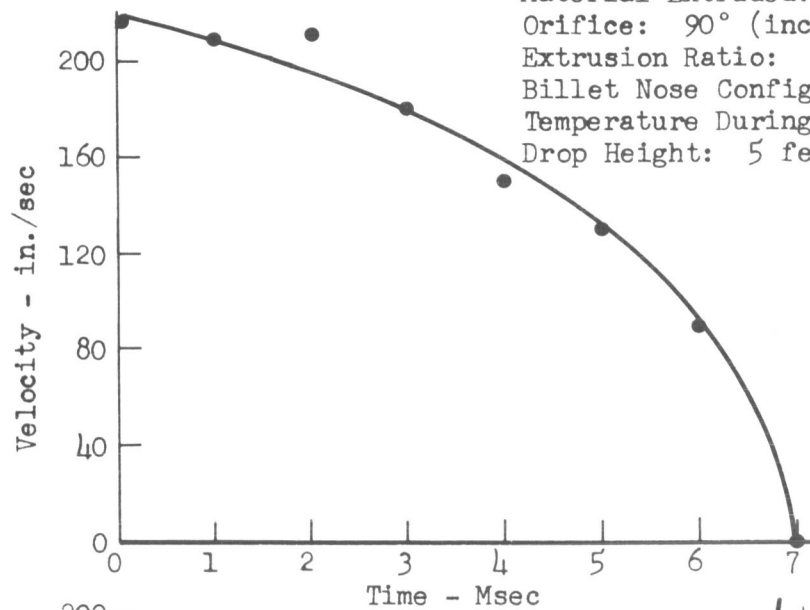


Figure 22

EFFECT OF BILLET NOSE CONFIGURATION ON DECELERATION: STRUT DESIGN NO. 2



Material Extruded: 1100-O Aluminum  
 Orifice:  $90^\circ$  (included)  
 Extrusion Ratio: 1.37  
 Billet Nose Configuration: Bored as Shown  
 Temperature During Drop:  $30^\circ\text{F}$   
 Drop Height: 5 feet



Cross Section of Extrudate

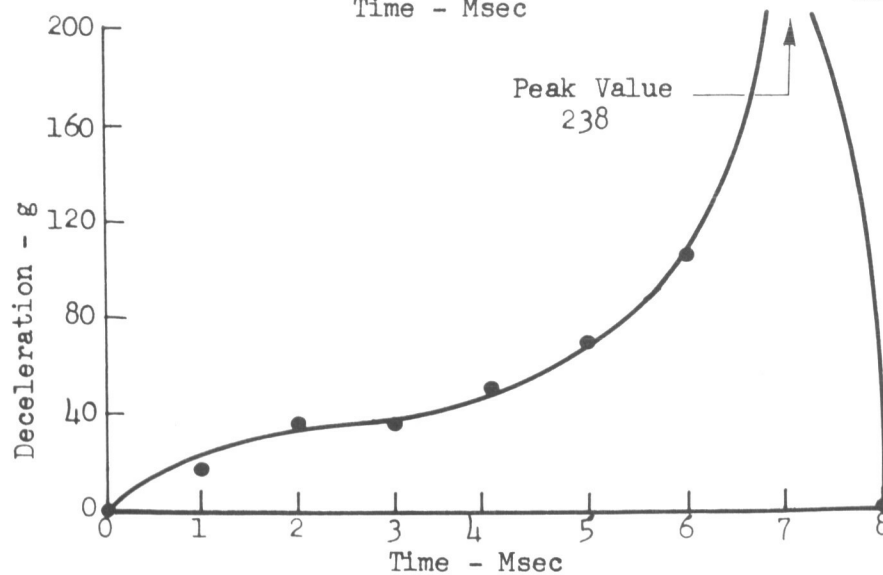


Figure 23

EFFECT OF BILLET NOSE CONFIGURATION ON DECELERATION: STRUT DESIGN NO. 2



the orifice ring of that part of the billet with the smallest annular area. The photograph in Figure 23, which shows the cross section of the extruded part of the billet after removal from the container, reveals the metal pileup which produced the high deceleration toward the end of the extrusion.

An attempt was made to ease this high deceleration by extending the large-diameter hole further into the billet, beyond the point of expected maximum ram travel. As evident in Figure 24, this produced uniform deceleration of 26 g's over most of the period. In this case, the rapid terminal increase could not be attributed to metal pileup due to change in hole size, as in the previous test. No bending or binding of the sliding parts of the apparatus occurred, as evidenced by the ease with which the ram and billet could be removed from the container.

An explanation offered for the terminal spike was that work hardening increased the yield strength of the metal during the latter portion of the extrusion. Microhardness measurements taken on the billets after their removal from the container showed a considerable hardness gradient along the length of the billet. The hardness was maximum in the extruded portion and diminished with increased distance from the orifice ring.

During the above, measurements were made of the temperature rise produced within the billets as a result of absorption of impact energy. The measurements were made with fine-wire thermocouples installed in radial holes drilled in the aluminum billets. Only negligible temperature rises were recorded at the start of extrusion where the greatest rise would be expected. Temperatures of about 40°F above ambient (30PF) were observed.

Additional measurements indicated the effect of billet preheating. These tests were made with annealed 1100-0 aluminum billets bored through-out with a 1-1/8-inch hole. Immediately before the drop, the billet temperature was raised to approximately 365°F by employing resistance heating tape around the billet container; this temperature was selected in order to reduce the ultimate tensile strength of the billet to approximately 50 percent of its original value at room temperature (13,000 psi). Hardness measurements on the Rockwell "H" scale were made before heating and again after dropping the heated billet. Typical results are presented in Figure 25.

#### Component Weight Studies

With the view to providing a shock strut assembly of minimum weight, consideration was given to the required container wall thickness and the required strut length.

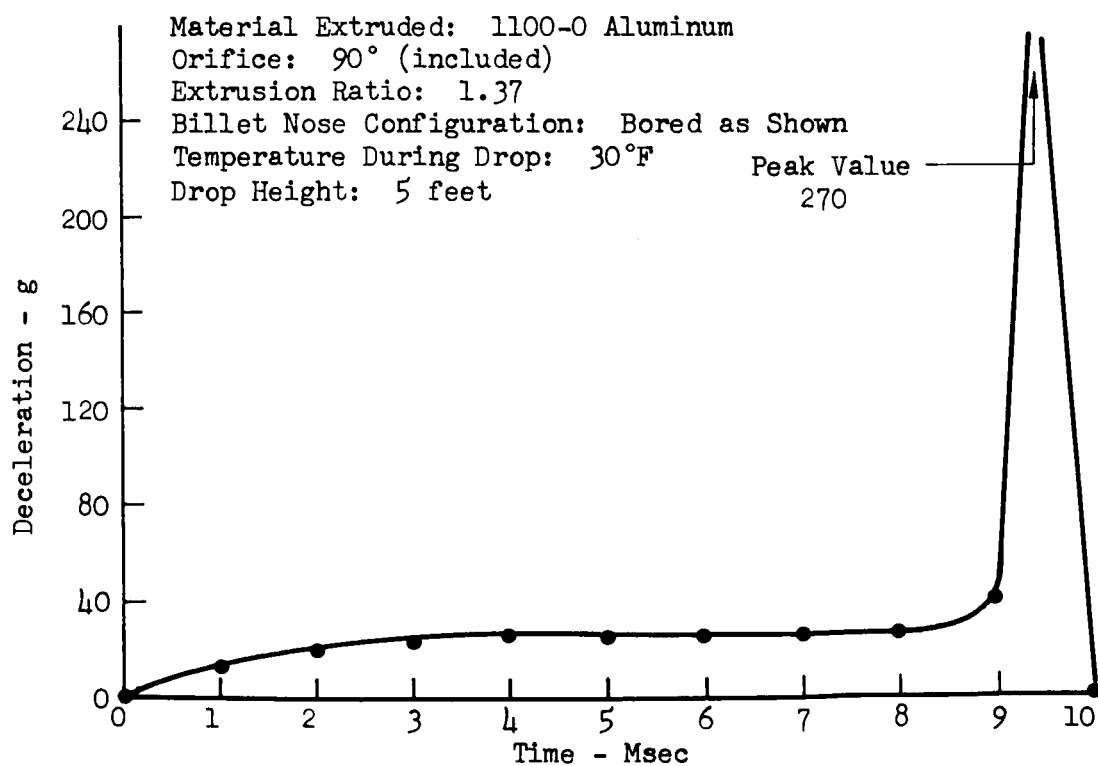
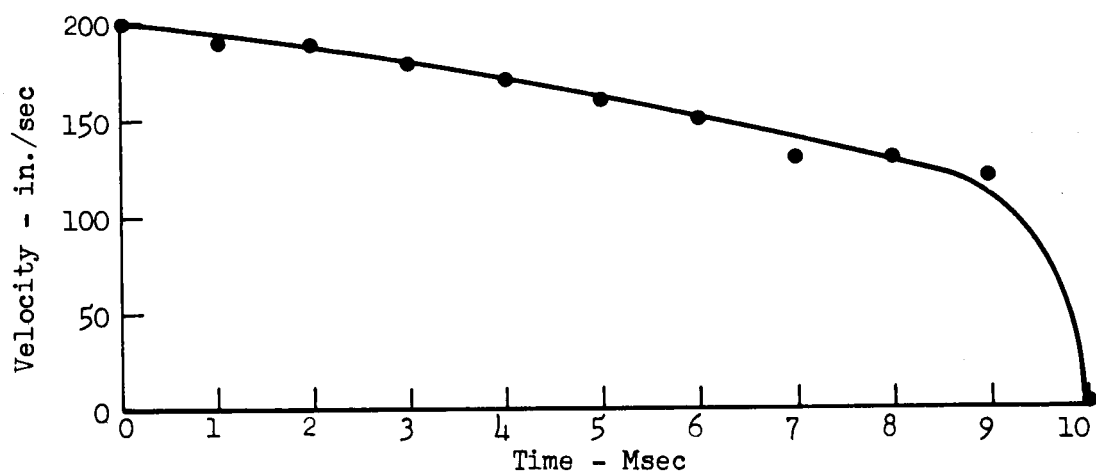
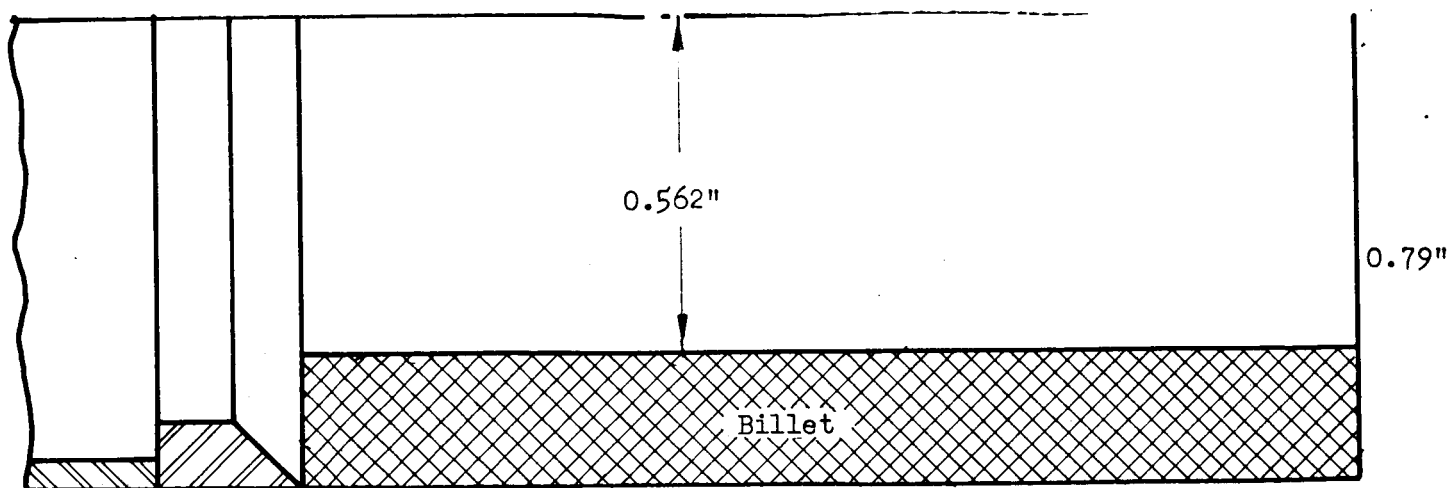
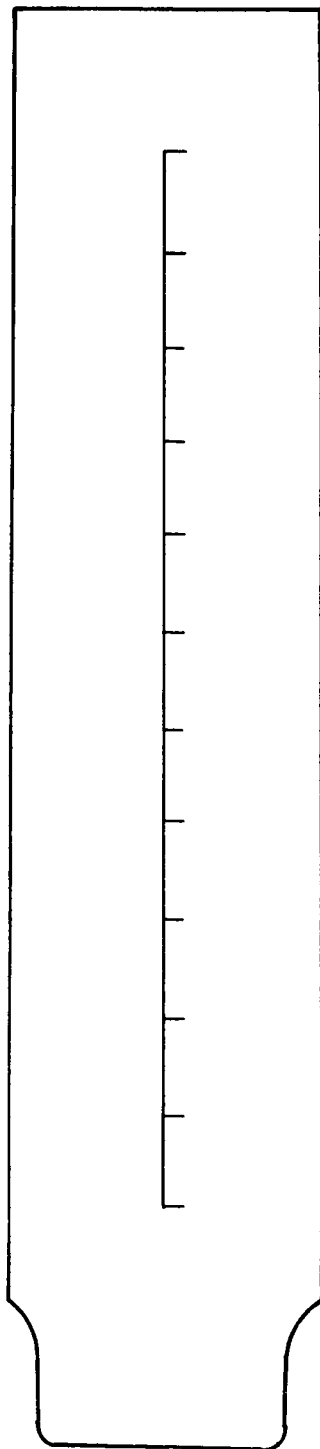


Figure 24

EFFECT OF BILLET NOSE CONFIGURATION ON DECELERATION: STRUT DESIGN NO. 2



Hardness - Rockwell "H" Scale

Billet: 1100-0 Aluminum  
 Outside Diameter: 1.6 inches  
 Through Hole: 1-1/8 inches  
 Temperature: 375°F

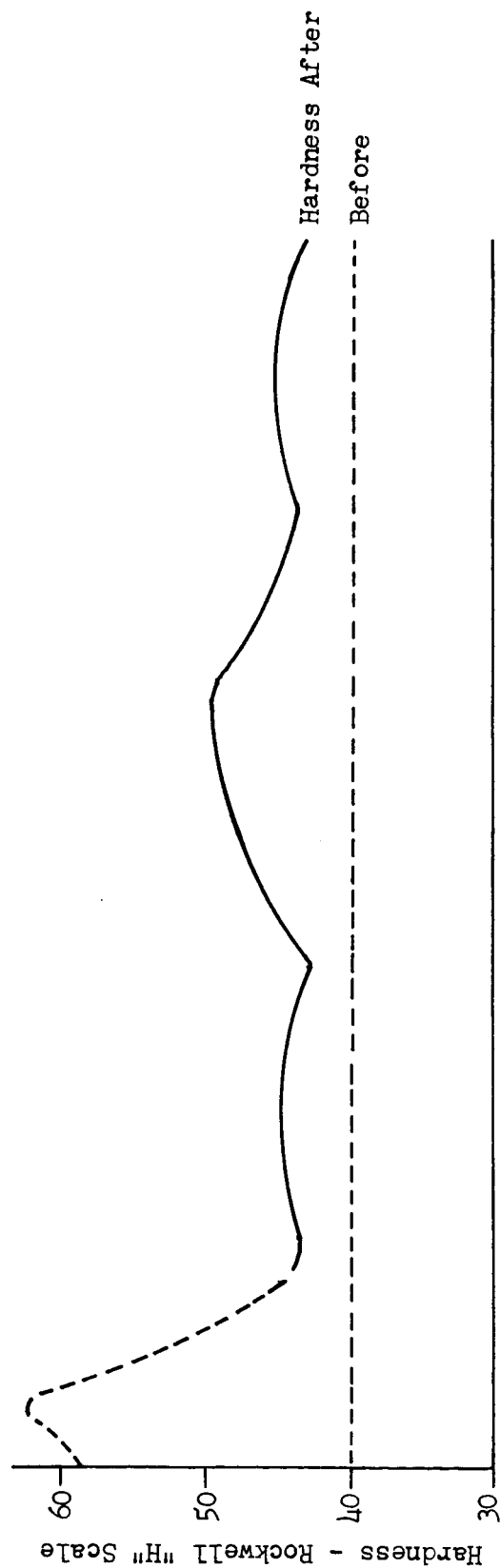


Figure 25:

WORK HARDENING OF ALUMINUM BILLETS, STRUT DESIGN NO. 2

The container walls of the second preliminary strut were approximately 15/32-inch thick. Hoop stress measurements made during drop tests using fully annealed aluminum 1100-0 as the billet material indicated peak stresses, for a 5-foot drop, of less than 300 psi.

The wall thickness of one container was reduced to 3/16 inch so that the stresses during aluminum extrusion would be increased to a realistic magnitude for comparison with the stresses that would be produced in the container by a fluid under pressure. The container was filled with oil (between two sections of a billet), and the weight was dropped a distance of 5 feet. Little energy was absorbed and the mass bounced, and a peak stress of 10,000 psi in the container wall was recorded. Stresses of 2500 to 3000 psi were recorded when the energy was absorbed (no bounce).

These observed low stresses indicated that with metal billets the container acts more as a guide for the ram than as a pressure-restraining member. A container of relatively thin-walled tubing with a similar telescoping used as the ram was thus indicated to be an effective low-weight energy absorber.

During the first few drops with the second strut, the length of the strut was also considered. Although the design included provision for 33 inches of billet, a ram travel of only 1-1/2 inches was observed for a 5-foot drop and 4-1/4 inches for a 20-foot drop. It was thus evident that the provision for ram travel could be greatly reduced in the final strut design, and that the length and weight of both container and ram could be reduced.

## CONCURRENT DEVELOPMENTS

### Billet Materials

Preliminary evaluation of candidate billet materials was conducted using lead billets with the first strut design and 1100-0 aluminum billets with the second design. The aluminum exhibited vastly superior energy absorption efficiency, which was computed according to the equation:

$$e = \frac{w s}{A_1 \rho \ell}, \quad (8)$$

where  $w$  is the weight of the load box,  $s$  is the height of the drop  $x \cos 5^\circ$ ,  $A_1$  is the billet cross-sectional area,  $\rho$  is the density of extrusion material and  $\ell$  is the distance of ram travel during deceleration. Here the volume of material utilized in the absorption process is defined as that volume of original billet that is displaced by the die (i.e., the cross-sectional area of the original billet times the distance traveled by the ram during extrusion).

For a solid lead billet with the first design shock strut (billet OD 2.24 inches, load weight 3 pounds), the ram travel for a 5-foot drop was 2.50 inches. This is equivalent to an absorption efficiency of 764 foot-pounds per pound. By contrast, the aluminum billet using the second design for the same drop height (billet OD 1.59 inches, load weight 270 pounds) resulted in ram travel of 1.875 inches, or an absorption efficiency of 7500 foot-pounds per pound. This pronounced effect of material on efficiency was confirmed by additional preliminary tests.

In addition to its relative superiority in absorption efficiency, aluminum has general advantages in machinability, cost, and other factors.

### Verification of Energy Balance

Verification of the validity of an observed deceleration profile in the above tests was made by comparing the energy absorbed (measured area under the deceleration curve) with the energy represented by the free-fall terminal velocity (in which frictional losses were disregarded). This comparison showed generally good agreement between the observed and the theoretical values of energy absorption.

### SUMMARY

Tests with the two preliminary struts established that the deceleration profile of an energy-absorbing event could be controlled by appropriate design of the orifice and the billet cross section. Initial work with bored-nose and drilled-through billets suggested the feasibility of a shock strut capable of producing the ideal deceleration profile.

The developmental data provided the basis for the design of an extrusion energy-absorbing system offering effectiveness in meeting a variety of end-use requirements. Specific design features determined from these data are summarized below.

Orifice Ring Entry Angle. - On the basis of the deceleration profile developed and the structural requirements for orifice rings during multiple use, a 90-degree included angle was chosen. A 60-degree angle was considered suitable for single-use situations where distortion of the ring would be inconsequential, or in cases where longer orifice ring throat depth might be used.

Billet Material. - Of the materials investigated, annealed 1100-O aluminum was the preferred billet material on the basis of absorption efficiency and general workability.

Billet Cross Section. - Tests enabled speculation that a cylindrical billet with an axial central hole extending through the entire length would be the most effective billet shape, with control of peak and mean deceleration levels being obtainable by selection of the hole diameter. Additional control of the deceleration profile was deemed possible by varying the hole diameter along the length of the billet.

Billet Length (Ram Travel). - In all cases observed, the ram travel fell within the range of from 2 to 4 inches, and the billet length can be adjusted accordingly.

Container Wall Thickness. - Steel tubing with wall thickness in the range of 0.20 to 0.25 inch was selected through observation of stresses developed during impact. Theoretically this thickness could be reduced to the order of 0.06 inch and still carry the stresses developed in the wall, but for experimental purposes a safety factor was provided.

## EXPERIMENTAL INVESTIGATION

The third shock strut design (Tables I and II) was based on information developed from measurements with the preliminary struts. Consideration of such design parameters as billet geometry, metallurgical properties of billets, and die area ratio were undertaken, as well as studies of the effects of load weight, drop height, impact angle, and soft contact surface.

The experiments performed with this strut are described in a sequence which illustrates the overall performance of the system. Tables V through VII record the drop conditions and evaluation data for these experiments.

### Evaluation Methods

As previously described, the performance of the shock strut was evaluated by two use criteria: deceleration profile and energy absorption efficiency. Data for all the experiments with this strut were obtained by use of the "Piezotron" accelerometer, and energy balance was verified in a manner analogous to that developed for the graphically derived data.

In tests with aluminum billets bored with a 5/8-inch central hole, typical terminal velocities obtained from integrated areas under the deceleration oscillogram were compared with theoretical free-fall terminal velocities. The areas under the oscillogram curve were determined with a planimeter. The data are tabulated in Table VIII.

The generally favorable correspondence between theoretical and planimetrically determined terminal velocities confirmed the validity of the accelerometer readings. Differences between these values are attributable to frictional effects in the drop system and to reading errors.

Comparison of the deceleration curves determined by the accelerometer and by graphical means, shown in Figure 26, indicates certain similarities and certain differences. For example, the duration of the energy absorption process is essentially the same for both the graphically and the accelerometrically determined curves. The average magnitudes of the deceleration are similar, but the impact sections of the curves differ. The record of the accelerometer shows that the true peak deceleration leads the graphically determined value due to the instantaneous response of the accelerometer. Figure 27 shows the graphically-determined curve for a 5-foot drop superimposed on the accelerometric curve.

Superimposed high-frequency vibrations evident on the oscillogram during the entire deceleration event are probably the result of Chladni-type ringing of drop system components; the frequency of these vibrations was approximately 2500 cps.

Table V

## DROPS USING DIE AREA RATIO OF 1.50:1

Material: 1100-O Aluminum

Test No.	Billet ID (in.)	Billet Area (in. <sup>2</sup> )	Drop Height (ft)	Impact Energy (ft-lb)	Length Extruded (in.)	Energy Absorption (ft-lb/lb)	Mode Deceleration (g)	Comments
97	Solid	1.00	5	1350	0.813	18,000	65	
99	Solid	1.00	5	1350	0.719	20,370	60	
102	Solid	1.00	10	2700	1.247	23,400	60	
103	Solid	1.00	10	2700	1.408	20,800	65	
93	0.6250	0.688	5	1350	0.906	19,150	55	
110	0.6250	0.688	5	1350	1.00	21,000	50	
94	0.6250	0.688	10	2700	1.3125	32,100	75	
111	0.6250	0.688	10	2700	1.683	25,000	65	
138	0.6250	0.690	10	2700	1.603	24,400	65	
96	0.6250	0.688	15	4050	1.906	33,200	65	
113	0.6250	0.688	15	4050	2.1875	28,000	65	
114	0.6250	0.688	17.5	4725	2.5625	28,700	65	
115	0.6250	0.688	20	5400	2.531	33,300	65	
116	0.6250	0.688	20	5400	2.781	29,500	65	
118	0.6250	0.688	22.5	6075	2.9675	33,000	65	
119	0.6250	0.688	25	6850	3.1875	31,400	65	
120	0.750	0.588	55	1350	1.4375	18,000	65	
130	0.760	0.588	10	2700	1.876	23,500	65	
								Insert of 0.060-inch wall titanium tubing.
121	0.750	0.588	10	2700	1.876	27,400	70	
131	0.750	0.588	15	4050	2.75	28,600	60	
125	0.8750	0.398	20	5400	3.125	31,200		
129	0.8750	0.398	5	1350	1.969	18,600		
134	0.880	0.390	10	2700	2.813	26,000	50	Onset rate 3500 g's
137	1.00	0.215	15	4050	3.00	32,400	25	
155	Solid	1.00	10	2700	5.374	28,800		
			15	5250*	2.50	27,600		Drop weight of 350 lb.



Table VI  
DROPS USING DIE AREA RATIO OF 1.23:1  
Material: 1100-O Aluminum

Test No.	Billet ID (in.)	Billet Area (in. <sup>2</sup> )	Drop Height (ft)	Impact Energy (ft-lb)	Length Extruded (in.)	Energy Absorption (ft-lb/lb)	Mode Deceleration (g)
81	Solid	1.00	5	1350	0.968	14,280	30
82	Solid	1.00	5	1350			30
83	Solid	1.00	5	1350			50
84	Solid	1.00	10	2700	1.468	18,800	
95	0.6250	0.688	10	2700	1.437	21,850	
96	0.6250	0.688	15	4050	1.906	27,800	
140	0.750	0.588	10	2700	1.938	25,700	
133	0.8750	0.398	10	2700	2.328	30,900	54
139	1.00	0.215	5	1350	3.875	16,000	

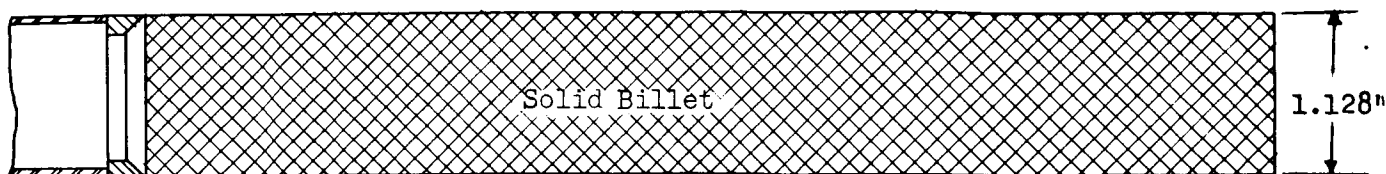
Table VII

## DROPS WITH 6061-T6 ALUMINUM ALLOY HOLLOW BILLETS

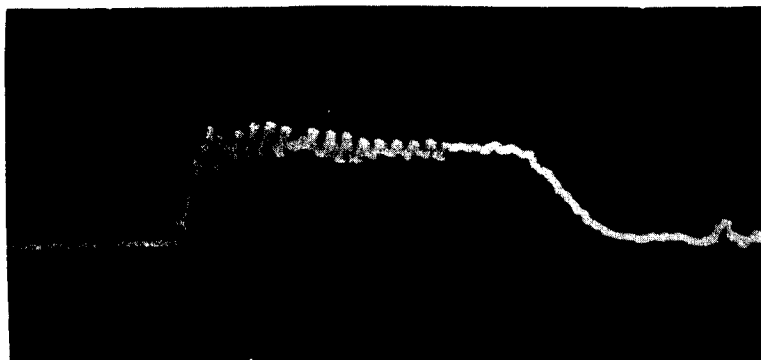
Test No.	Ratio	Billet ID (in.)	Billet Area (in. <sup>2</sup> )	Drop Height (ft)	Impact Energy (ft-lb)	Length Extruded (in.)	Energy Absorption (ft-lb/lb)	Mode Deceleration (g)	Comments
150	1.23:1	1.009	0.200	10	2700	3.4375	39,900	30	
152	1.23:1	1.009	0.200	15	4050	4.50	45,750	30	
157	1.23:1	1.009	0.200	5	1350	3.50	19,750		Solution treated
151	1.50:1	1.009	0.200	10	2700	2.0	68,000	58	
153	1.50:1	1.009	0.200	15	4050	2.375	86,750	61	
154		0.750		10	2700	0.8125	17,050	102	Compound billet. Heat-treated to Rockwell (T15) 58, 76, 81.
158	1.50:1	1.009	0.200	10	2700	2.850	48,300	37	Solution treated.
163	1.50:1	1.009	0.200	10	4450	3.25	70,250	39.5	

Table VIII  
ACCELEROMETER DATA VERIFICATION

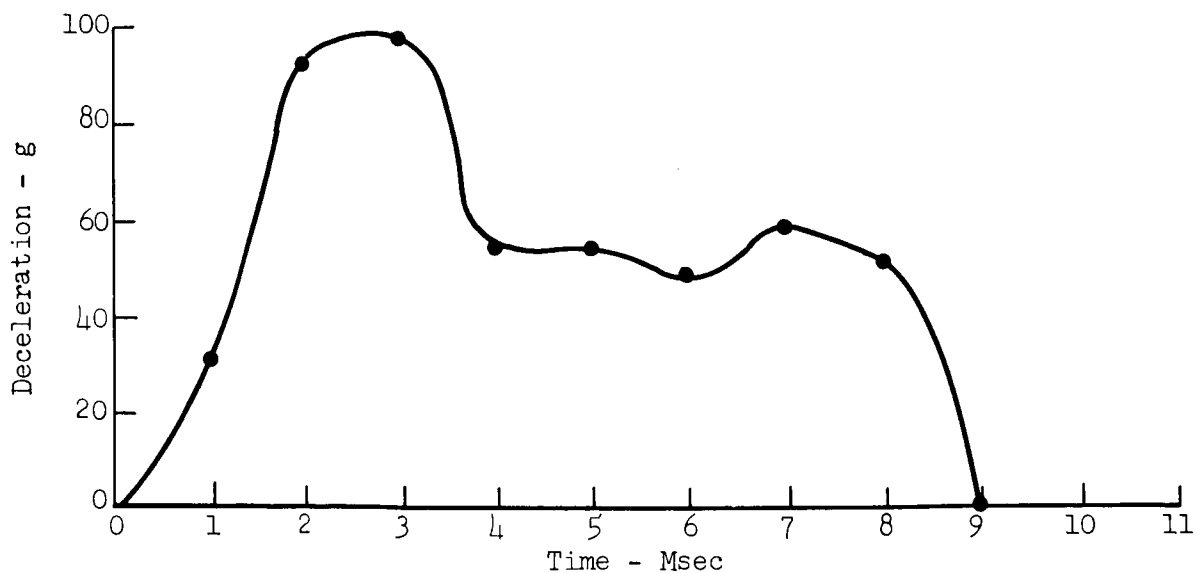
Drop No.	Drop Height (ft)	Terminal Velocity (ft/sec) Determined from	
		Area Under Oscillogram	Theoretical Free-Fall
120	5	18.2	17.9
138	10	23.8	25.4
114	17.5	30.2	33.6
116	20	31.15	35.9
119	25	35.1	40.2



Material Extruded: 1100-0 Aluminum  
 Orifice: 90° (included)  
 Extrusion Ratio: 1.50  
 Billet Nose Configuration: Solid  
 Temperature During Drop: 76°F  
 Drop Height: 5 feet



A. Accelerometric Curve



B. Graphically Derived Curve

Figure 26

DECELERATION PROFILES: COMPARISON OF ACQUISITION METHODS, STRUT DESIGN NO. 3

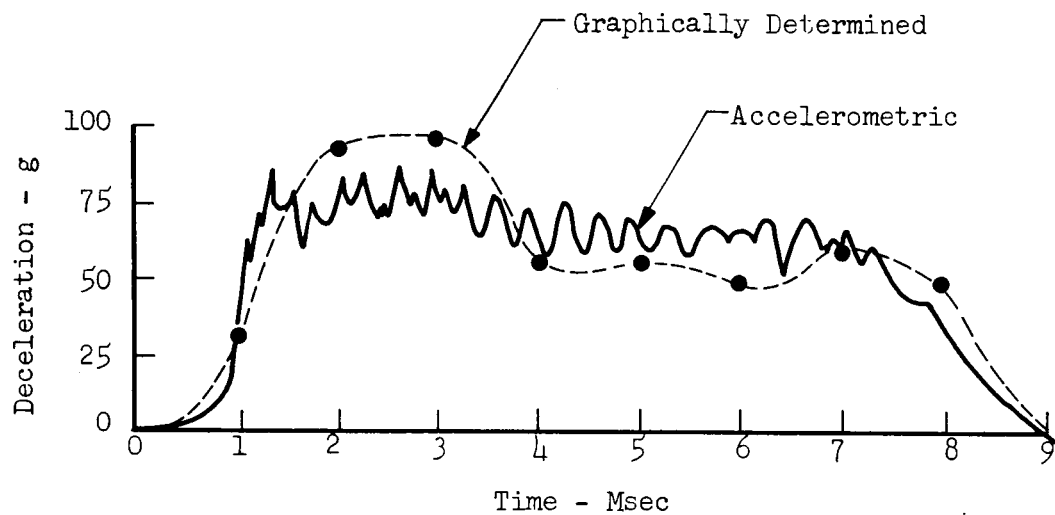


Figure 27

GRAPHICALLY DETERMINED CURVE SUPERIMPOSED ON  
ACCELEROMETRIC CURVE: STRUT DESIGN NO. 3

In certain of the profiles, a curve reversal effect was noted near onset; this is probably attributable to flexure of the base plate to which the accelerometer was attached. This anomaly is evident particularly in the case of low-energy drops where the restoring force of the base plate and of components mechanically connected to the base plate may be sufficient to cause the accelerometer to sense a reversal of the direction of motion.

Evaluation in terms of energy absorption efficiency was by calculation from impact energy and weight of extruded material for each drop, in the manner described in the Introduction.

### Investigation of Design Effects

The performance characteristics of greatest significance were found to be influenced largely by the design of the billet and die.

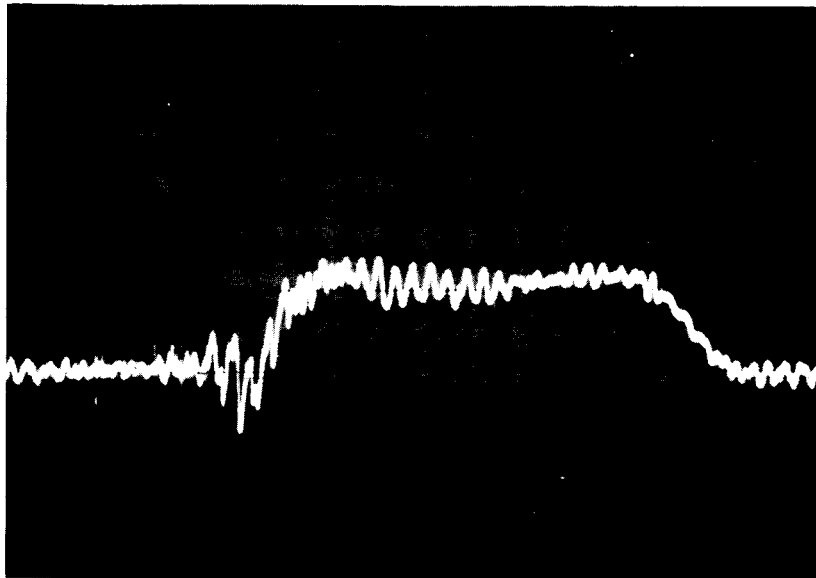
Billet Cross Section. - Using 1100-0 annealed aluminum billets and a die area ratio of 1.50:1, a series of drops was made to establish the effects of billet cross section on deceleration profile and energy absorption efficiency. Experiments were performed with solid circular billets and with four annular billet shapes, having respective inner diameters of 5/8 inch, 3/4 inch, 7/8 inch, and 1 inch.

Deceleration profiles and energy absorption values for 10-foot drops with the solid billet, the billet of 5/8-inch bore, and the billet of 1-inch bore are presented for comparison in Figures 28, 29, and 30. Data from additional drop-tests at varying heights are shown in Figures A-1 to A-6, Appendix A.

No pronounced onset spikes are evident in the three 10-foot drop records shown, and no terminal spikes were evident. In the test with the solid billet, deceleration onset was relatively sharp, whereas by contrast, the billet of 5/8-inch bore produced a more gradual onset to the same g-level. This effect can be attributed to the altered geometry. Attention is also directed to Figure A-7 which, although not depicting the termination of the event, shows the onset rate of approximately 3500 g's per second.

The deceleration modes recorded for the solid billet and the billet of 5/8-inch bore were virtually identical at a 65-g level. A slightly longer duration of the extrusion event will be noted for the bored billet. The 30-g deceleration mode shown for the billet of 1-inch bore illustrates the capabilities of the large-bore billet in reducing mode g-level.

The bored billets produced from 30 to 50 percent greater length of extruded billet material, but less mass of extrudate. The energy absorption efficiency value was thus higher for the bored billets.



#### BILLET

Material: Al 1100-0

Cross Section:

ID: 0 (Solid)

OD: 1.128 in.

#### DIE

Entry Area: 1 sq. in.

Exit Area: 0.666 sq. in.

Area Ratio: 1.50:1

#### OSCILLOSCOPE SETTINGS

Sweep: 2 ms/cm      Vertical Gain: .5 v/cm

Accelerometer Sensitivity: 10 mv/g

#### DECELERATION PROFILE

Mode g-level: 65 g's      Duration of Event: 12-1/2 ms

#### ENERGY ABSORPTION

Drop Height: 10 ft      Distance of Ram Travel: 1.408 in.

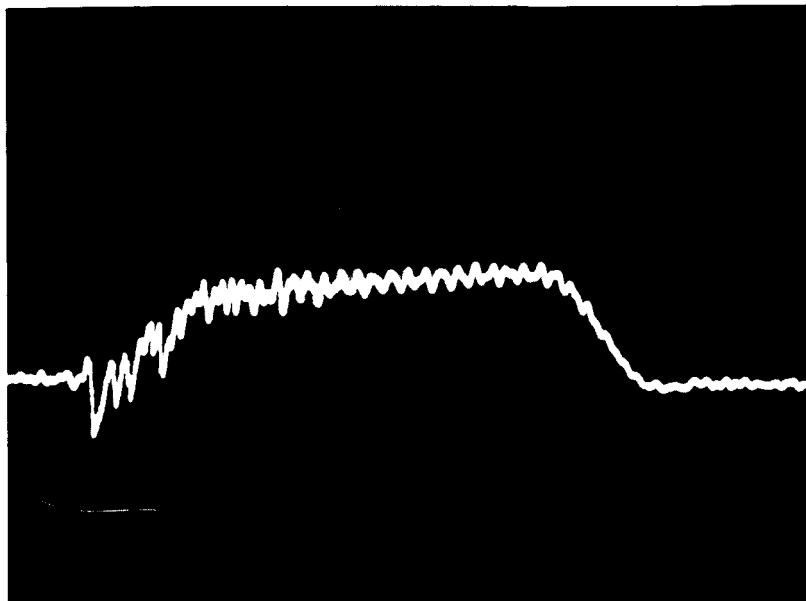
Load Weight: 270 lb

Impact Energy: 2700 ft-lb       $e = 19,700 \text{ ft-lb/lb}$

Figure 28

SHOCK STRUT PERFORMANCE

Drop No. 103



#### BILLET

Material: Al 1100-0

Cross Section:

ID: 0.625 in.

OD: 1.128 in.

#### DIE

Entry Area: 1 sq. in.

Exit Area: 0.666 sq. in.

Area Ratio: 1.50:1

#### OSCILLOSCOPE SETTINGS

Sweep: 2 ms/cm      Vertical Gain: .5 v/cm

Accelerometer Sensitivity: 10 mv/g

#### DECELERATION PROFILE

Mode g-level: 65 g's      Duration of Event: 13-1/2 ms

#### ENERGY ABSORPTION

Drop Height: 10 ft

Distance of Ram Travel: 1.683 in.

Load Weight: 270 lb

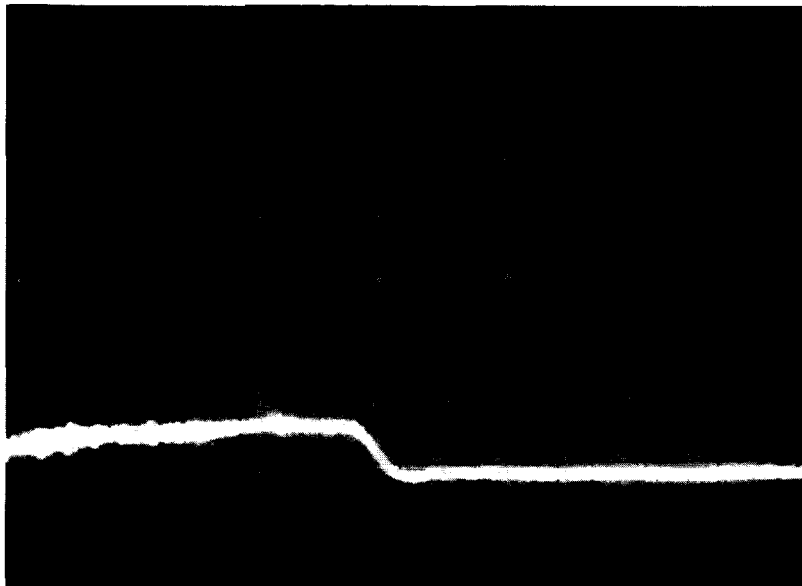
Impact Energy: 2700 ft-lb       $e = 25,700 \text{ ft-lb/lb}$

Figure 29

SHOCK STRUT PERFORMANCE

Drop No. 111





#### BILLET

Material: Al 1100-0

Cross Section:

ID: 1 in.

OD: 1.128 in.

#### DIE

Entry Area: 1 sq. in.

Exit Area: 0.666 sq. in.

Area Ratio: 1.50:1

#### OSCILLOSCOPE SETTINGS

Sweep: 2 ms/cm      Vertical Gain: 15 v/cm

Accelerometer Sensitivity: 10 mv/g

#### DECELERATION PROFILE

Mode g-level: 25 g's      Duration of Event: Indeterminate ms

#### ENERGY ABSORPTION

Drop Height: 10 ft

Distance of Ram Travel: 5.374 in.

Load Weight: 270 lb

Impact Energy: 2700 ft-lb       $e = 28,800 \text{ ft-lb/lb}$

Figure 30

SHOCK STRUT PERFORMANCE

Drop No. 137

In summary, the effects of altered geometry were shown in reduced onset shock, longer duration of the event, and increased energy absorption efficiency.

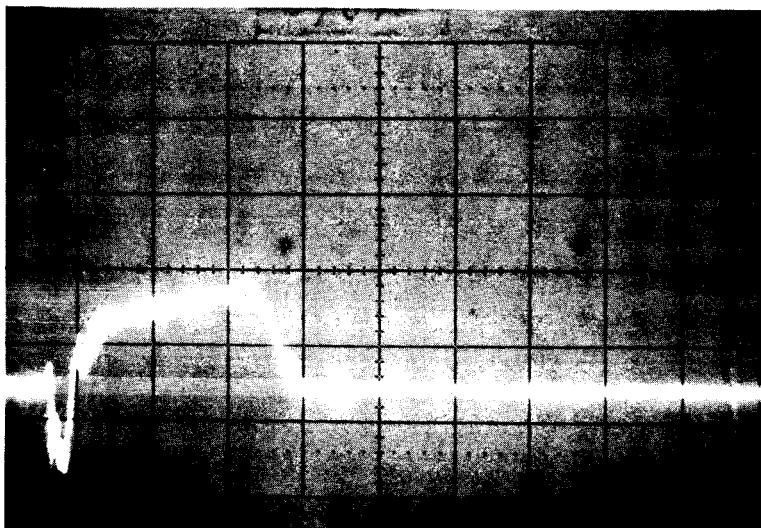
In the case of the 1100-0 aluminum alloy billet material, the practical limits of billet bore-diameter were indicated by tests with the 1-inch bore. Upon examination of the billet after impact, slight indentations indicative of incipient buckling were noted in the unextruded portions of the billet, furnishing visible evidence that the limits of wall strength were being reached with this billet design and material.

Billet Metallurgical Properties. - The majority of tests employed annealed 1100-0 aluminum (yield strength 8500 psi, Rockwell 20 Superficial 15-T hardness) as the billet material. Experimentation with this relatively soft alloy was dictated by its observed capabilities for elimination of onset and terminal spikes and for reducing mode g-levels. The indications of the foregoing geometry studies, however, particularly those from tests with large-bore billets, were projected into a further materials investigation.

Commercially available as-received 6061-T6 aluminum alloy tubing (1-1/8-inch OD, 0.058-inch wall thickness, and 1-inch ID) was employed as a billet precisely simulating the geometrical characteristics of the 1-inch billet-bore previously tested with the 1100-0 alloy, but possessing differing metallurgical properties, i.e., yield strength of approximately 40,000 psi and Rockwell 81 Superficial 15-T measurement. A hollow billet of this composition offered the observed advantages of thin-wall geometry while possessing greater wall strength. Results of hollow billet drops at heights of 10 and 15 feet are shown in Figures 31 and 32.

These drop tests resulted in the highest energy absorption efficiency ratings recorded (in excess of 80,000 ft-lb/lb), with the corresponding mode g-levels remaining substantially below 100 g's. These efficiencies were several times higher than those obtainable by alternative absorption systems /1, 2/. Although the geometrical factor must be appropriately weighed in the interpretation of the results, the more-than-doubled efficiency rise in these drops was obviously attributable to the higher yield strength and hardness of the 6061-T6 material. The relative roles of the latter factors were indeterminate.

In a further test, the same 6061-T6 aluminum alloy tubing was solution heat-treated to a different temper, i.e., yield strength approximately 20,000 psi and hardness measurement of 61-65 by Rockwell Superficial 15-T scale. A drop using this hollow billet yielded the data presented in Figure 33. By comparison with the as-received hollow billet results, this test demonstrated the effect of the reduction of yield strength and hardness. Note the lowered deceleration mode of the drop as well as the corresponding reduction in energy absorption efficiency.



#### BILLET

Material: Al 6061-T6

#### Cross Section:

ID: 1.009 in.

OD: 1.125 in.

#### DIE

Entry Area: 1 sq. in.

Exit Area: 0.666 sq. in.

Area Ratio: 1.50:1

#### OSCILLOSCOPE SETTINGS

Sweep: 5 ms/cm Vertical Gain: 0.5 v/cm

Accelerometer Sensitivity: 10 mv/g

#### DECELERATION PROFILE

Mode g-level: 58 g's Duration of Event: 16.5 ms

#### ENERGY ABSORPTION

Drop Height: 10 ft

Distance of Ram Travel: 2.0 in.

Load Weight: 270 lb

Impact Energy: 2700 ft-lb  $e = 68,000$  ft-lb/lb

Figure 31

SHOCK STRUT PERFORMANCE

Drop No. 151

BILLET

Material: Al 6061-T6

Cross Section:

ID: 1.009

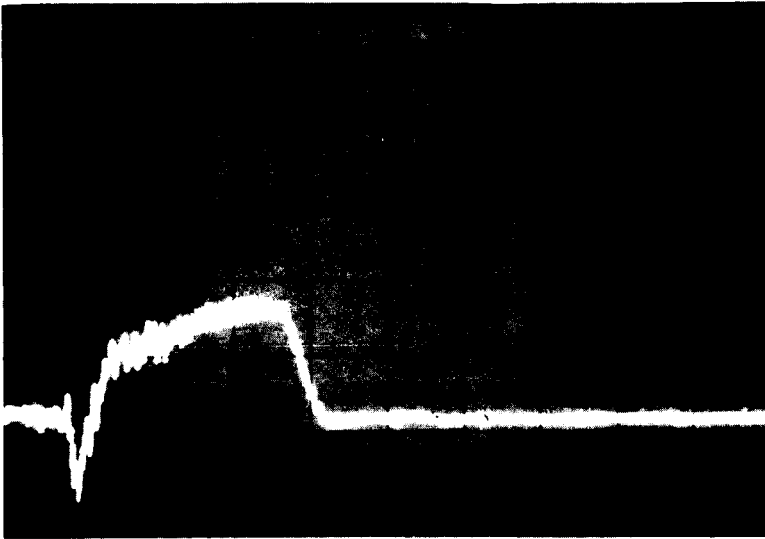
OD: 1.125

DIE

Entry Area: 1 sq. in.

Exit Area: 0.666 sq. in.

Area Ratio: 1.50:1



OSCILLOSCOPE SETTINGS

Sweep: 5 ms/cm      Vertical Gain: 0.5 v/cm

Accelerometer Sensitivity: 10 mv/g

DECELERATION PROFILE

Mode g-level: 61 g's      Duration of Event: 16 ms

ENERGY ABSORPTION

Drop Height: 15 ft      Distance of Ram Travel: 2.3750 in.

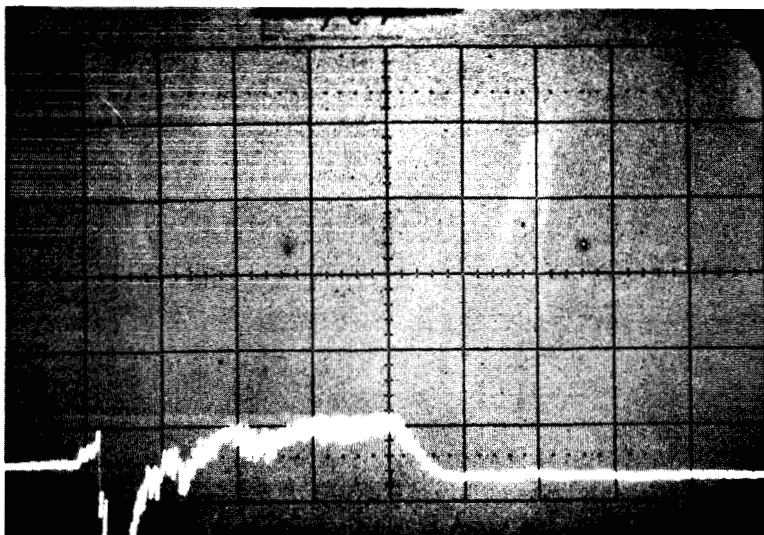
Load Weight: 270 lb

Impact Energy: 4050 ft-lb       $e = 86,750 \text{ ft-lb/lb}$

Figure 32

SHOCK STRUT PERFORMANCE

Drop No. 153



#### BILLET

Material: Al 6061 Solution  
Treated

#### Cross Section:

ID: 1.009 in.  
OD: 1.125 in.

#### DIE

Entry Area: 1 sq. in.  
Exit Area: 0.666 sq. in.  
Area Ratio: 1.50:1

#### OSCILLOSCOPE SETTINGS

Sweep: 5 ms/cm Vertical Gain: 0.5 v/cm

Accelerometer Sensitivity: 10 mv/g

#### DECELERATION PROFILE

Mode g-level: 37 g's Duration of Event: 21 ms

#### ENERGY ABSORPTION

Drop Height: 10 ft Distance of Ram Travel: 2.85 in.

Load Weight: 270 lb

Impact Energy: 2700 ft-lb  $e = 48,200 \text{ ft-lb/lb}$

Figure 33

SHOCK STRUT PERFORMANCE

Drop No. 158

To investigate the effect of within-billet variation of metallurgical properties, compound billets were designed to provide radial variation and axial variation of metallurgical properties.

For the radially varied compound billet, a titanium\* tube of 3/4-inch OD and 0.035-inch wall thickness was inserted into an 1100-0 aluminum billet of 3/4-inch central bore. Because of titanium's high-strength low-weight characteristics, it was postulated that a beneficial effect on energy absorption might result from radially compounding titanium with aluminum. The deceleration profile obtained from a drop with this billet design is shown in Figure 34. By comparison with drops using all-aluminum billets of similar bore, no significant effects of the alteration were recorded either for deceleration profile or energy absorption efficiency. The titanium tubing was found to be deformed by buckling, indicating that the tubing had contributed in the absorption of total impact energy.

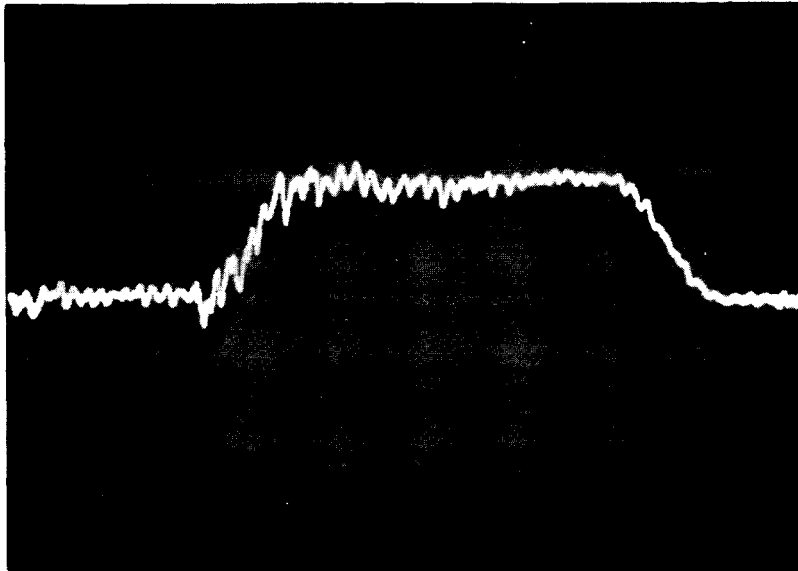
For the axially compounded billets, cylindrical sections of 6061-T5 aluminum, heat-treated to varying hardnesses, were sequentially assembled in the billet position within the container. These sections were in the form of 1/2-inch-long annular washers with a 3/4-inch central hole, permitting assembly of a bored-typed billet of varying hardness. To assure two transitions of hardness throughout the expected length of ram travel, the sections were heat-treated to produce three grades of Rockwell Superficial T-15 hardness, as follows: Two bottom segments, Rockwell 58, solution heat-treated to the T-4 condition; next two segments, Rockwell 76, partially aged at 350°F for 1 hour; upper segment, Rockwell 81, as received. Figure 35 shows the design of the graduated annular billet.

The resultant data for a drop height of 10 feet, depicted in Figure 36, shows no observable change in deceleration level with change of hardness gradients of billet material. Note that the mode deceleration exceeds 100 g's. Because of the high g-level, no further investigation of this type billet was undertaken.

Die Area Ratio. - In the experiments with the final strut design, orifices with two die area ratios (ratio of area of die entry to area of die exit) were employed: A die with entry 1.128 inches in diameter (entry area, 1 square inch) and with exit diameter of 0.920 inch (exit area 0.666 square inch) effected an area ratio of 1.50:1. The exit diameter of the second die was 1.020 inches (exit area 0.815 square inch), effecting an area ratio of 1.23:1. The effect of die area ratio on deceleration profile and energy absorption efficiency was investigated in drop tests employing billets of both 1100-0 and 6061-T6 aluminum alloys.

---

\* ASTM B 338-65, Grade 2.



#### BILLET

Material: 1100-O, with 0.035"  
annular titanium insert

#### Cross Section:

ID: (Al) 0.750 in.  
OD: 1.128 in.

#### DIE

Entry Area: 1 sq. in.  
Exit Area: 0.666 sq. in.  
Area Ratio: 1.50:1

#### OSCILLOSCOPE SETTINGS

Sweep: 2 ms/cm      Vertical Gain: 0.5 v/cm

Accelerometer Sensitivity: 10 mv/g

#### DECELERATION PROFILE

Mode g-level: 65 g's      Duration of Event: 12 ms

#### ENERGY ABSORPTION

Drop Height: 10 ft      Distance of Ram Travel: 1.813 in.

Load Weight: 270 lb

Impact Energy: 2700 ft-lb       $e = 23,500 \text{ ft-lb/lb}$  (Ti calculated)  
27,400 ft-lb/lb (Only Al calculated)

Figure 34

SHOCK STRUT PERFORMANCE

Drop No. 130

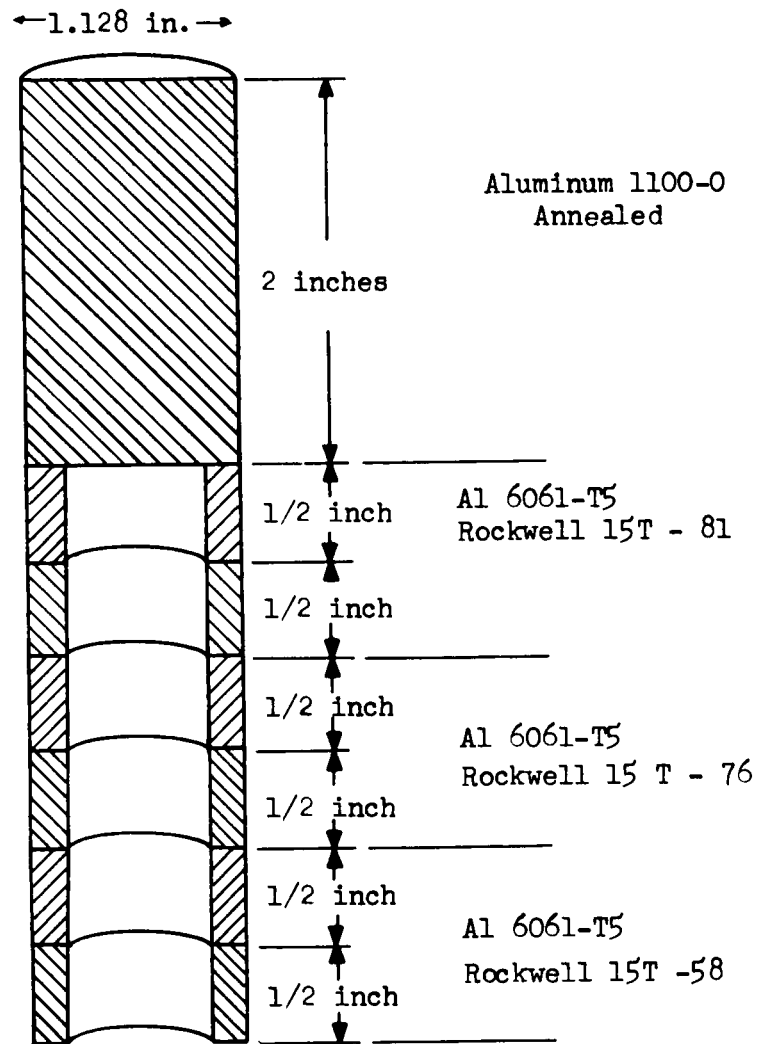
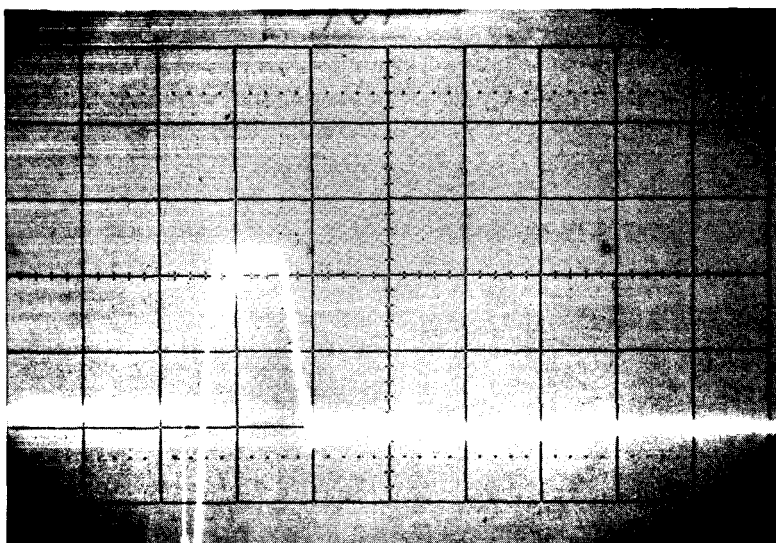


Figure 35

DESIGN OF 6061-T5 BILLET, AXIALLY GRADED FOR HARDNESS





#### BILLET

Material: Al 6061 Axial Compound

#### Cross Section:

ID: 0.750 in.

OD: 1.128 in.

#### DIE

Entry Area: 1 sq. in.

Exit Area: 0.666 sq. in.

Area Ratio: 1.50:1

#### OSCILLOSCOPE SETTINGS

Sweep: 5 ms/cm      Vertical Gain: 0.5 v/cm

Accelerometer Sensitivity: 10 mv/g

#### DECELERATION PROFILE

Mode g-level: 102 g's      Duration of Event: 8 ms

#### ENERGY ABSORPTION

Drop Height: 10 ft      Distance of Ram Travel: 0.8125 in.

Load Weight: 270 lb

Impact Energy: 2700 ft-lb       $e = 61,150 \text{ ft-lb/lb}$

Figure 36

SHOCK STRUT PERFORMANCE

Drop No. 154

Drop tests were made with a 1100-O aluminum billet having a 5/8-inch bore. Data obtained using an orifice ring with a die area ratio of 1.23:1 and those acquired using a die ratio of 1.50:1 are provided in Figures 37 and 38, respectively, both of which depict 10-foot drops. With the use of these soft billets, deceleration profiles at the two ratios are not significantly different. Their mode g-levels are virtually identical at approximately 65 g's and the durations of the events are also comparable.

6061-T6 Aluminum Alloy Hollow Billets. - Further die area ratio comparisons were conducted using 6061-T6 aluminum alloy tubing as the billets. Results of 10-foot drop tests at the two ratios are shown in Figures 39 and 40. Contrary to the results shown for the softer, lower-yield 1100-O aluminum billet material, die area ratio exerted a significant influence on deceleration profile when the hard, high-yield hollow billet was employed. The 1.23:1 ratio effected a mode g-level of 30 g's as opposed to a 58-g level for the 1.50:1 ratio, and the duration of the event was considerably longer in the test of the 1.23:1 orifice ring. Energy absorption efficiency is also shown to be affected by the die area ratio, a substantially higher absorption value being recorded for the 1.50:1 ratio.

Results of die area ratio tests under the same conditions but at 15-foot drop heights are presented in Figures 41 and 42, with the results evidencing consistency, in all respects discussed above, with those recorded for the 10-foot drop heights.

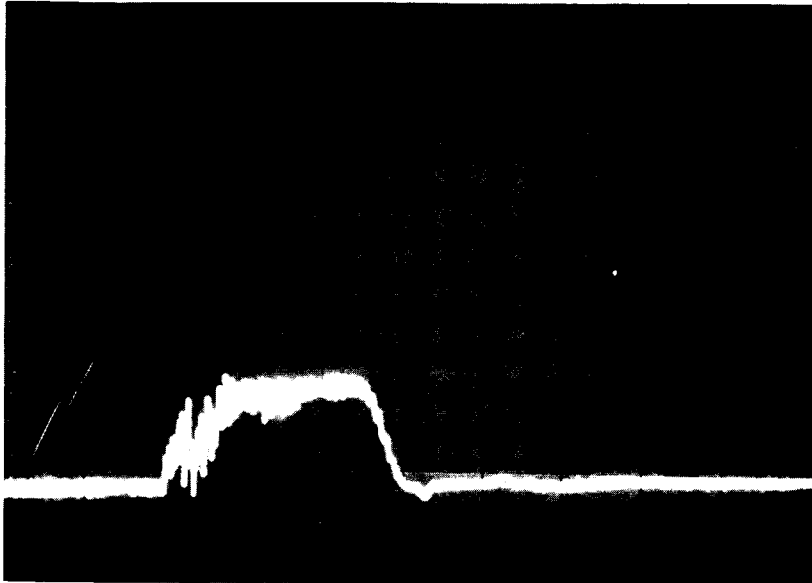
Effect of Drop Height. - The effect of drop height on deceleration profile and energy absorption efficiency was assessed by test drops from seven graduated heights, using billets with a 5/8-inch bore and an extrusion ratio of 1.50:1. Profiles and data on these drops are shown in Figures 43 through 49.

It is obvious from these data that the deceleration mode remains essentially constant throughout the series, implying that the energy absorption mechanism gives rise to constant force, independent of drop height (terminal velocity). The duration of the event was consistently extended with each increase in drop height, and greater heights consistently increased the length of the billet extruded. Calculations indicate that slight energy absorption efficiency increases also occurred with increases in drop height.

Effect of Load Weight. - To assess the effect of load weight, the 270-pound\* load routinely used was increased to provide a total load weight of 445 pounds, or a weight increase of approximately 64 percent. A 10-foot drop was then made using a 6061-T6 aluminum alloy billet with 1-inch inside diameter. The results of this drop are shown in Figure 50. For comparison, data from a drop at the same conditions but using a normal 270-pound load are presented in Figure 51.

---

\* Actual load, 274 pounds 4 ounces, designated 270 pounds to allow for frictional losses in the system.



BILLET

Material: A1 1100-0

Cross Section:

ID: 0.625 in.

OD: 1.128 in.

DIE

Entry Area: 1 sq. in.

Exit Area: 0.815 sq. in.

Area Ratio: 1.23:1

OSCILLOSCOPE SETTINGS

Sweep: 5 ms/cm Vertical Gain: 0.5 v/cm

Accelerometer Sensitivity: 10 mv/g

DECELERATION PROFILE

Mode g-level: 65 g's Duration of Event: 15 ms

ENERGY ABSORPTION

Drop Height: 10 ft

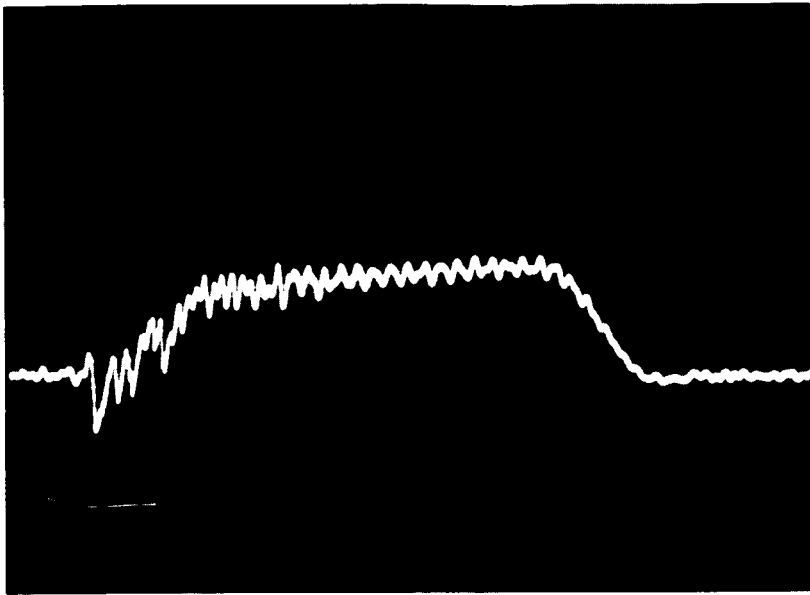
Load Weight: 270 lb

Impact Energy: 2700 ft-lb

Figure 37

SHOCK STRUT PERFORMANCE

Drop No. 143



#### BILLET

Material: Al 1100-0

Cross Section:

ID: 0.625 in.

OD: 1.128 in.

#### DIE

Entry Area: 1 sq. in.

Exit Area: 0.666 sq. in.

Area Ratio: 1.50:1

#### OSCILLOSCOPE SETTINGS

Sweep: 2 ms/cm Vertical Gain: 0.5 v/cm

Accelerometer Sensitivity: 10 mv/g

#### DECELERATION PROFILE

Mode g-level: 65 g's Duration of Event: 14 ms

#### ENERGY ABSORPTION

Drop Height: 10 ft

Distance of Ram Travel: 2.97 in.

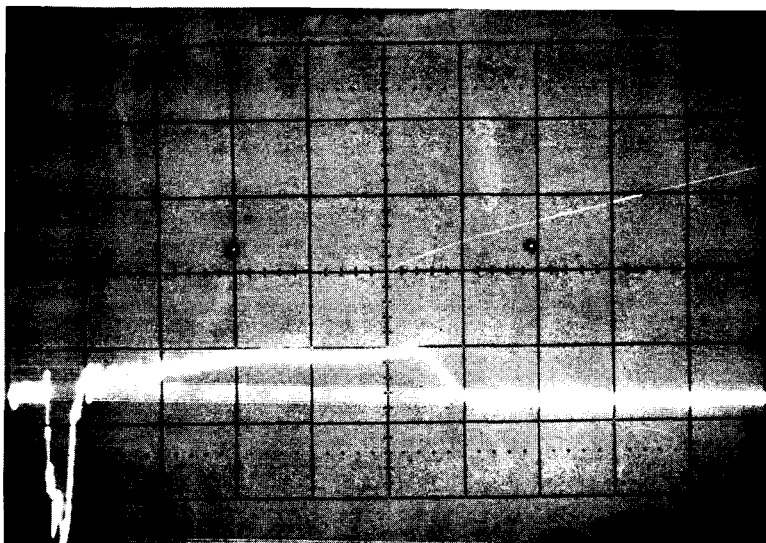
Load Weight: 270 lb

Impact Energy: 2700 ft-lb  $e = 25,000 \text{ ft-lb/lb}$

Figure 38

SHOCK STRUT PERFORMANCE

Drop No. 111



#### BILLET

Material: Al 6061-T6

#### Cross Section:

ID: 1.009 in.

OD: 1.125 in.

#### DIE

Entry Area: 1 sq. in.

Exit Area: 0.815 sq. in.

Area Ratio: 1.23:1

#### OSCILLOSCOPE SETTINGS

Sweep: 5 ms/cm      Vertical Gain: 0.5 v/cm

Accelerometer Sensitivity: 10 mv/g

#### DECELERATION PROFILE

Mode g-level: 30 g's      Duration of Event: 28 ms

#### ENERGY ABSORPTION

Drop Height: 10 ft      Distance of Ram Travel: 3.4375 in.

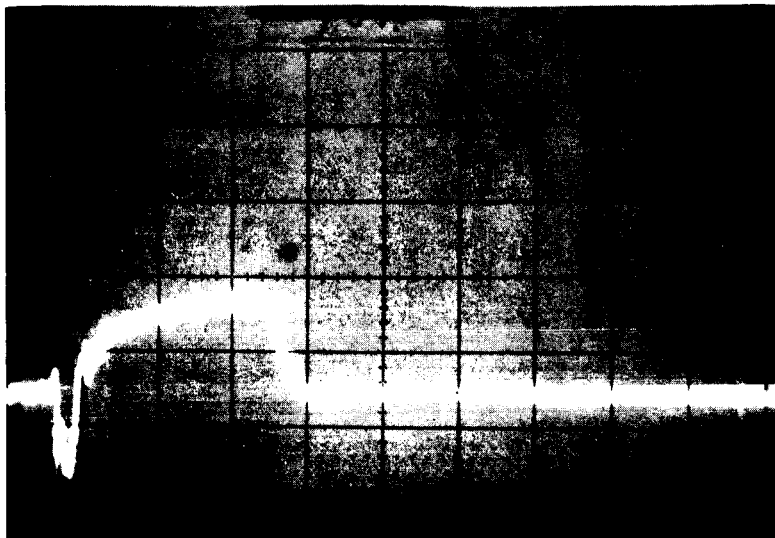
Load Weight: 270 lb

Impact Energy: 2700 ft-lb       $e = 39,900 \text{ ft-lb/lb}$

Figure 39

SHOCK STRUT PERFORMANCE

Drop No. 150



#### BILLET

Material: Al 6061-T6

#### Cross Section:

ID: 1.009 in.

OD: 1.125 in.

#### DIE

Entry Area: 1 sq. in.

Exit Area: 0.666 sq. in.

Area Ratio: 1.50:1

#### OSCILLOSCOPE SETTINGS

Sweep: 5 ms/cm      Vertical Gain: 0.5 v/cm

Accelerometer Sensitivity: 10 mv/g

#### DECELERATION PROFILE

Mode g-level: 58 g's      Duration of Event: 16.5 ms

#### ENERGY ABSORPTION

Drop Height: 10 ft

Distance of Ram Travel: 2.0 in.

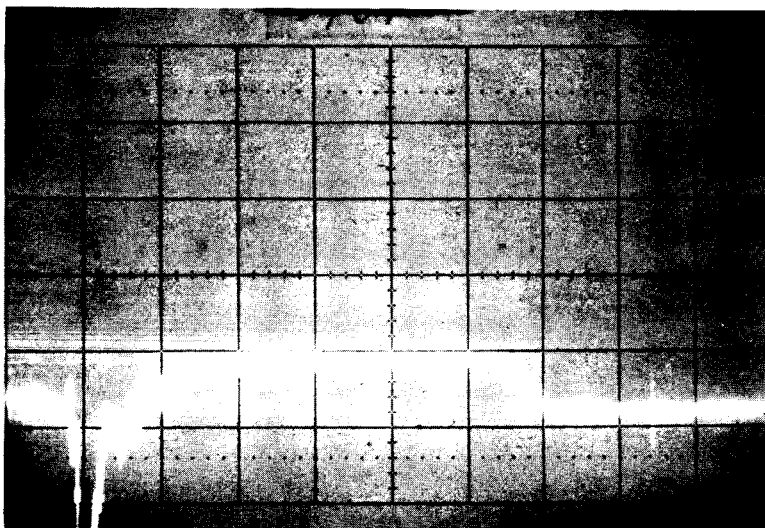
Load Weight: 270 lb

Impact Energy: 2700 ft-lb       $e = 68,000 \text{ ft-lb/lb}$

Figure 40

SHOCK STRUT PERFORMANCE

Drop No. 151



#### BILLET

Material: Al 6061-T6

#### Cross Section:

ID: 1.009 in.

OD: 1.125 in.

#### DIE

Entry Area: 1 sq. in.

Exit Area: 0.815 sq. in.

Area Ratio: 1.23:1

#### OSCILLOSCOPE SETTINGS

Sweep: 5 ms/cm      Vertical Gain: 0.5 v/cm

Accelerometer Sensitivity: 10 mv/g

#### DECELERATION PROFILE

Mode g-level: 30 g's      Duration of Event: 31 ms

#### ENERGY ABSORPTION

Drop Height: 15 ft      Distance of Ram Travel: 4.50 in.

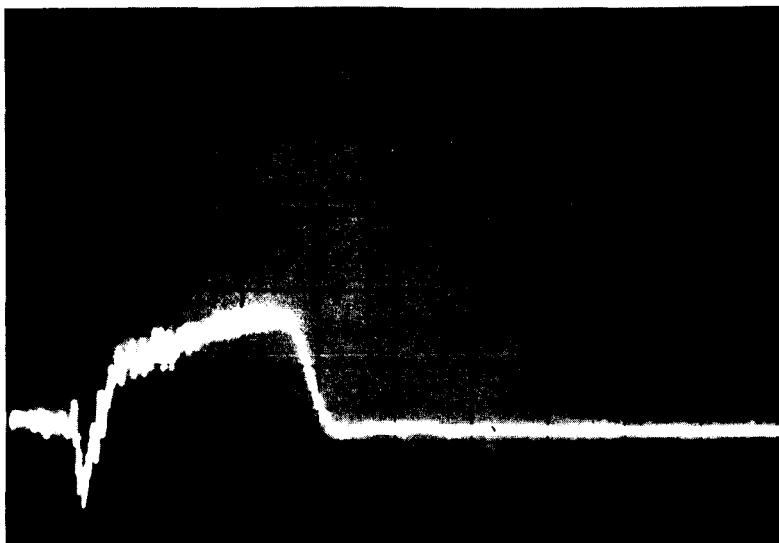
Load Weight: 270 lb

Impact Energy: 4050 ft-lb       $e = 45,750 \text{ ft-lb/lb}$

Figure 41

SHOCK STRUT PERFORMANCE

Drop No. 152



BILLET

Material: Al 6061-T6

Cross Section:

ID: 1.009

OD: 1.125

DIE

Entry Area: 1 sq. in.

Exit Area: 0.666 sq. in.

Area Ratio: 1.50:1

OSCILLOSCOPE SETTINGS

Sweep: 5 ms/cm      Vertical Gain: 0.5 v/cm

Accelerometer Sensitivity: 10 mv/g

DECELERATION PROFILE

Mode g-level: 61 g's      Duration of Event: 16 ms

ENERGY ABSORPTION

Drop Height: 15 ft

Distance of Ram Travel: 2.375 in.

Load Weight: 270 lb

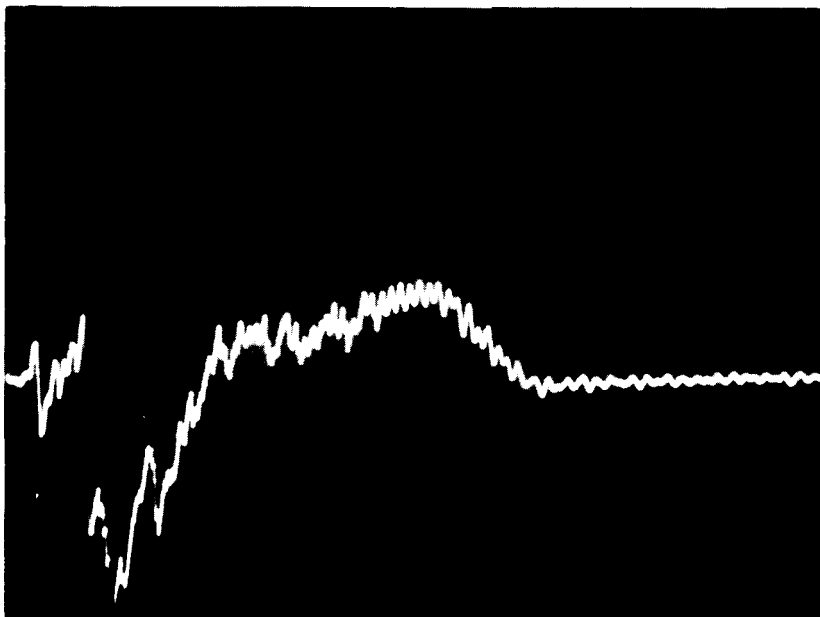
Impact Energy: 4050 ft-lb     $e = 86,750 \text{ ft-lb/lb}$

Figure 42

SHOCK STRUT PERFORMANCE

Drop No. 153





#### BILLET

Material: Al 1100-O

Cross Section:

ID: 0.625 in.

OD: 1.128 in.

#### DIE

Entry Area: 1 sq. in.

Exit Area: 0.666 sq. in.

Area Ratio: 1.50:1

#### OSCILLOSCOPE SETTINGS

Sweep: 2 ms/cm      Vertical Gain: 0.5 v/cm

Accelerometer Sensitivity: 10 mv/g

#### DECELERATION PROFILE

Mode g-level: 50 g's      Duration of Event: 11 ms

#### ENERGY ABSORPTION

Drop Height: 5 ft      Distance of Ram Travel: 1.0 in.

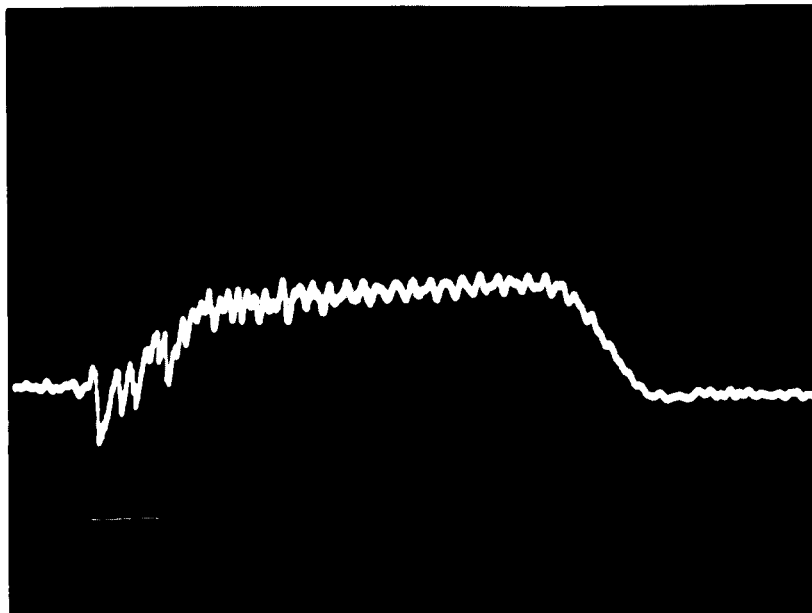
Load Weight: 270 lb

Impact Energy: 1350 ft-lb       $e = 21,000 \text{ ft-lb/lb}$

Figure 43

SHOCK STRUT PERFORMANCE

Drop No. 110



#### BILLET

Material: Al 1100-0

#### Cross Section:

ID: 0.625 in.

OD: 1.128 in.

#### DIE

Entry Area: 1 sq. in.

Exit Area: 0.666 sq. in.

Area Ratio: 1.50:1

#### OSCILLOSCOPE SETTINGS

Sweep: 2 ms/cm      Vertical Gain: 0.5 v/cm

Accelerometer Sensitivity: 10 mv/g

#### DECELERATION PROFILE

Mode g-level: 65 g's      Duration of Event: 13-1/2 ms

#### ENERGY ABSORPTION

Drop Height: 10 ft

Distance of Ram Travel: 2.97 in.

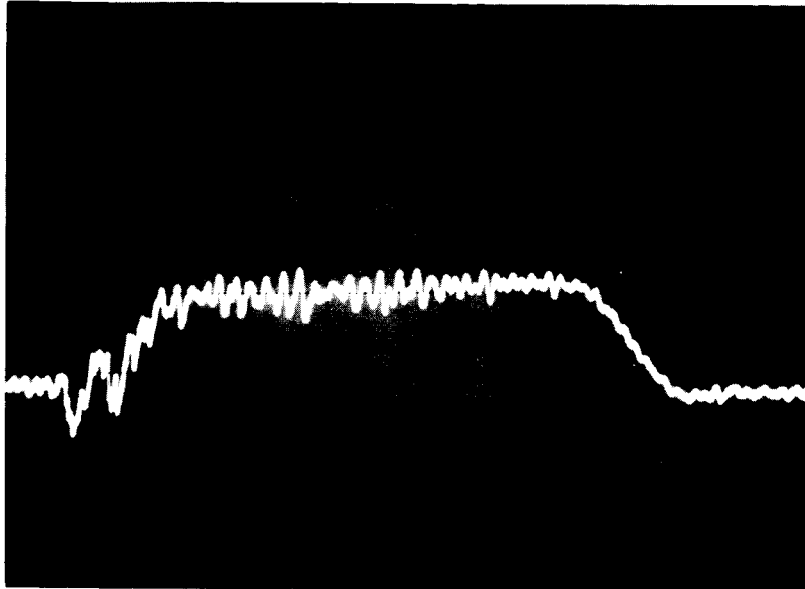
Load Weight: 270 lb

Impact Energy: 2700 ft-lb       $e = 25,000 \text{ ft-lb/lb}$

Figure 44

SHOCK STRUT PERFORMANCE

Drop No. 111



#### BILLET

Material: Al 1100-0

Cross Section:

ID: 0.625 in.

OD: 1.128 in.

#### DIE

Entry Area: 1 sq. in.

Exit Area: 0.666 sq. in.

Area Ratio: 1.50:1

#### OSCILLOSCOPE SETTINGS

Sweep: 2 ms/cm      Vertical Gain: 0.5 v/cm

Accelerometer Sensitivity: 10 mv/g

#### DECELERATION PROFILE

Mode g-level: 65 g's      Duration of Event: 15 ms

#### ENERGY ABSORPTION

Drop Height: 15 ft      Distance of Ram Travel: 2.1875 in.

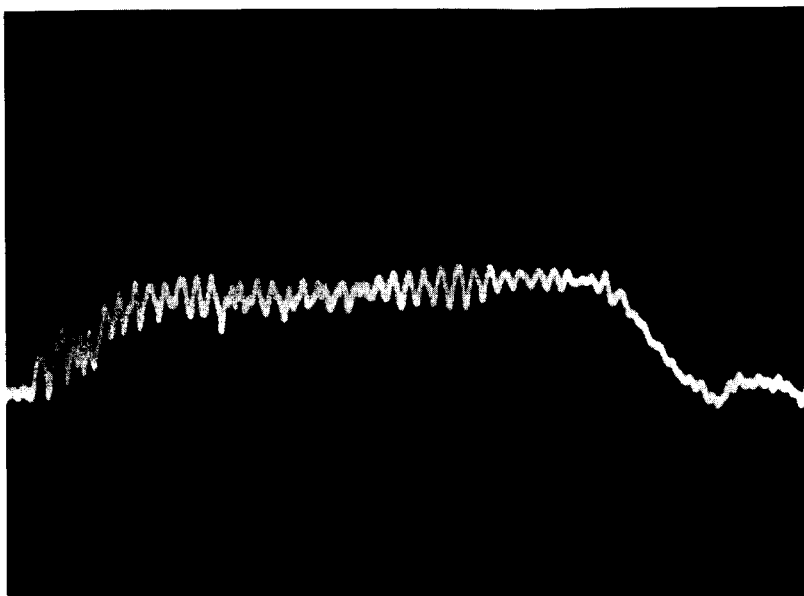
Load Weight: 270 lb

Impact Energy: 4050 ft-lb       $e = 28,000$  ft-lb/lb

Figure 45

SHOCK STRUT PERFORMANCE

Drop No. 113



#### BILLET

Material: Al 1100-0

Cross Section:

ID: 0.625 in.

OD: 1.128 in.

#### DIE

Entry Area: 1 sq. in.

Exit Area: 0.666 sq. in.

Area Ratio: 1.50:1

#### OSCILLOSCOPE SETTINGS

Sweep: 2 ms/cm      Vertical Gain: 0.5 v/cm

Accelerometer Sensitivity: 10 mv/g

#### DECELERATION PROFILE

Mode g-level: 65 g's      Duration of Event: 16 ms

#### ENERGY ABSORPTION

Drop Height: 17.5 ft      Distance of Ram Travel: 2.5625 in.

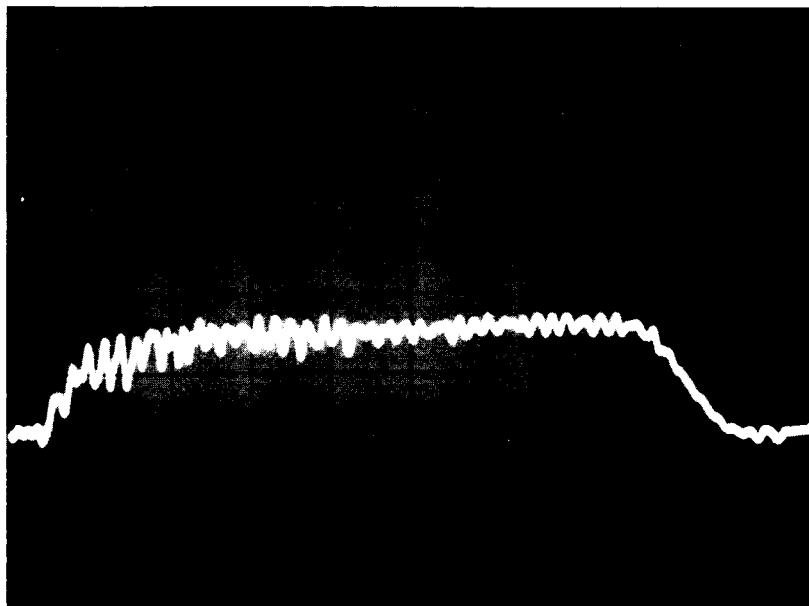
Load Weight: 270 lb

Impact Energy: 4725 ft-lb       $e = 28,700 \text{ ft-lb/lb}$

Figure 46

SHOCK STRUT PERFORMANCE

Drop No. 114



#### BILLET

Material: Al 1100-0

Cross Section:

ID: 0.625 in.

OD: 1.128 in.

#### DIE

Entry Area: 1 sq. in.

Exit Area: 0.666 sq. in.

Area Ratio: 1.50:1

#### OSCILLOSCOPE SETTINGS

Sweep: 2 ms/cm      Vertical Gain: 0.5 v/cm

Accelerometer Sensitivity: 10 mv/g

#### DECELERATION PROFILE

Mode g-level: 65 g's      Duration of Event: 17 ms

#### ENERGY ABSORPTION

Drop Height: 20 ft      Distance of Ram Travel: 2.781 in.

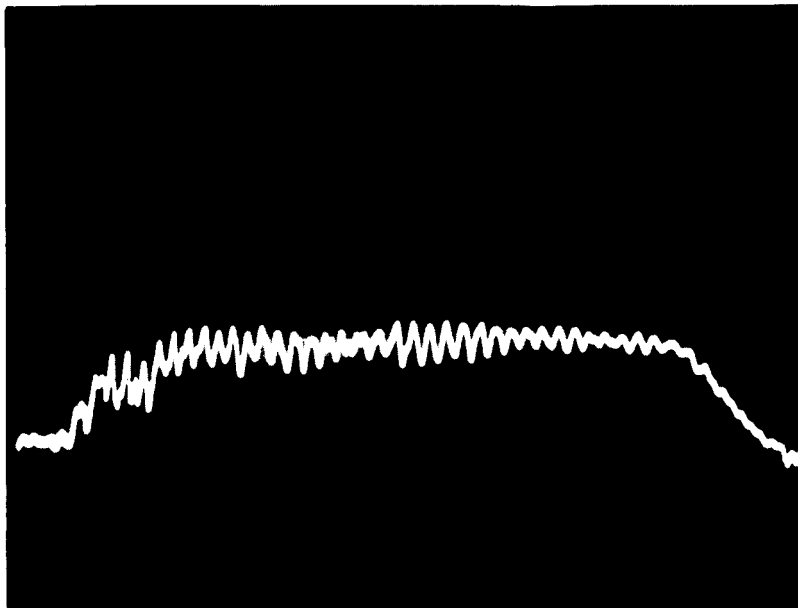
Load Weight: 270 lb

Impact Energy: 5400 ft-lb       $e = 29,500 \text{ ft-lb/lb}$

Figure 47

SHOCK STRUT PERFORMANCE

Drop No. 116



#### BILLET

Material: Al 1100-0

Cross Section:

ID: 0.625 in.

OD: 1.128 in.

#### DIE

Entry Area: 1 sq. in.

Exit Area: 0.666 sq. in.

Area Ratio: 1.50:1

#### OSCILLOSCOPE SETTINGS

Sweep: 2 ms/cm      Vertical Gain: 0.5 v/cm

Accelerometer Sensitivity: 10 mv/g

#### DECELERATION PROFILE

Mode g-level: 65 g's      Duration of Event: 17 ms

#### ENERGY ABSORPTION

Drop Height: 22.5 ft      Distance of Ram Travel: 2.9675 in.

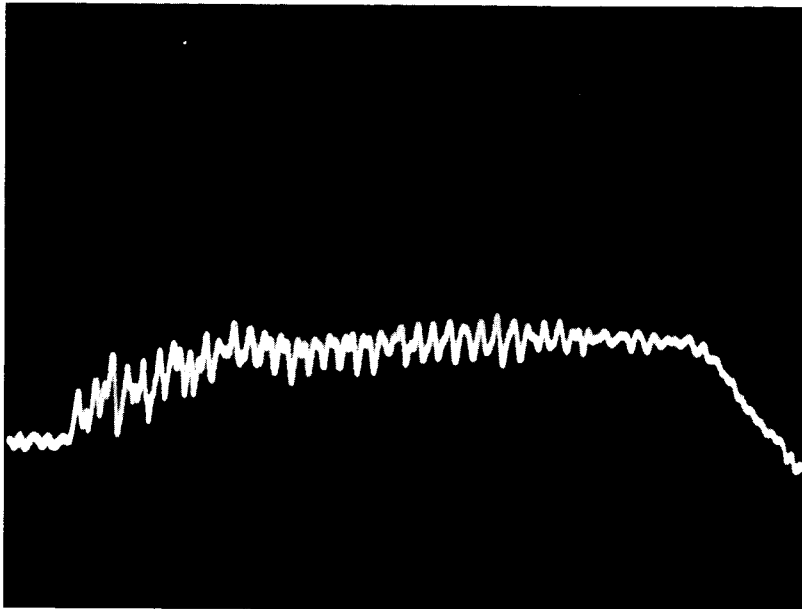
Load Weight: 270 lb

Impact Energy: 6075 ft-lb       $e = 33,000$  ft-lb/lb

Figure 48

SHOCK STRUT PERFORMANCE

Drop No. 117



#### BILLET

Material: Al 1100-0

#### Cross Section:

ID: 0.625 in.

OD: 1.128 in.

#### DIE

Entry Area: 1 sq. in.

Exit Area: 0.666 sq. in.

Area Ratio: 1.50:1

#### OSCILLOSCOPE SETTINGS

Sweep: 2 ms/cm      Vertical Gain: 0.5 v/cm

Accelerometer Sensitivity: 10 mv/g

#### DECELERATION PROFILE

Mode g-level: 65 g's      Duration of Event: 18 ms

#### ENERGY ABSORPTION

Drop Height: 25 ft      Distance of Ram Travel: 3.1875 in.

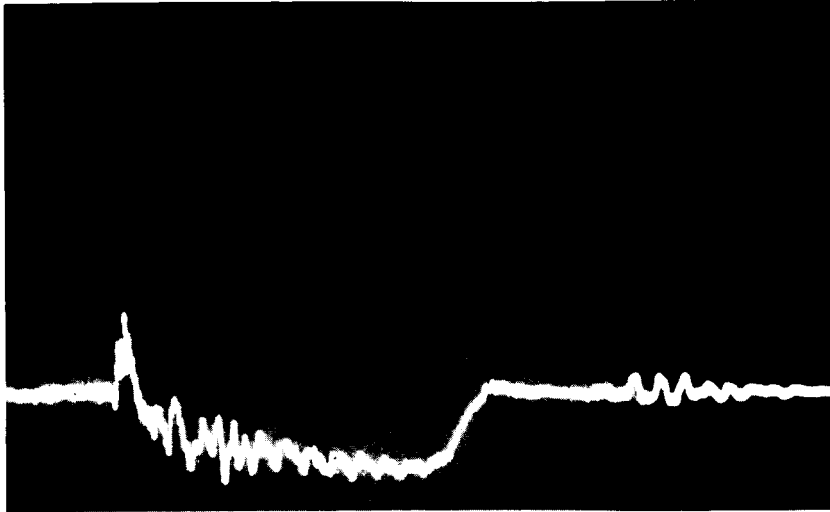
Load Weight: 270 lb

Impact Energy: 6750 ft-lb       $e = 31,400 \text{ ft-lb/lb}$

Figure 49

SHOCK STRUT PERFORMANCE

Drop No. 119



#### BILLET

Material: Al 6061-T6

Cross Section:

ID: 1.009 in.

OD: 1.125 in.

#### DIE

Entry Area: 1 sq. in.

Exit Area: 0.666 sq. in.

Area Ratio: 1.50:1

#### OSCILLOSCOPE SETTINGS

Sweep: 5 ms/cm      Vertical Gain: 0.5 v/cm (Negative Polarity)

Accelerometer Sensitivity: 10 mv/g

#### DECELERATION PROFILE

Mode g-level: 39.5 g's      Duration of Event: 23 ms

#### ENERGY ABSORPTION

Drop Height: 10 ft      Distance of Ram Travel: 3.25 in.

Load Weight: 445 lb

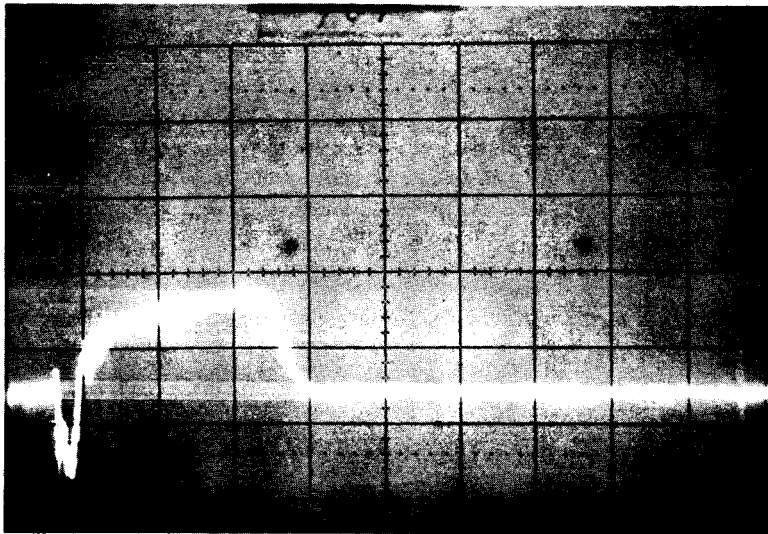
Impact Energy: 4450 ft-lb       $e = 70,250 \text{ ft-lb/lb}$

Figure 50

SHOCK STRUT PERFORMANCE

Drop No. 163





#### BILLET

Material: Al 6061-T6

#### Cross Section:

ID: 1.009 in.

OD: 1.125 in.

#### DIE

Entry Area: 1 sq. in.

Exit Area: 0.666 sq. in.

Area Ratio: 1.50:1

#### OSCILLOSCOPE SETTINGS

Sweep: 5 ms/cm      Vertical Gain: 0.5 v/cm

Accelerometer Sensitivity: 10 mv/g

#### DECELERATION PROFILE

Mode g-level: 58 g's      Duration of Event: 16.5 ms

#### ENERGY ABSORPTION

Drop Height: 10 ft

Distance of Ram Travel: 2.0 in.

Load Weight: 270 lb

Impact Energy: 2700 ft-lb       $e = 68,000 \text{ ft-lb/lb}$

Figure 51

SHOCK STRUT PERFORMANCE

Drop No. 151

The distance of ram travel for the heavier load exceeded that for the lighter load by approximately 62 percent, and a 39 percent longer duration of the event was recorded. A comparison of the deceleration profiles indicates that the heavier weight reduced the mode by approximately 31 percent. This effect is analytically predictable from considerations of the physical significance of the deceleration profile. The area under the profile is equatable to the terminal velocity of the load. Since terminal velocity from a given drop height is independent of magnitude of load, the area under the profile (or terminal velocity) must remain constant, regardless of load. As observed, the duration of the deceleration event (and the length of ram travel) increased with increase in load. Thus the mode g-levels for the longer duration events must be lower than those of shorter duration events to produce equivalent profile areas.

In the cases illustrated, planimetric measurements of the areas under the profiles indicated a terminal velocity of 25.5 ft/sec for Figure 50 and 26.0 ft/sec for Figure 51. These values are within the limits of experimental and reading error with respect to each other and to the free-fall velocity from 10 feet of 25.4 feet per second.

It was also observed that the velocity of load descent after impact (i.e. extrusion velocity) increased with increase in load. For the 270-pound load (Figure 51) this extrusion velocity was 0.125 inch per millisecond, while for the 445-pound load the extrusion velocity increased approximately 13 percent to 0.141 inch per millisecond. The decrease of extrusion force (mode g-level) with increase in load (and increase in extrusion velocity) may be attributable to the fact that recovery from work hardening is a rate process\*. Thus, the extrusion velocity may influence the yield strength to in turn influence extrusion force.

Oblique Impact. - Shock strut performance during oblique impact was evaluated by dropping the apparatus onto a contact plate set at an angle of approximately 13 degrees from the perpendicular to the line of descent. Severe bending of the shock strut assembly resulted from the drop, as shown in Figure 52. Extrusion was negligible, and absorption by deformation bending occurred. It thus appears that for the shock strut to function as an inverse extrusion system, perpendicular delivery of impact force is essential.

Soft Contact Surface. - The effect of soft contact surface was evaluated by dropping the strut into 4 inches of moist sand. The resultant deceleration profile is shown in Figure 53. The deceleration mode level of 65 g's is the same as that observed for impacts of the same system on hard surfaces, and the duration of the event also was not significantly changed.

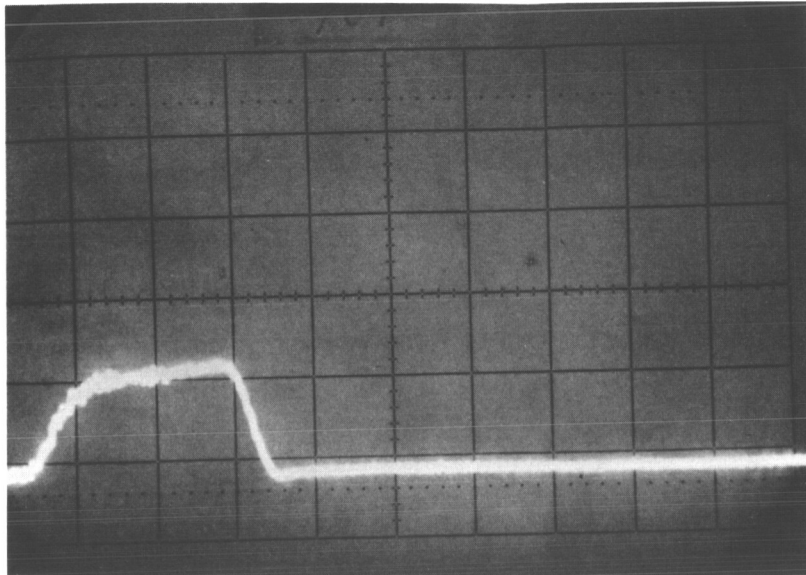
---

\* Pearson and Parkins, op. cit. 27



Figure 52

BENDING OF SHOCK STRUT AS RESULT OF OBLIQUE IMPACT TEST



#### BILLET

Material: Al 1100-O

Cross Section:

ID: 0.625 in.

OD: 1.128 in.

#### DIE

Entry Area: 1 sq. in.

Exit Area: 0.666 sq. in.

Area Ratio: 1.50:1

#### OSCILLOSCOPE SETTINGS

Sweep: 5 ms/cm      Vertical Gain: 0.5 v/cm

Accelerometer Sensitivity: 10 mv/g

#### DECELERATION PROFILE

Mode g-level: 65 g's      Duration of Event: 15 ms

#### ENERGY ABSORPTION

Drop Height: 10 ft      Distance of Ram Travel: 1.603 in.

Load Weight: 270 lb

Impact Energy: 2700 ft-lb       $e = 24,400 \text{ ft-lb/lb}$

Figure 53

SHOCK STRUT PERFORMANCE

Drop No. 138

## System Design Considerations

Performance data from experiments with the third-design strut permitted further evaluations of overall shock strut design.

Evaluation of Extrusion Factor. - The mode deceleration level developed on impact was indicated through these experiments to be a function of extrusion system design and load, independent of terminal velocity. Representative values of the factor were calculated for constant load by the following equations:

$$\phi = \frac{F}{YA \ln A_1 A_2} = \frac{F}{8500 \times 1 \times 4050} = \frac{F}{3440}$$

where     $Y = 8500 \text{ psi}$   
            $m = \frac{270 \text{ lb}}{1 \text{ g}}$   
            $A_1 = 1.00 \text{ in.}^2$   
            $A_2 = .663 \text{ in.}^2$   
            $A_1/A_2 = 1.5$   
            $\ln = A_1/A_2 = 0.4050.$

The following table indicates variation of extrusion factor with variation in billet bore diameter.

Table IX

### EXTRUSION FACTOR VARIATION WITH BILLET GEOMETRY

$A_1/A_2 = 1.50$   
 1100-0 Aluminum  
 Load Weight: 270 lbs

Test No.	Billet Description	Mode Deceleration	Average Force (ma)	Extrusion Factor, $\phi$
113	5/8-inch bore	65	17,550	5.12
129	7/8-inch bore	50	13,500	3.92
137	1-inch bore	25	6,750	1.96

The variations noted in the value of  $\phi$  negates the possibility of deriving an extrusion factor which is universally applicable in the design of struts to meet varied use conditions.

Length of Ram Travel. - In designing a shock strut to meet particular landing requirements, the deceleration profile will be controlled most directly by billet cross-sectional shape and billet metallurgical properties; thus for a specified billet configuration and material condition, the distance of ram travel will be determined by impact energy. The length of billet required under any specified set of conditions may be predicted by equating the impact energy to the work performed by the ram travel, as follows:

$$Fl = E$$

$$(ma)l = mgs \quad (8)$$

Using data from the test drops it was found that the actual length,  $l$ , is generally in good agreement with this equation. For example, in employing the 6061-T6 hollow-billet with the 1.50:1 die, a 270-pound load, and at a 15-foot drop height (Figure 32), the mode deceleration is approximately 65 g's and the theoretical length of ram travel  $l$  is:

$$l = \frac{15 \text{ ft} \times 270 \text{ lb}}{270 \text{ lb/g} \times 65 \text{ g's}} = 0.23 \text{ ft or } 2.77 \text{ in.}$$

The actual observed ram travel was 2.38 inches. The small difference between theoretical and observed ram travel may be attributable to frictional losses and to absorption of energy during onset and during terminal portions of the deceleration event while the deceleration level was changing with time.

Container Thickness. - Since billet metallurgical properties and cross-sectional geometry participate in the control of deceleration levels and consequently the forces developed in the system, the minimum thickness of the billet container also becomes a function of the billet.

A drop of a 270-pound load from 20 feet with a strut incorporating a 1100-O aluminum billet of 3/4-inch bore produced a measured hoop (circumferential) strain of 0.001 inch. The corresponding observed stress is then 29,000 psi, assuming a Young's modulus of  $29 \times 10^6$  psi for the 4340 steel. The minimum container-wall thickness needed to carry the stress developed in the container wall may be calculated as follows:

(1) The equivalent internal pressure is determined using a thick-walled cylinder formula, since the dimensions of the present container (wall-thickness, 0.181, OD, 1.132) place it in that category. Thus the equivalent pressure  $\frac{1}{2}P$ ,

4 Roark, Raymond J., Formulas for Stress and Strain, McGraw Hill, Inc., New York, 1954.

$$p = \sigma \frac{r_2^2 (r_2^2 + r_1^2)}{r_1^2 (r_2^2 + r_1^2)} \quad (9)$$

where  $\sigma$  = observed hoop stress (29,000 psi)  
 $r_1$  = inner radius of billet container (0.565 in.)  
 $r_2$  = outer radius of billet container (0.753 in.)

In the case at hand,  $p = 23,100$  psi.

(2) This equivalent internal pressure may then be used in a thin-walled cylinder formula to determine the minimum wall thickness capable of carrying the pressure. Assuming that the steel used has an ultimate tensile strength UTS = 225,000 psi (as is attainable with 4340 steel), the minimum wall thickness  $t$  is

$$t = \frac{p(r_1 + t/2)}{\text{UTS}},$$

or, in the case at hand,  $t = 0.064$  inch.

System Weight. - From the two foregoing considerations, i.e., length of ram travel and billet container thickness, the minimum shock strut system-weight per length of billet required can be determined.

For effective performance (to prevent cocking of the ram in the container, and to prevent bottoming of the ram) the container length should be approximately 40 percent greater than that of the billet; the length of the ram should be about 10 percent greater than that of the billet.\*

Thus, the shock strut weight per length of billet required is

$$w = \ell(\rho_1 A_1) + 1.40 \ell(\rho_2 A_2) + 1.10 \ell(\rho_3 A_3)$$

where  $\ell$  = length of billet required  
 $\rho_1$  = density of billet material  
 $\rho_2$  = density of container material  
 $\rho_3$  = density of ram material  
 $A_1$  = cross-sectional area of billet  
 $A_2$  = cross-sectional area of container  
 $A_3$  = cross-sectional area of ram

---

\* In one-time-use situations, the ram end cap would not be required, and it is assumed that the adapter ring (or its equivalent) may be fabricated directly as a part of the body of the load-vehicle structure.

A probable case, using a 6061-T6 aluminum hollow billet (1-inch ID, 0.058-inch wall thickness) in a 4340 steel container (1.130-inch ID, 0.060-inch wall thickness) with a 4340 steel ram (1.125-inch OD and 0.095-inch wall thickness), would be stated

$$\begin{aligned}w &= \mathcal{L}(0.0975 \times 0.2020) + 1.40 \mathcal{L}(0.2853 \times 0.110) + 1.10 \mathcal{L}(0.2853 \times 0.165) \\&= \mathcal{L}(0.0197 + 0.0438 + 0.0518) = \mathcal{L}(0.1153) \text{ pounds.}\end{aligned}$$

Thus, in this case, the weight of the shock strut system per inch of billet required is 0.1153 pounds.



## SUMMARY AND DISCUSSION

### Constant Force

The inverse extrusion process was selected for investigation because it theoretically offered a system concept for energy absorption at constant force levels. Experimental work conducted during the program substantiated this theoretical position. Within the range of loads and drop heights tested, impact energy was absorbed under essentially constant force conditions, as indicated by the essentially constant mode deceleration levels achieved throughout each event. The maximum g-level developed on impact was observed to be independent of impact velocity and to vary inversely with magnitude of the dropping load. Process control through strut design and through load distribution was thus indicated.

### Major Design Effects

The major control for both deceleration and absorption performance of the system was found to reside in the physical and geometrical characteristics of the billet. Die characteristics were also found to affect performance to an extent varying with variation in billet composition and geometry.

Effects on Deceleration Profile. - Billet cross-section was observed to exert primary control over deceleration profile, in particular, over deceleration onset rate and deceleration mode level. The mode or "plateau" deceleration level was varied from a maximum of approximately 65 g's to a minimum approaching 20 g's as the billet cross-sectional configuration was varied from solid circular to thin-walled annular. Deceleration onset rate decreased in a similar manner, generally becoming more gradual with the thinner-wall annular sections. Minimum onset rates of approximately 3500 g/sec were observed.

Billet metallurgical properties, especially hardness, were also found to affect the profile and particularly the deceleration onset rate.

Effects on Energy Absorption Efficiency. - Energy absorption efficiency was found to be influenced predominantly by billet metallurgical properties (hardness and yield strength), which, in experiments employing 6061-T6 aluminum alloy tubing as the billet, were proven more significant to absorption efficiency than either die area ratio or billet geometric factors. In these experiments, energy absorption efficiencies substantially in excess of 60,000 foot-pounds per pound (based upon weight of billet expended only) were readily attained, appearing to exceed by factors of two or more the efficiencies of the best-known alternative systems.

## Design for Use

Inasmuch as the two performance criteria--deceleration mode level and energy absorption efficiency--must be selected or "traded off" in individual use situations, this experimental work provides empirical data suitable for use in the design of shock struts to meet particular end-use requirements.

Billet-Material Selection. - Billet material selection is governed by considerations of weight, yield strength, and hardness. Aluminum alloys were found to adequately meet the requirements for light weight and reasonably high yield strength. The particular alloy and temper selected for a given use will depend upon the deceleration profile mode level and energy absorption efficiency desired. In general, high absorption efficiencies may be attained by using harder material, but at the expense of higher deceleration levels.

Strut Design. - The design of a shock strut to meet particular use requirements can be accomplished if the weight and terminal velocity of the landing vehicle are known and if the desired characteristics of the deceleration profile are determinable.

The third experimental shock strut design of this program, utilizing a thin-wall billet (OD 1.128 inches, ID 1 inch) is light-weight and versatile and may be considered a reference system. The graphs shown in Figures 54 and 55 are derived therefrom and may be applied in designing a shock strut for particular use. It should be noted that additional data and additional graphs may be needed for impact of loads other than those used herein; however, the method employed would be similar.

For example, if a deceleration mode of 50 g's may be tolerated (e.g. for instrument landing) and a strut is required to absorb energy from the impact of a 400-pound load landing at a velocity of 40 feet per second (kinetic energy at impact of approximately 10,000 foot-pounds). Figure 54 may be used to determine the billet temper needed to produce the 50-g deceleration mode at the desired weight.\* This graph indicates that the 1.50:1 die area ratio system may be used with billets of any temper and be within the acceptable g-level.

The energy absorption efficiency associated with the selected system may be obtained from Figure 55 or from extrapolation thereof. The billet-length determination necessary to complete the strut design may be derived from the work energy equation. For example, since the exact mode g-level to be developed for a 400-pound load is not determinable directly from Figure 54, the level at 445 pounds may be used. This level will be a conservative estimate for purposes of computing length of ram travel, since

---

\* This graph includes data for the 1.50:1 die area system only; additional data at varying load weights may be compiled to develop similar graphs for 1.23:1 or other systems.

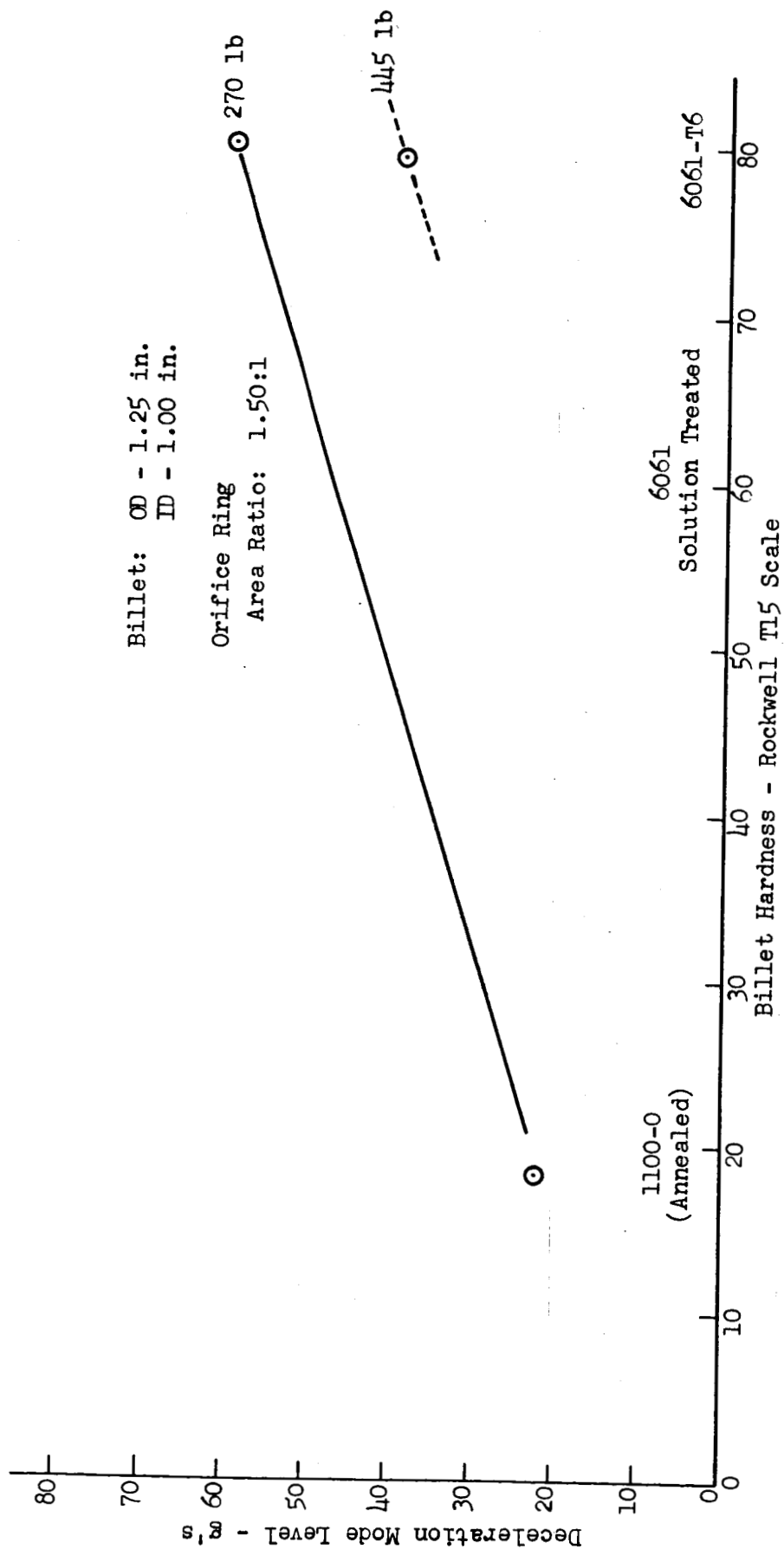


Figure 54

DECELERATION MODE AS A FUNCTION OF BILLET HARDNESS AND LOAD WEIGHT

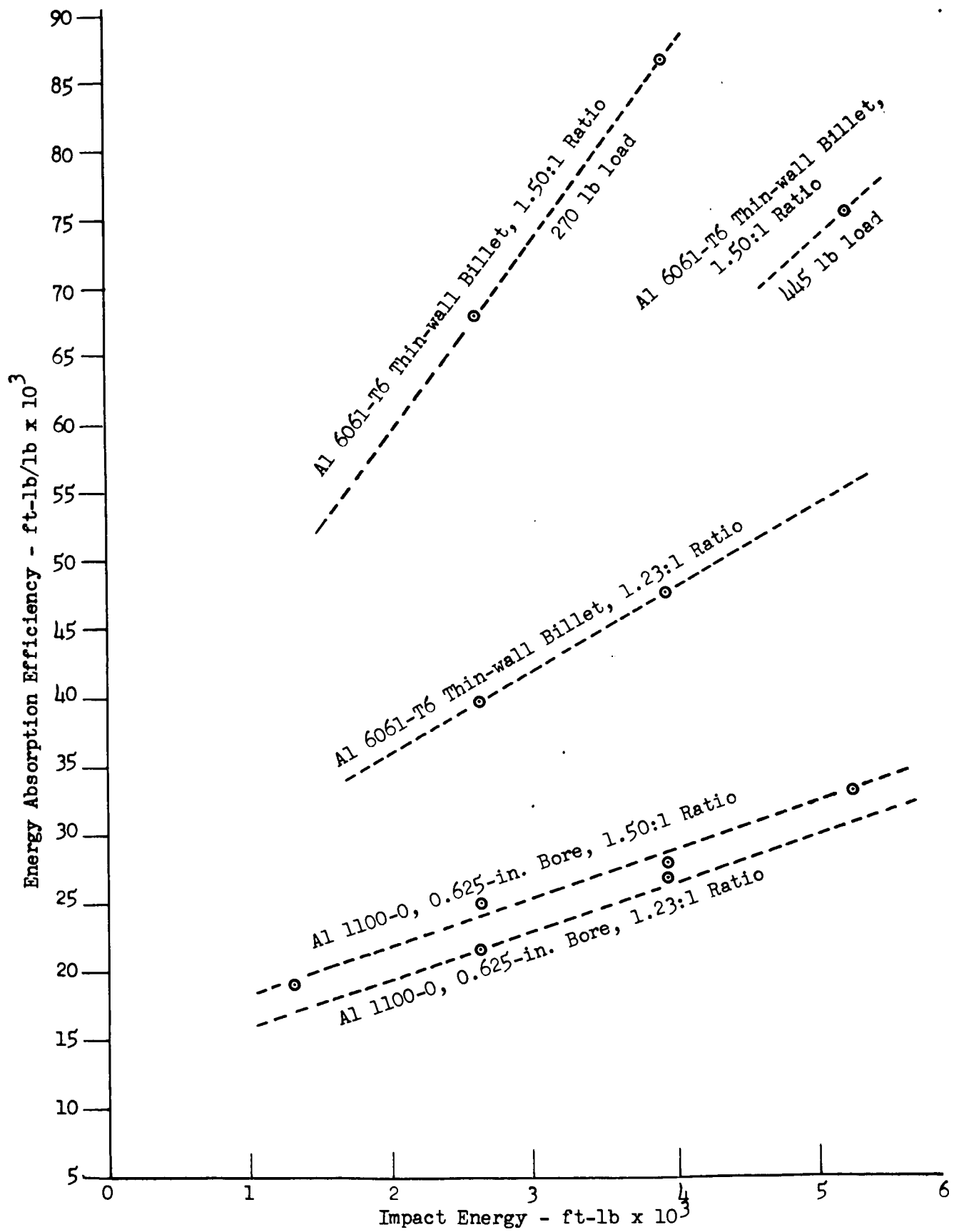


Figure 55

ENERGY ABSORPTION EFFICIENCY AS A FUNCTION OF IMPACT ENERGY

the heavier load is associated with lower g-level, and hence longer ram travel. Thus, using 40 g's as the estimated deceleration mode, the length of ram travel is found to be:

$$l = \frac{10,000 \text{ ft-lb}}{(445 \times 40) \text{ lb}} = 6.8 \text{ inches.}$$

#### Limitations of Shock Strut Concept

The most significant limitation of the shock strut design concept is that, in its current form, it requires essentially perpendicular impact for proper functioning. It is possible, however, that susceptibility to damage upon oblique landing may be reduced by proper support mechanism (e.g., spherical sections as contact members), in order to provide essentially axial load delivery to the shock strut.

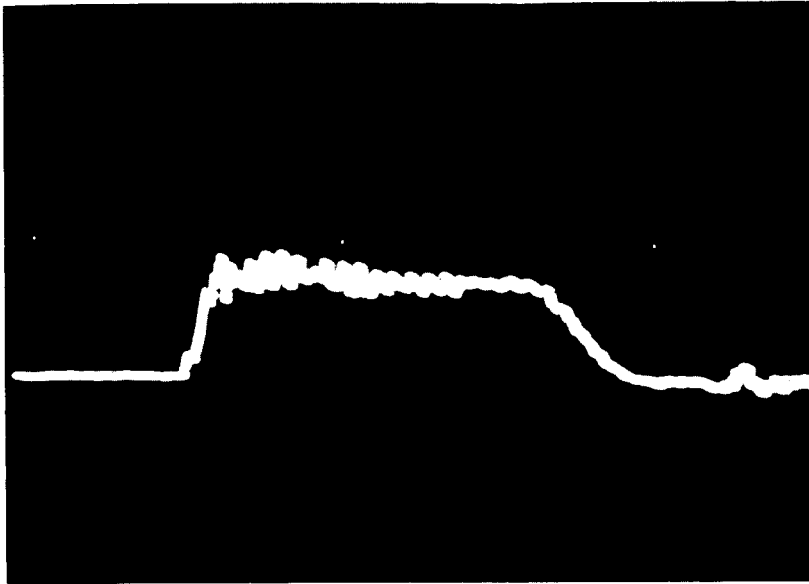
The data acquired in this work has not established lower limits on peak deceleration g-loading. If lower peak levels are desired, they should be attainable by additional variations of billet hardness, die entry angle, die extrusion ratio, and/or load weight.

## CONCLUSIONS

1. The inverse extrusion process was demonstrated to be effective in absorption of impact energy, with essentially constant force levels developed during absorption.
2. Aluminum was found to be a satisfactory material for use in shock strut billets. The particular alloy and temper required will vary with end-use objectives.
3. Deceleration profile is influenced most significantly by geometric and physical properties of the billets. Thin-walled annular cross-sectional shapes were found to be most effective with regard to peak deceleration and energy absorption efficiencies developed.
4. Small diameter components (billet diameter 1.125 inch) were found to be adequate in absorbing impact energies up to at least 6500 foot-pounds. Component length requirement was determined to vary directly with impact energy and with the characteristics of the billet and the extrusion ring.
5. Using 6061 aluminum alloy thin-wall billets, peak deceleration levels within the range of 25 to 65 g's were obtained with variation of temper from T-6 to solution-treated, and with variation of load from 270 pounds to 445 pounds. The associated energy absorption efficiencies ranged upward from 60,000 to over 80,000 foot-pounds per pound, calculated on the basis of weight of billet expended only. These efficiencies appear to be significantly higher than those of alternative energy absorption systems, considering weight of energy absorptive materials only.
6. Design of shock struts for specific end-use requirements may be accomplished using empirical data to determine component cross-sectional shape and metallurgical properties, and the conservation of energy equation to determine component lengths.

APPENDIX A

ADDITIONAL SHOCK STRUT PERFORMANCE DATA



#### BILLET

Material: Al 1100-0

Cross Section:

ID: 0 (Solid)

OD: 1.128 in.

#### DIE

Entry Area: 1 sq. in.

Exit Area: 0.666 sq. in.

Area Ratio: 1.50:1

#### OSCILLOSCOPE SETTINGS

Sweep: 2 ms/cm      Vertical Gain: 0.5 v/cm

Accelerometer Sensitivity: 10 mv/g

#### DECELERATION PROFILE

Mode g-level: 65 g's      Duration of Event: 11 ms

#### ENERGY ABSORPTION

Drop Height: 5 ft      Distance of Ram Travel: 0.813 in.

Load Weight: 270 lb

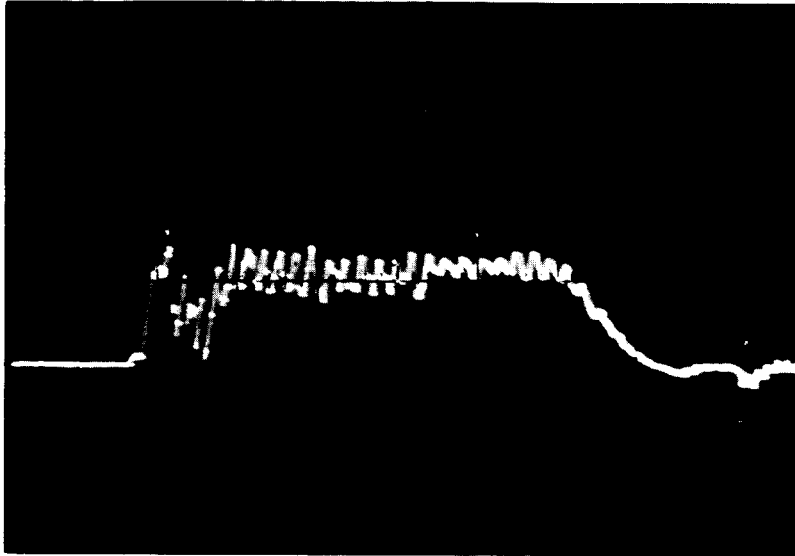
Impact Energy: 1350 ft-lb       $e = 18,000 \text{ ft-lb/lb}$

Figure A-1

SHOCK STRUT PERFORMANCE

Drop No. 97





#### BILLET

Material: Al 1100-0

Cross Section:

ID: 0 (Solid)

OD: 1.128 in.

#### DIE

Entry Area: 1 sq. in.

Exit Area: 0.666 sq. in.

Area Ratio: 1.50:1

#### OSCILLOSCOPE SETTINGS

Sweep: 2 ms/cm Vertical Gain: 0.5 v/cm

Accelerometer Sensitivity: 10 mv/g

#### DECELERATION PROFILE

Mode g-level: 60 g's Duration of Event: 12-1/2 ms

#### ENERGY ABSORPTION

Drop Height: 10 ft Distance of Ram Travel: 1.287 in.

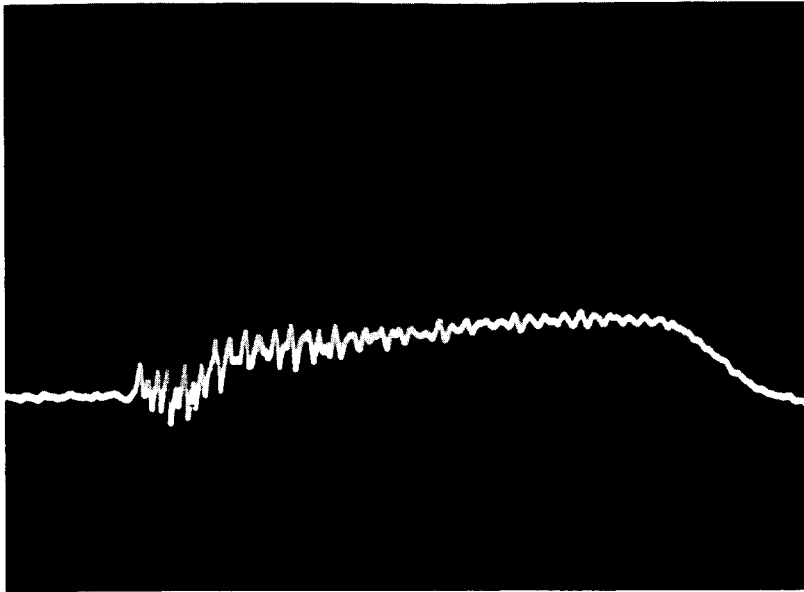
Load Weight: 270 lb

Impact Energy: 2700 ft-lb  $e = 23,400$  ft-lb/lb

Figure A-2

SHOCK STRUT PERFORMANCE

Drop No. 102



#### BILLET

Material: A1 1100-O

Cross Section:

ID: 0.750 in.

OD: 1.128 in.

#### DIE

Entry Area: 1 sq. in.

Exit Area: 0.666 sq. in.

Area Ratio: 1.50:1

#### OSCILLOSCOPE SETTINGS

Sweep: 2 ms/cm      Vertical Gain: 0.5 v/cm

Accelerometer Sensitivity: 10 mv/g

#### DECELERATION PROFILE

Mode g-level: 50 g's      Duration of Event: 16 ms

#### ENERGY ABSORPTION

Drop Height: 5 ft      Distance of Ram Travel: 1.4375 in.

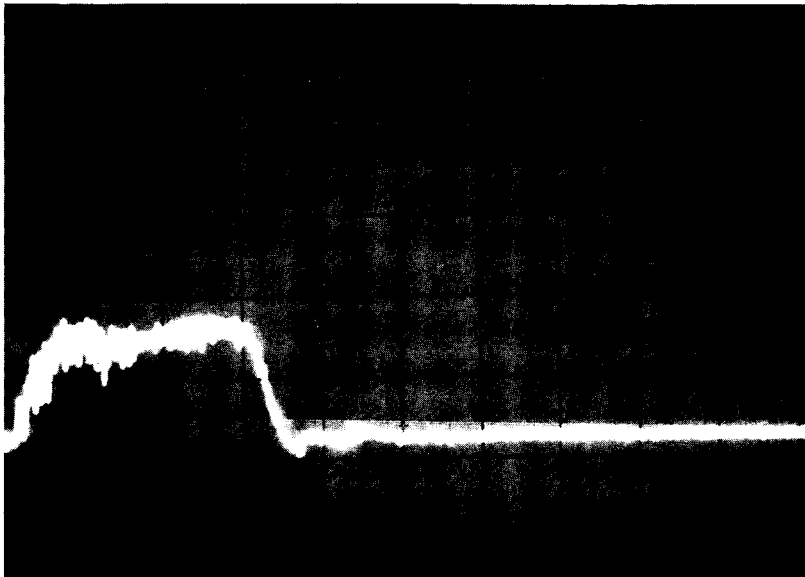
Load Weight: 270 lb

Impact Energy: 1350 ft-lb       $e = 18,000 \text{ ft-lb/lb}$

Figure A-3

SHOCK STRUT PERFORMANCE

Drop No. 120



#### BILLET

Material: Al 1100-O

Cross Section:

ID: 0.625 in.

OD: 1.128 in.

#### DIE

Entry Area: 1 sq. in.

Exit Area: 0.666 sq. in.

Area Ratio: 1.50:1

#### OSCILLOSCOPE SETTINGS

Sweep: 5 ms/cm    Vertical Gain: 0.5 v/cm

Accelerometer Sensitivity: 10 mv/g

#### DECELERATION PROFILE

Mode g-level: 65 g's    Duration of Event: 18 ms

#### ENERGY ABSORPTION

Drop Height: 20 ft    Distance of Ram Travel: 2.531 in.

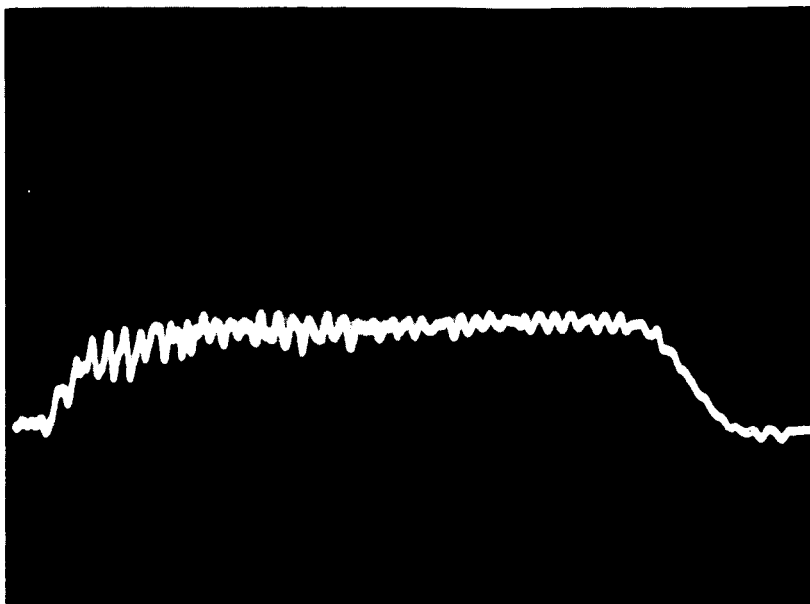
Load Weight: 270 lb

Impact Energy: 5400 ft-lb     $e = 33,300 \text{ ft-lb/lb}$

Figure A-4

SHOCK STRUT PERFORMANCE

Drop No. 115



BILLET

Material: Al 1100-O

Cross Section:

ID: 0.625 in.

OD: 1.128 in.

DIE

Entry Area: 1 sq. in.

Exit Area: 0.666 sq. in.

Area Ratio: 1.50:1

OSCILLOSCOPE SETTINGS

Sweep: 2 ms/cm    Vertical Gain: 0.5 v/cm

Accelerometer Sensitivity: 10 mv/g

DECELERATION PROFILE

Mode g-level: 65 g's    Duration of Event: 17 ms

ENERGY ABSORPTION

Drop Height: 20 ft

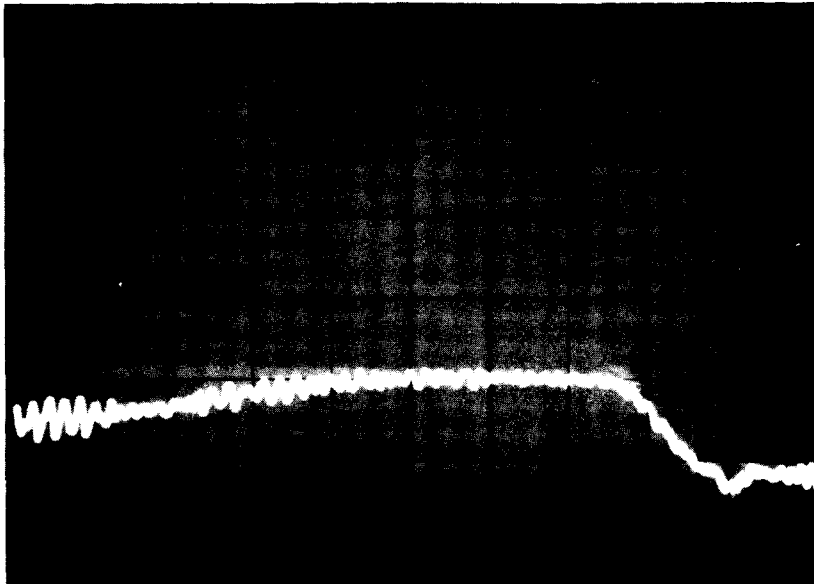
Load Weight: 270 lb

Impact Energy: 5400 ft-lb     $e = 29,500 \text{ ft-lb/lb}$

Figure A-5

SHOCK STRUT PERFORMANCE

Drop No. 116



BILLET

Material: Al 1100-0

Cross Section:

ID: 0.875 in.

OD: 1.128 in.

DIE

Entry Area: 1 sq. in.

Exit Area: 0.666 sq. in.

Area Ratio: 1.50:1

OSCILLOSCOPE SETTINGS

Sweep: 2 ms/cm      Vertical Gain: 0.5 v/cm

Accelerometer Sensitivity: 10 mv/g

DECELERATION PROFILE

Mode g-level: 55 g's      Duration of Event: Indeterminate ms

ENERGY ABSORPTION

Drop Height: 15 ft      Distance of Ram Travel: 3-3/8 in.

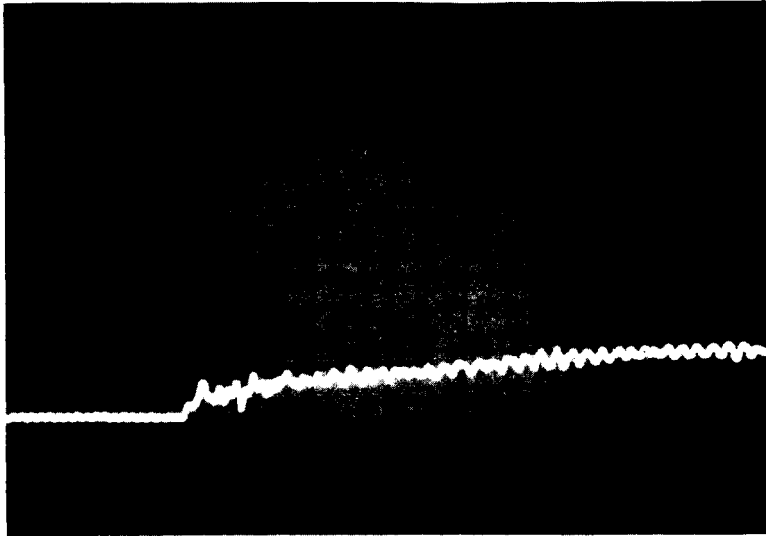
Load Weight: 270 lb

Impact Energy: 3050 ft-lb

Figure A-6

SHOCK STRUT PERFORMANCE

Drop No. 135



#### BILLET

Material: Al 1100-0

Cross Section:

ID: 0.875 in.

OD: 1.128 in.

#### DIE

Entry Area: 1 sq. in.

Exit Area: 0.666 sq. in.

Area Ratio: 1.50:1

#### OSCILLOSCOPE SETTINGS

Sweep: 2 ms/cm      Vertical Gain: 0.5 v/cm

Accelerometer Sensitivity: 10 mv/g

#### DECELERATION PROFILE

Mode g-level: 50 g's      Duration of Event: Indeterminate ms

#### ENERGY ABSORPTION

Drop Height: 10 ft

Load Weight: 270 lb

Figure A-7

SHOCK STRUT PERFORMANCE

Drop No. 129